THE
PHYSICAL REVIEW
A Journal of Experimental and Theoretical Physics Established by E. L. Nichols in 1893
VOL. 53, NO. 8 APRIL 15, 1938 SECOND SERIES

Cosmic-Ray Ionization in the Neighborhood of a Lead Block

EDWIN G. SCHNEIDER*
Harvard University, Cambridge, Massachusetts
(Received February 21, 1938)

A study of the relative occurrence of the more frequent cosmic-ray phenomena in the neighborhood of a 6 mm thick sheet of lead has been made by analyzing 2500 stereoscopic photographs of electron tracks. In order to avoid selectivity of the apparatus for certain types of events, the cloud chamber was not triggered by a counting device, but was operated by manual and mechanical controls. These photographs show that about three quarters of the ionization is due to single particles, about one-fifth is due to photon produced pairs, and approximately one-twentieth is caused by secondaries ejected by particles.

SINCE an ionization chamber measures the total ionization in a moderately large region, an estimate of the number of ionizing particles may be made, but practically no information concerning the actual paths of the particles can be obtained. A group of G-M counters, on the other hand, may give some indication of the particle path, but fails to record the total number of particles involved. Because of these limitations neither of these devices is entirely suitable for a detailed study of the ionization in the neighborhood of a block of absorbing material. For this purpose the use of a cloud chamber is highly desirable because the exact paths and numbers of ionizing particles may be obtained and the approximate amount of ionization may be determined from the density of the tracks. In order to avoid a great many exposures which show no cosmic rays, it is customary to use G-M counters singly or in groups to start the expansion of the chamber. This practice greatly enhances the probability of obtaining a photograph of a cosmic-ray phenomenon, the discharge of the counters being a necessary condition for the taking of the picture. Because of the geometry of the counter array certain configurations of ionizing particles will be more apt to discharge the counters than other configurations with the result that certain phenomena are favored. If the discharge of two or more counters is required, events involving a large number of particles will be almost certain to start the expansion of the chamber.

This selection of particular particle configurations and of large groups of particles may be avoided by taking photographs at random time intervals. Unless an extremely large number of these random photographs are taken, this procedure will give the relative occurrence of only the more common cosmic-ray events. Pictures of electron tracks have been taken with a cloud chamber which was not controlled by a counting device.[1] Since these pictures show a great complexity of secondary radiation from a massive magnet surrounding the chamber, they cannot be

* Now with the Philco Radio and Television Company.

[1] C. D. Anderson, Phys. Rev. **44**, 406 (1933); P. Kunze, Zeits. f. Physik **80**, 559 (1933).

considered as typical for an isolated block of lead.

In order to reduce to a minimum the secondary radiation from material outside of the region of observation, a cloud chamber[2] with 3 mm thick glass walls was placed in a room having only a thin wooden roof. A plate of lead 6 mm thick and 175 cm² in area was mounted horizontally across the center of the chamber. A pair of Helmholtz coils giving a magnetic field of 600 gauss, constant to 10 percent over the sensitive region of the chamber, permitted the measurement of electron energies up to about 10 Mev with reasonable accuracy. Two cameras mounted 30° off the normal to the cloud chamber were used to obtain stereoscopic views of the tracks.

All single electrons and all electron pairs having a total energy less than 3 Mev were discarded from the data because of the difficulty of separating cosmic-ray secondaries of such low energy from electrons ejected by radioactive contamination.

In Table I are given the results of 2500 pictures taken at random in time.

In Table I no attempt has been made to separate electrons and positrons since the magnetic field was insufficient to determine the sign of the charge on the high energy particles. In the energy range where the charge could be determined there were about three positrons for every five electrons. There is also a possibility that many of the penetrating particles having an ionization density about that of an electron are not electrons.[3]

A comparison of the number of electrons above and below the plate shows that the ionization is not greatly altered by the introduction of 6 mm of lead. There is, however, a slight increase in ionization below the lead similar to that found by Street and Young during some ionization chamber studies in the same room.[4] Schindler[5] has suggested that the increase in ionization when a few millimeters of dense material are inserted above an ionization chamber is due to the establishment of a new equilibrium between the primary and secondary radiation. It is apparent from the table that the new equilibrium is established chiefly by absorption of low energy particles and photons rather than through a reaction of the penetrating radiation with the lead. This fact is most strikingly illustrated by the number of electron pairs which appear below the lead. About one-fifth of the ionization below the plate is due to electron pairs, over half of these pairs having a total energy less than 10 Mev. Presumably all of these pairs are produced by photons since no other tracks appear in the immediate neighborhood.

TABLE I. *Classification of tracks.*

Electron Tracks Passing Through or Terminating on the Lead Plate	
Total Number of Electron Tracks Above Lead	438
Total Number of Electron Tracks Below Lead	450
Single Electrons	
Penetrating the Lead	257
Above Lead Only	136
Number of These with Energy Between 3 and 10 Mev	34
Below Lead Only	86
With Energy Between 3 and 10 Mev	24
Electron Pairs	
Above Lead	18
With Total Energy Between 3 and 10 Mev	17
Below Lead	42
With Total Energy Between 3 and 10 Mev	26
Single Electron Entering Lead, Two Leaving	4
Single Electron Entering Lead, Three Leaving	5
More Complicated Phenomena	0
Number of Tracks Not Touching Lead	647

The ionization chamber data of Street and Young[4] permit another comparison. If their curves for the ionization under very thick layers of lead are assumed to give the intensity of the penetrating component of the cosmic radiation, an extrapolation can be made to obtain the intensity of this component under thin layers of lead. A comparison of the extrapolated and measured curves shows that 0.57 is the ratio of the absorbed to the penetrating radiation for 6 mm of lead. The ratio of the number of single electrons appearing only above the lead to those which penetrate the lead is 0.53, a value which may be considered in agreement with the ionization chamber measurements.

Danforth and Lipman[6] have made a more direct determination of the intensity of the low energy component of the cosmic radiation by means of very thin walled counters. They find that 20 percent of the electrons have energies less

[2] Street and Stevenson, Rev. Sci. Inst. **7**, 347 (1936).
[3] Street and Stevenson, Phys. Rev. **52**, 1003 (1937); Neddermeyer, Phys. Rev. **53**, 102 (1938).
[4] Street and Young, Phys. Rev. **46**, 823 (1934).
[5] Schindler, Zeits. f. Physik **72**, 625 (1931).
[6] Danforth and Lipman, J. Frank. Inst. **217**, 73 (1934).

than 10 Mev and greater than 1 Mev, that 10 percent have energies between 5 and 10 Mev, and that an absorbing sheet of 4 g/cm² reduced the number of electrons by 20 percent. The cloud chamber results in Table I above show that about 9 percent of the incident electrons have energies between 3 and 10 Mev and that the lead sheet of 6.8 g/cm² removed about 35 percent of the incident electrons. Since these two sets of experiments were conducted under different types of roofing material, the agreement may be considered satisfactory. Any change in the material above the region of observation would probably have a large effect on the low energy radiation.

The assumption that all of the single tracks appearing only above the lead are due to absorbed electrons may be invalid since some of these tracks may be due to electrons ejected in an upward direction by photons. Since the number of electron pairs above the lead is small, it is very unlikely that many of these single tracks are due to photons. Furthermore, since practically all of the pairs above the lead are of low energy, it is probable that many of them are reflected electrons rather than pairs. For these reasons this assumption, that all single electron tracks above the lead represent only absorbed electrons, cannot introduce a large error.

The sensitive time of the cloud chamber after an expansion and the integrated time of observation can be calculated from the data in the table if the number of cosmic rays incident on a unit area in a unit time is known. Ionization chamber and counter data indicate that 1.5 cosmic-ray electrons/cm²/min. may be expected in the room in which the cloud chamber was operated. Since 438 cosmic-ray electrons were incident on the 175 cm² of lead in 2500 photographs, the integrated time of exposure must have been 100 sec. and the chamber was sensitive for about 0.04 sec. after each expansion.

A rough calculation of the intensity of incident photons may be made if the absorption coefficient of the photons is known. According to Heitler[7] the absorption coefficient of the photons capable of ejecting the observed electrons lies between 0.5/cm of lead for the energies between 3 and 10 Mev and 1.5/cm for the very high energies. There are 128 single electrons or electron pairs presumably corresponding to 128 absorbed photons which had sufficient energy to cause electrons to escape below the lead with a remaining energy greater than 3 Mev. A lower limit to the photon intensity may be set by assuming an average absorption coefficient of 1.0/cm and assuming that all electrons ejected by these photons appear in the gas. These assumptions give 0.7 photons/cm²/sec. as the incident intensity. The assumption that all ejected electrons escape into the gas is obviously wrong since high energy electrons suffer an energy loss of about 10 Mev/mm or more[8] in the average energy range of the observed electrons. Furthermore, in practically all cases the electron pairs appeared to originate at a point within 1 mm of the surface of the lead. In view of these facts it seems more likely that the incident photon intensity is several times that of the electron intensity rather than about half as indicated by the value given above.

Since no shower phenomena involving the ejection of three or more electrons were observed, it seems safe to assume that at sea level only a few percent of the ionization below a 6 mm block of lead can be due to large showers. About 75 percent of this ionization is due to single particles, about 20 percent is due to photon produced pairs and about 5 percent results from the ejection of secondary electrons by high energy particles.

In conclusion the author wishes to thank Dr. J. C. Street for his helpful suggestions during the preparation of this paper.

[7] Heitler, *Quantum Theory of Radiation* (Oxford, 1936).
[8] Anderson and Neddermeyer, Phys. Rev. **50**, 270 (1936).

The Absorption of High Energy Electrons. Part III

A. J. RUHLIG AND H. R. CRANE
University of Michigan, Ann Arbor, Michigan

(Received February 25, 1938)

Losses in lead of electrons with energies both above and below the range previously used (2 to 11 Mev) have been measured. For the low energy group electrons from radioactive P^{32} were sent through lead laminae of two thicknesses placed in the center of a cloud chamber. In this energy region the losses in lead should be due almost entirely to ionization processes. The experimental values for the energy losses are from 2 to 4 times those given by the Bloch formula. For the high energy group the electrons and positrons produced by the $Li+H^1$ gamma-radiation were used. The values found are about 50 percent greater than the calculated losses due to ionization and radiation, but are in good accord with the previous experimental values.

INTRODUCTION

THE first two papers of this series[1,2] dealt with the loss in energy which electrons with kinetic energies ranging from 2 to 11 Mev undergo in traversing carbon and lead absorbers. The apparently anomalous behavior of electrons at somewhat lower energies noticed by various experimenters[3,4] led to the present extension which includes the energy losses in lead experienced by electrons with an energy of about 1 Mev. Because of the importance, especially for cosmic-ray data, of a comparison between the energy losses of electrons and those of positrons we have also measured the losses in lead of positrons having initial kinetic energies between 5 and 15 Mev. We have considered separately the cases in which particles are scattered through an angle of more than 90 degrees and thus are reflected from the absorber. It is probable that such information will be important to any theory which deals with the effect of scattering on the observed energy loss.

EXPERIMENTAL TECHNIQUE

Low energy group

The beta-rays emitted by phosphorus bombarded by deuterons in the Michigan cyclotron provided a convenient source of electrons, because of the long (fourteen day) half-life. This P^{32} source was placed about 15 cm away from a small Cellophane window, 0.1 mm thick, in the wall of the cloud chamber.[5] As a rough selector lead blocks were placed between the source and the window in the magnetic field around the chamber. These blocks were arranged so that electrons of various energies, ranging from 0.35 to 1.35 Mev, were allowed to enter the chamber. The magnetic field employed was 460 oersteds, kept constant to within 5 percent.

Since air at 0.8 atmospheres pressure was used in the cloud chamber throughout the experiment, it was necessary in the case of the lowest energy group (0.5 Mev) to discard a considerable number of tracks which were visibly scattered in the gas. For this reason we cannot place as much faith in the results for the 0.5 Mev group as for those of higher energy. Two different lead laminae were used as absorbers, placed across the center of the chamber. Their thicknesses, as determined by weighing, were 0.0038 and 0.0066 cm.

The energy losses were determined by measuring the momenta of the electrons in terms of their radii of curvature on both sides of the absorber. To aid in achieving an impersonal selection of the tracks, that side of the chamber on which the particles emerged was hidden from view during the measuring of the incident energy. Stereoscopic pictures were taken in the experiments on the low energy electrons by use of an arrangement with a single mirror in which both the direct and the indirect views were photographed side by side on the same film. This reduced the possibility of counting as one track what might in reality be two parts of two different tracks.

[1,2] Turin and Crane, Phys. Rev. **52**, 63; **52**, 610 (1937).
[3] Laslett and Hurst, Phys. Rev. **52**, 1035 (1937).
[4] Skobeltzyn and Stepanowa, Nature **137**, 234 (1935); Leprince-Ringuet, Ann. de physique **7**, 5 (1937); Klarmann and Bothe, Zeits. f. Physik **101**, 489 (1936).
[5] Crane, Rev. Sci. Inst. **8**, 440 (1937).

High energy group

As a source of high energy positrons and electrons, we used the gamma-radiation emitted in the $Li+H^1$ reaction.[6] The protons were accelerated by the high voltage apparatus previously described.[7] The gamma-rays coming from the lithium target struck a sheet of lead about 3 mm thick which was placed against the inside wall of the cloud chamber. The pairs emerging from the lead passed through an absorber of lead, 0.038 cm thick, placed across the center of the chamber. The magnetic field had a value of 2850 oersteds ± 2 percent.

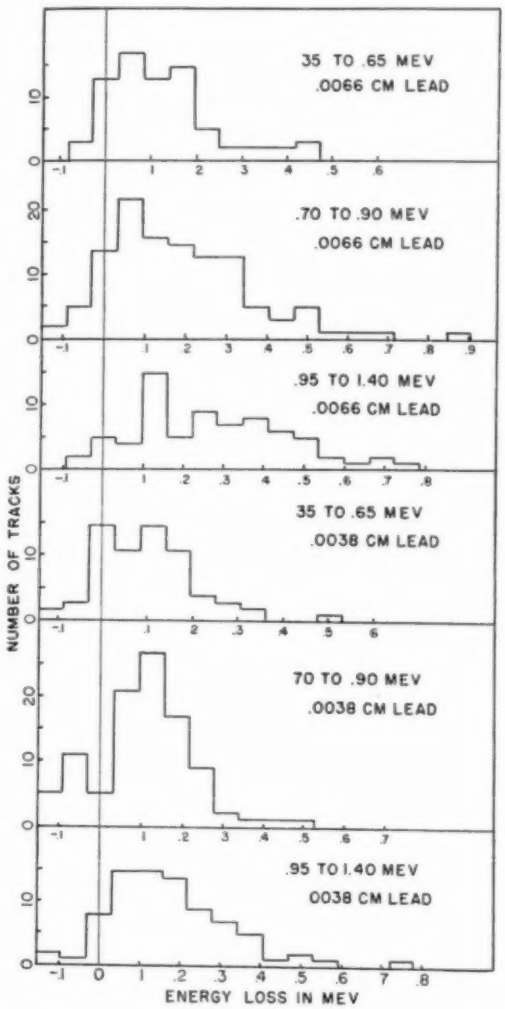

FIG. 1. Energy losses for electrons traversing lead laminae of thicknesses 0.0038 cm and 0.0066 cm.

[6] Gaerttner and Crane, Phys. Rev. **52**, 582 (1937); Delsasso, Fowler and Lauritsen, Phys. Rev. **51**, 391 (1937).
[7] Crane, Phys. Rev. **52**, 11 (1937).

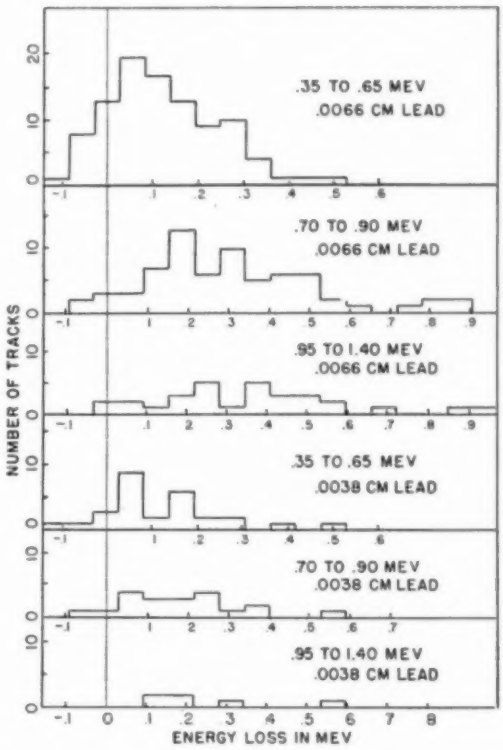

FIG. 2. Energy losses for electrons reflected from lead laminae of thicknesses 0.0038 cm and 0.0066 cm.

RESULTS

Histograms showing the distribution of energy losses among the electrons for the groups of various energies are plotted in Figs. 1 to 4. A summary of the energy loss data obtained from these histograms is given in Tables I to V. In Table I the losses for the two different thicknesses of lead are in good agreement, being about 10 percent higher for the thinner absorber. The energy loss per unit length has not been given for the reflected electrons in Tables II and V, since there is no way to estimate the minimum

TABLE I. *Energy losses of electrons traversing lead absorbers.*

THICKNESS OF ABSORBER	NUMBER OF ELECTRONS	ENERGY RANGE IN MEV	AVERAGE ENERGY IN MEV	AVERAGE LOSS IN MEV/CM	THEORETICAL LOSS IN MEV/CM
0.0038 cm	69	0.35 to 0.65	0.55	23	11
	101	0.7 to 0.9	0.79	28	11
	81	0.95 to 1.4	1.08	48	11
	251		0.82	33	11
0.0066 cm	61	0.35 to 0.65	0.57	19	11
	117	0.7 to 0.9	0.80	27	11
	71	0.95 to 1.4	1.08	44	11
	249		0.82	30	11

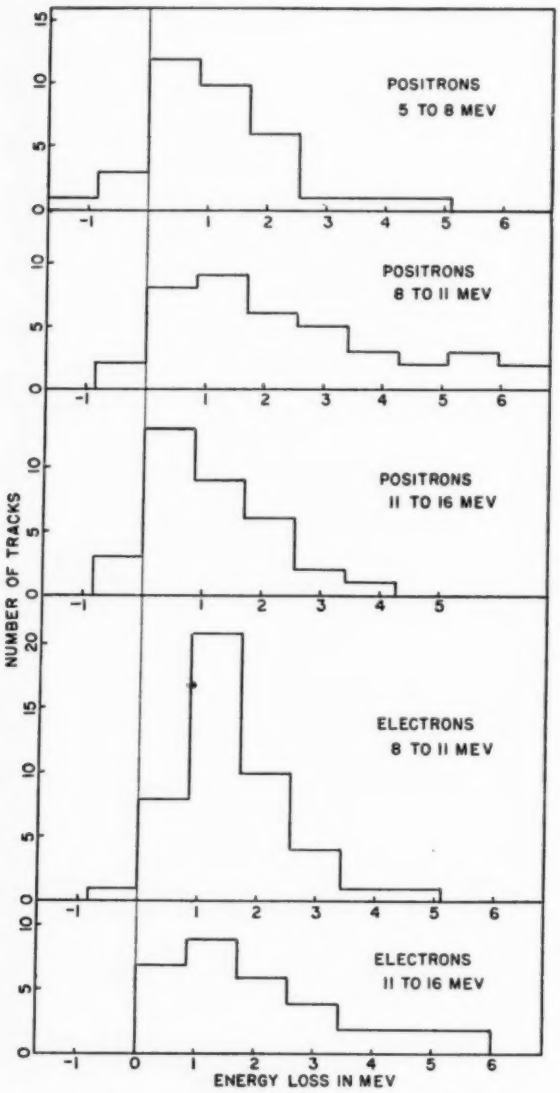

FIG. 3. Energy losses of positrons and of electrons traversing a lead lamina of thickness 0.038 cm.

length of path within the absorber of such reflected particles. The reflections summarized in Table V were obtained from the photographs which were taken for the previous investigation of the energy losses of Li^8 beta-rays.[2] The values predicted by theory[8] are also given in the tables for comparison.

DISCUSSION

For electrons below 1 Mev the radiation losses indicated by the Bethe-Heitler theory are negligible, even in lead. The energy losses should

[8] Heitler, *Quantum Theory of Radiation*, p. 217.

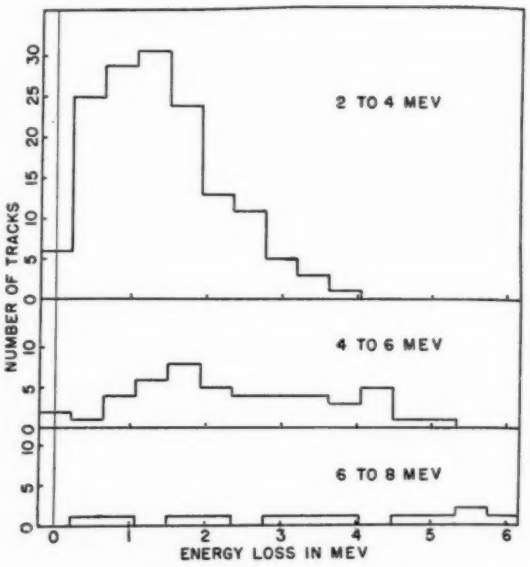

FIG. 4. Energy losses of electrons reflected from a lead lamina of thickness 0.05 cm.

be due almost entirely to ionization processes, and should therefore not change markedly with incident energy. For this reason the sharp increase which we observe in energy loss for 1 Mev electrons as compared to the loss for 0.5 Mev electrons is difficult to interpret. Because this increase occurs for both thicknesses of absorber and for both traversals and reflections it is hard to doubt its reality. If the actual thickness of the absorber should be multiplied

TABLE II. *Energy losses of electrons reflected from lead absorbers.*

THICKNESS OF ABSORBER	NUMBER OF ELECTRONS	ENERGY RANGE IN MEV	AVERAGE ENERGY IN MEV	AVERAGE ENERGY LOSS IN MEV
0.0038 cm	28	0.35 to 0.65	0.56	0.13
	20	0.7 to 0.9	0.77	0.18
	6	0.95 to 1.4	1.04	0.26
	54		0.69	0.16
0.0066 cm	98	0.35 to 0.65	0.59	0.13
	69	0.7 to 0.9	0.79	0.30
	31	0.95 to 1.4	1.07	0.38
	198		0.73	0.23

TABLE III. *Energy losses of positrons traversing lead.*

THICKNESS OF ABSORBER	NUMBER OF POSITRONS	ENERGY RANGE IN MEV	AVERAGE ENERGY IN MEV	AVERAGE LOSS IN MEV/CM	THEORETICAL ENERGY LOSS IN MEV/CM
0.038 cm	35	5 to 8	5.8	30	21
	47	8 to 11	9.5	40	28
	33	11 to 16	12.3	49	33

by some factor larger than unity because of the increase in path length in the absorber due to scattering, we would expect this factor to be larger for the lower energy group, since scattering increases greatly with decreasing energy. Thus the actual increase in energy loss more than compensates for this factor.

It might be supposed that for some reason the large losses of the lowest energy group are not considered in the data. This might be due to the fact that tracks of very small radii of curvature are more easily missed in the cloud chamber or discarded because of scattering. Or again, it could be because of a smaller probability for particles which have lost most of their energy emerging from the lead absorber. If this were so, however, the fractional losses would be appreciably higher for the 1 Mev electrons than for those with less energy (unless there are some compensating factors). But experimentally there are no appreciable differences in fractional losses among the three energy groups.

In addition to the variation of energy loss with energy the data indicate an experimental loss which is about three times the value given by the Bloch formula. This agrees with the work of Laslett and Hurst,[3] who found a factor 2.6 times theory in the region from 1.5 to 4.5 Mev. Whether this can be accounted for on the basis of an increase in path length in the absorber due to multiple scattering cannot be answered at present. If one postulates that there are large radiative losses already for electrons below 1 Mev, this might be difficult to reconcile with experiences regarding the efficiency of high voltage x-ray tubes.

TABLE IV. *Energy losses of electrons traversing lead.*

Thickness of Absorber	Number of Electrons	Energy Range in Mev	Average Energy in Mev	Average Loss in Mev/cm	Theoretical Energy Loss in Mev/cm
0.038 cm	33 41	8 to 11 11 to 16	9.5 12.7	34 61	28 34

TABLE V. *Energy losses of electrons reflected from lead.*

Thickness of Absorber	Number of Electrons	Energy Range in Mev	Average Energy Loss in Mev
0.05 cm	146 50 12	2 to 4 4 to 6 6 to 8	1.30 2.38 3.47

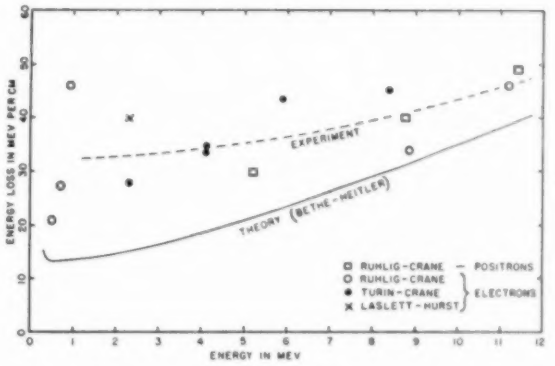

FIG. 5. Differential energy loss of positrons and electrons in lead for various incident energies, compared to theoretical values.

The values found here for high energy electrons and positrons are in good agreement with those previously reported. We have summarized the experimental values for energy losses in lead in Fig. 5. It is seen that the experimental values are appreciably higher than theory, but theory may be as much as 30 percent too low because of the approximations made in the derivation. We have not found any marked difference between the losses of positrons and those of electrons, as were indicated for the cosmic-ray region by Crussard.[9] This is in agreement with the work of Anderson and Neddermeyer[10] and Blackett and Wilson[11] in the cosmic-ray region, and with the results of Curtis[12] for the losses of low energy positrons in aluminum.

In the fourth part of this series of papers, now being prepared by M. M. Slawsky and H. R. Crane, there will be presented experimental data on multiple scattering for the energy range for which loss measurements have been made, and an attempt will be made to discover whether the effects of scattering are sufficient to account for the observed energy loss.

We wish to thank Professor J. M. Cork, Dr. R. L. Thornton and the other members of the Michigan cyclotron group for supplying the radioactive phosphorus. This research was made possible through the generosity of the Horace H. Rackham Foundation.

[9] Crussard, J. de phys. **8**, 213 (1937).
[10] Anderson and Neddermeyer, Phys. Rev. **51**, 884 (1937).
[11] Blackett and Wilson, Proc. Roy. Soc. **A160**, 304 (1937).
[12] Curtis, Phys. Rev. **53**, 206 (1938).

Disintegration of the Deuteron by Alpha-Particles*

H. L. SCHULTZ
Sloane Physics Laboratory, Yale University, New Haven, Connecticut
(Received February 7, 1938)

The noncapture disintegration of the deuteron by fast alpha-particles has been observed. Neutrons emitted in the transmutation were detected with the aid of a BF_3 filled ionization chamber surrounded by paraffin and connected to a high gain amplifier thyratron recording system. Both Ra C′ and Th C′ alpha-particles were used to bombard a gaseous target of heavy hydrogen. Essentially "thin layer" technique was employed in obtaining cross sections for the disintegration process by comparing the neutron yields from D_2 and N_2 under identical conditions. Mean cross sections of 0.12×10^{-26} cm² and 0.30×10^{-26} cm² were obtained for the range intervals 5.7 to 6.9 cm and 7.4 to 8.6 cm, respectively. These experimental values are lower than theoretical estimates obtained from computations made by Massey and Mohr who used an approximation method.

I. INTRODUCTION

PREVIOUS to the present work several attempts had been made to observe the noncapture disintegration of the deuteron according to

$$_1H^2+{}_2He^4\rightarrow{}_1H^1+{}_0n^1+({}_2He^4).$$

Rutherford and Kempton[1] using a H_2 filled ionization chamber amplifier arrangement found no detectable yield of neutrons when D_2O was bombarded by polonium alpha-particles. Dunning[2] performed the same experiment with radon instead of polonium, and with the aid of a similar but improved detection apparatus obtained indications of a small neutron yield of doubtful origin. Recently, McCarthy[3] of this laboratory has made with a Wilson cloud chamber and Th C+C′ alpha-particles a study of the range-velocity relation for recoil deuterons. The analysis of a large number of photographs failed to reveal a deuteron disintegration.

The method of distorted wave functions has been applied by Massey and Mohr[4] in calculating cross sections for the process in question at several alpha-particle energies. These calculations indicate an order of magnitude for the disintegration yield sufficient to permit experimental detection, at least for Th C′ particles. Energetically, the reaction is possible for alpha-particle energies greater than three times the binding energy of $_1H^2$.

Since data on the interactions of light nuclei are fundamental in nuclear theory, it was considered desirable to search for the neutrons emitted from deuterium under fast alpha-particle bombardment (especially by Th C′ particles). The search was made with a more sensitive method of detection, in particular for lower energy neutrons, than employed by the previous investigators. As recently pointed out by Bethe,[5] the method of calculation adopted by Massey and Mohr is probably not applicable to nuclear problems. Thus, an experimental determination of cross section for several incident energies will be valuable in connection with any more rigorous theoretical treatment that may be made in the future.

Positive results have been obtained with the aid of a highly sensitive BF_3 filled ionization chamber paraffin arrangement for detecting neutrons. The use of a target of D_2 gas (1.2 cm air equivalent absorption) made it possible to compare directly the relative neutron yields from deuterium and nitrogen from which comparison cross sections for D_2 were obtained. The data of Fahlenbrach[6] on the absolute neutron yields

* Part of a dissertation presented to the Faculty of the Graduate School of Yale University in candidacy for the degree of Doctor of Philosophy.

[1] Lord Rutherford and A. E. Kempton, Proc. Roy. Soc. **A143**, 724 (1933).

[2] J. R. Dunning and G. B. Pegram, Phys. Rev. **45**, 275 (1934).

[3] J. T. McCarthy, Dissertation, Yale University (1937).

[4] H. S. W. Massey and C. B. O. Mohr, Proc. Roy. Soc. **A148**, 206 (1935).

[5] H. A. Bethe, Rev. Mod. Phys. **9**, 69 (1937).

[6] H. Fahlenbrach, Zeits. f. Physik **94**, 607 (1935).

from nitrogen under alpha-particle bombardment have been applied. The final results with both Ra C′ alpha-particles and Th C′ alpha-particles consist of two mean cross sections which are 0.12×10^{-26} cm² for the range interval 5.7–6.9 cm, 0.30×10^{-26} cm² for the range interval 7.4–8.6 cm.

II. Experimental Technique

A. Detection equipment

An experimental study of the reaction

$$_1H^2+{}_2He^4\rightarrow{}_1H^1+{}_0n^1+({}_2He^4)$$

must be concerned with the detection of at least one of the two final products, neutron or proton. Any attempt to count the small number of disintegration protons must involve considerable difficulty due to the presence of projected deuterons and "natural" protons emitted from radioactive sources. In addition, strong β- and γ-radiation from the sources may cause trouble. Modifications in geometry undertaken to improve the situation in all of these respects will lead to a serious reduction in numbers counted. Hence, the only alternative is to count the neutrons also emitted. Unfortunately, this causes the determination of cross sections to be much less direct.

Of the several methods of neutron detection available for investigation of the reaction in question, the one chosen must satisfy the requirements of (1) high sensitivity especially for neutrons of energies below the fast region, and (2) suitability for obtaining absolute yields.

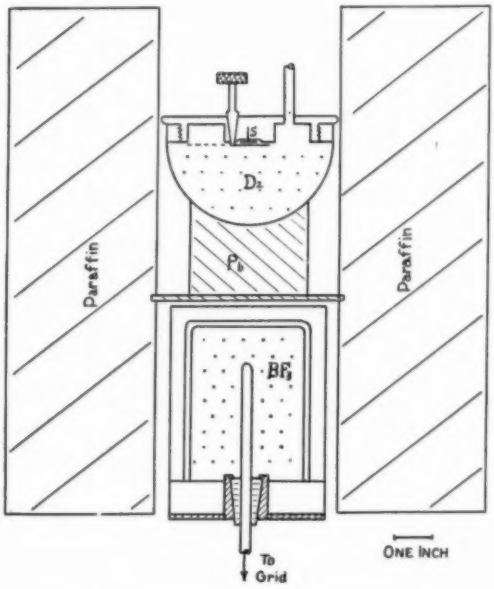

Fig. 1. Source and detector arrangement.

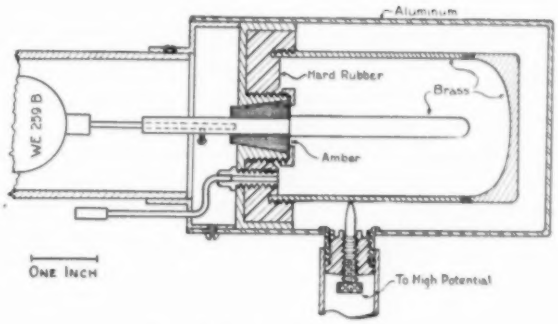

Fig. 2. Ionization chamber.

Chadwick and Goldhaber,[7] Dunning and his co-workers,[8] Fink[9] and others have emphasized the large detection efficiencies of B and Li lined ionization chambers for slow neutrons. Goldhaber[10] and Tuve and Hafstad[11] have in particular applied this method to the detection of fast neutrons by slowing them down in paraffin. The BF_3 filled chamber is not only more sensitive than a similar B or Li lined chamber, but also surpasses the usual artificial radioactive detector. It thus appeared that a BF_3 filled ionization chamber surrounded by paraffin and connected to the conventional high gain amplifier offered the best possibilities for the detection of neutron yields from deuterium. The advantages of this method may be summarized as follows:

(1) High sensitivity as a result of (a) large effective solid angles for counting due to the paraffin surroundings, and (b) high disintegration probability for B by slow neutrons.

(2) Ultimate detection of heavy particles (alpha-particles from the disintegration of B by neutrons), thus giving high ionization currents and less difficulty in recording.

(3) Continuity of detection efficiency with neutron energy, i.e., absence of resonance phenomena.

The location of the ionization chamber in relation to the cylindrical paraffin block used and neutron source is shown in Fig. 1. Details of

[7] J. Chadwick and M. Goldhaber, Proc. Camb. Phil. Soc. **31**, 612 (1935).
[8] J. R. Dunning, G. B. Pegram, G. A. Fink and D. P. Mitchell, Phys. Rev. **48**, 265 (1935).
[9] G. A. Fink, Phys. Rev. **50**, 738 (1936).
[10] M. Goldhaber, Nature **137**, 824 (1936).
[11] M. A. Tuve and L. R. Hafstad, Phys. Rev. **50**, 490 (1936).

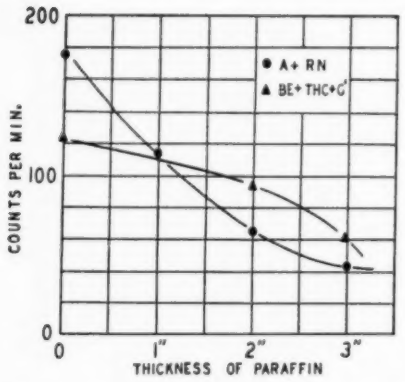

FIG. 3. Variation of detection efficiency with thickness of paraffin between neutron source and BF_3 chamber.

construction of the ionization chamber are given in Fig. 2. This type of design provided for large effective counting volume. The large depth obtainable with this arrangement appeared desirable in view of neutron scattering from all sections along the inner paraffin wall. This chamber was filled to 1 atmosphere with BF_3. At this pressure a collecting potential of 1400 volts gave good uniformity in the size of pulses observed on a cathode-ray oscillograph.

The lead (or copper) block, placed between the neutron source and ionization chamber as indicated in Fig. 1 served to reduce disturbance caused by γ-radiation from the sources employed, and to scatter some of the fast neutrons originally directed toward the chamber into the paraffin. Replacement of the lead block by layers of paraffin of various thicknesses gave a marked diminution in the number of neutrons counted. This decrease in sensitivity was found to be more rapid for sources of neutrons of lower energies. Fig. 3 depicts the variation in counting efficiency with thickness of paraffin interposed between the source and ionization chamber for two different neutron sources. These were Be+Th(C+C′) and A+Rn, the latter reaction having been recently observed in this laboratory and known to represent a source of neutrons of considerably lower energy than that of the Be+Th(C+C′) combination. It was also noted that without any paraffin between the source and chamber, the variation of detection sensitivity with position of the neutron source was not appreciable over the distance of separation implied in the above experiments. Thus the cylindrical paraffin block acts to concentrate the neutrons emitted from the source into a beam of slow ones, hence emphasizing the role of back scattering and accounting in part for the high detection sensitivity noted with this arrangement. These observations are in accord with those of Hopwood and Chalmers[12] and of Fink[9] in connection with the neutron "howitzer."

Frequent checks on the detection sensitivity of the entire arrangement (i.e., amplifier and recording circuit included) were made with radioactive sources of known activity by counting neutrons emitted from a standard Be target. This factor remained constant during the course of the present work. Some idea of the large sensitivity obtainable with this type of apparatus may be gained from the fact that, using air (N_2) as a target in the hemispherical container to be described later, on the average at least one neutron out of every 1000 emitted in the reaction

$$_7N^{14}+{}_2He^4\rightarrow{}_9F^{17*}+{}_0n^1$$

could be recorded.

The amplifier and recording circuit were of conventional design after Wynn-Williams and Ward[13] and Dunning.[14] Since the counting rates dealt with did not exceed 50 per minute, a simple self-extinguishing thyratron circuit with a "Cenco" high impedance counter gave satisfactory results in recording disintegrations.

In view of the small yields from D_2, considerable effort was spent in reducing the ionization chamber background. The final figure attained was 1.4 counts per minute, and this reading was found to be duplicated day after day.

B. Radioactive sources

Two types of sources, namely the active deposits of thorium and of radium were employed. These were collected on 9 mm silver buttons by the recoil method.

Determination of the alpha-ray activities of these sources was effected by directly counting with a small proportional counter the number of alpha-particles emitted in a small solid angle per

[12] F. L. Hopwood and T. A. Chalmers, Nature **135**, 341 (1935).
[13] C. E. Wynn-Williams and F. A. B. Ward, Proc. Roy. Soc. **A131**, 391 (1931).
[14] J. R. Dunning, Rev. Sci. Inst. **5**, 387 (1934).

unit time. The method of employing a γ-ray electroscope and standard radium source was open to the criticism that considerable radioactive material might be deposited on the back side of the button, this portion not being useful for transmutation purposes in the target arrangement adopted.

Although source strengths are given in millicuries, it is to be noted that the final cross sections are free from any error caused by inaccuracy in expressing activities in this unit.

The sources of radium active deposit were usually of from 10 to 15 millicuries initial strength, while sources of Th C′ particles generally did not exceed one millicurie. The subsequent data imply that strengths of the latter type sources are given in terms of the 8.6 cm particles, since Th C (4.8 cm) alpha-particles also present contribute very little or not at all to neutron yields from nitrogen and deuterium, respectively.

All the sources were found to exhibit what appeared to be a weak neutron emission. With the detection system already described, a source placed in an evacuated copper or silver container resulted in a noticeable increase in the chamber background. With air in the ionization chamber, this effect was not noted, and, hence, it is unreasonable to attribute it to instantaneous accumulations of ionization caused by secondary β-rays. In any case, with the lead block between the source and ionization chamber, the γ-radiation produced negligible disturbance. This spurious activity appeared to be greater (per millicurie of alpha-activity) for sources of Th C′ particles than for radium active deposits, and in each case depended somewhat on the surface conditions of the buttons employed for collection. For thorium active deposit on silver, the effect amounted to about one count per minute per millicurie. Considerations in regard to the stability of nuclei indicate that the spontaneous emission of neutrons is unfavorable. This and further experiments led to the conclusion that the background activity must be attributed to such factors as contamination of the surface of the source button by light elements, thus giving rise to neutron emission under the alpha-particle bombardment.

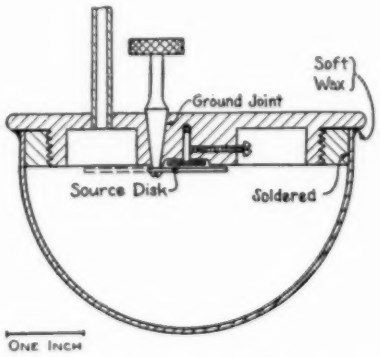

FIG. 4. Deuterium container.

C. Target arrangements

Preliminary experiments with targets of $Ca(OD)_2$ and D_2O indicated the small magnitude of the neutron yield from deuterium by alpha-particles, and emphasized the need of using deuterium in as pure a form as possible in order to be certain of results. The use of the gaseous form also had the advantage that a more direct comparison between the yields from deuterium and nitrogen was possible.

The final arrangement for bombardment is shown in Fig. 4. The source of alpha-particles was located at the center of curvature of the 5.5 cm radius copper container. With D_2 at 76 cm pressure, the total absorption for the alpha-particles was 1.2 cm air equivalent. This factor is not in general correct for all angles since a point source was not employed. Errors introduced in this respect are unimportant in view of the small absorption of the target. This arrangement allowed approximately a solid angle of 2π for bombardment. It seemed that 1.2 cm absorption was a reasonable compromise between the magnitude of the yield convenient for detection and spread in alpha-particle energy. Furthermore, with this absorption the nuclear photo-effect should result in a negligible contribution to the neutron yield.

In order to avoid the difficulty introduced by the stray neutron background associated with the radioactive sources, the arrangement was fitted with a ground joint such that, from the exterior, a thin copper plate could be turned over the source. The thickness of this plate was sufficient to stop all alpha-particles. Thus, this device enabled background counts to be conveniently recorded without removing the D_2 each time such a count was desired.[15]

[15] W. J. Henderson and L. N. Ridenour (Phys. Rev. **52**, 40 (1937)) have recently observed the emission of neutrons

D. Experimental procedure

With a given source, counting was done over periods with the source button alternately exposed to D_2 and covered by the copper absorber. The same procedure was adopted in obtaining yields from nitrogen by bombarding air at 17 cm pressure. At this pressure air gives approximately the same absorption as D_2 at atmospheric pressure.

The time intervals referred to above in which counting was done, were chosen of such length (depending upon the kind of source used) that over each such interval the decay curve of the source could be closely approximated by a straight line. Thus, with this procedure, correction for course decay was easily carried out by using strengths appropriate to the midpoints of these counting periods.

III. Results

The data obtained are summarized in Table I, and the total numbers of counts actually recorded are given in Table II. In the latter table R_α denotes the maximum air range of the alpha-particle in the target substance, i.e. $R_\alpha=0$ for example refers to background recordings. Thus,

Table I. *Net yields from* D_2 *and from air in number of counts per minute per millicurie.*

Source	Target D_2 (76 cm)	Target air (17 cm)
Ra C′	0.32	1.75
Th C′	0.77	2.46

Table II. *Total counts.*

Source	R_α	Target D_2 (76 cm)	Target air (17 cm)
Ra C′	0	1928	609
	6.9	2436	1343
Th C′	0	3115	806
	8.6	3937	1251

from Cu under bombardment of 7–8 Mev alpha-particles from a cyclotron. The use of Cu in the target arrangement just described, however, introduced no difficulty in the present case, since control experiments showed that the yield from this element was not detectable above the natural chamber background.

taking into account the amount of nitrogen present in air, the observed yields from a N_2 target of 1.2 cm absorption would have been 2.18 and 3.08 counts per minute per millicurie for Ra C′ and Th C′ particles, respectively. These data in all represent about 70 hours of recording.

In obtaining cross sections for deuterium, the data of Fahlenbrach[6] on the absolute neutron yields from nitrogen under alpha-particle bombardment have been applied. Fahlenbrach has investigated the reaction

$$_7N^{14}+{}_2He^4\rightarrow{}_9F^{17*}+{}_0n^1$$

by observing the positron emission from radioactive $_9F^{17*}$. Using his excitation curve, one finds the mean cross section $\bar{\sigma}$ for N^{14} in the range interval 5.7 to 6.9 cm is 3.8×10^{-26} cm^2, which corresponds to a range of alpha-particle of 6.3 cm.

Now the effective cross section for transmutation may be defined by

$$\sigma(E)=(dp(E)/dx)(1/N), \tag{1}$$

where $dp(E)$ is the probability of a transmutation occurring as a result of bombardment by a particle of kinetic energy E when this particle traverses a layer of thickness dx of the substance bombarded. N is the number of atoms per unit volume of the target material. If it is desirable to employ range interval rather than actual thickness, then

$$\begin{aligned}\sigma(E)&=(dp(E)/dR_s)(1/N)\\&=(b/N)(dp(E)/dR_b)\end{aligned} \tag{2}$$

where R_b and R_s are the ranges of particles in the target and in standard air, respectively. The quantity b is defined by $R_s=bR_b$ and N has the same significance as in the preceding relation. Under the conditions of the present experiment where essentially a "thin" target has been employed, it is sufficiently accurate to use $\Delta p(E)/\Delta R_s$ instead of the differential expression above. In this case, the value of σ obtained will be the mean effective cross section appropriate to the midpoint of the interval ΔR_s (1.2 cm).

Thus, from an experimental determination of X, the ratio of the neutron yield from D_2 to that from N_2 under identical conditions, and from a knowledge of $\bar{\sigma}_N$, the mean cross section for nitrogen, $\bar{\sigma}_D$ for deuterium may be obtained

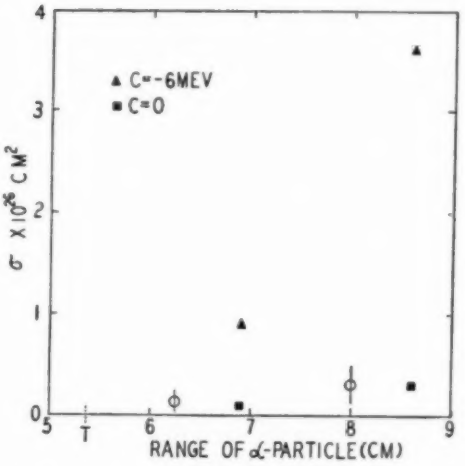

FIG. 5. Comparison between experimental and theoretical (after Massey and Mohr) cross sections. Circles denote experimental values. The theoretical points are for two values of C (the average alpha-particle deuteron interaction).

by application of the relation

$$\bar{\sigma}_D = \bar{\sigma}_N \cdot X \cdot (p_{N_2}/p_{D_2}), \qquad (3)$$

an immediate consequence of Eq. (1) or (2). p_{N_2} and p_{D_2} are the pressures of N_2 and D_2, respectively, as used in the hemispherical target arrangement. Therefore, for the alpha-particle range interval 5.7 to 6.9 cm, $\bar{\sigma}_D$ is 0.12×10^{-26} cm^2 corresponding to a range of 6.3 cm.

Rather than rely entirely upon Fahlenbrach's results for higher energies, the method that was adopted in obtaining $\bar{\sigma}_N$ for the range interval 7.4 to 8.6 cm is as follows:

The ratio of the neutron yield from N_2 in the range interval 7.4 to 8.6 cm and the yield in the interval 5.7 to 6.9 cm was multiplied by $\bar{\sigma}_N$ corresponding to 6.3 cm range of alpha-particle. This procedure gives a good approximation to $\bar{\sigma}_N$ at the alpha-particle range 8.0 cm, this value being 5.4×10^{-26} cm^2. (This is in agreement with the value obtained by extrapolating Fahlenbrach's curve to 8.6 cm range.) Finally $\bar{\sigma}_D$ appropriate to 8.0 cm range may be calculated in the same manner as that used in obtaining $\bar{\sigma}_D$ at 6.3 cm with the result $\bar{\sigma}_D = 0.30\times10^{-26}$ cm^2 at 8.0 cm.

Haxel[16] has also given cross sections for the emission of neutrons from nitrogen under alpha-particle bombardment. These values are somewhat smaller than the corresponding ones employed in making the above calculations for deuterium. However, these data do not appear to be as complete as those published by Fahlenbrach; moreover, some preliminary experiments on nitrogen with the present apparatus give a form of excitation function more in agreement with that of the latter worker. Thus, it seemed desirable to apply the results of Fahlenbrach in obtaining the cross sections for deuterium. However, the results so calculated probably represent upper limits, particularly if both sets of data on nitrogen are considered.

Theoretical cross sections of σ_D as given by the treatment of Massey and Mohr are plotted in Fig. 5. Each point implies the value 2.2 Mev as the binding energy of the deuteron. The two sets of points indicated are for two assumed values of C (the average alpha-particle deuteron interaction). Circles are used to represent the experimental values of σ_D on the same diagram, and estimated experimental errors in these values are given by vertical lines through these points. T denotes the threshold range for the reaction.

IV. Discussion

The data obtained definitely establish a neutron yield when deuterium is bombarded by the fast alpha-particles of Ra C′ or of Th C′. An explanation of the emission of neutrons from deuterium in terms of a reaction involving the capture of the alpha-particle is probably excluded in view of existing information concerning mass defects in the lighter nuclei.

Obviously, the number of experimental points obtained is much too small to permit any very definite conclusions about the excitation function for the process in question. Nevertheless, these points taken in conjunction with the threshold range value corresponding to an alpha-particle energy of 6.6 Mev, necessary for the reaction to begin, lie on a smooth curve, and thus suggest a reasonable excitation function.

The validity of the comparison method employed in obtaining cross sections may be questioned in view of possible variation of detection sensitivity with neutron energy. However, since the two reactions involved are no

[16] O. Haxel, Zeits. f. Physik **93**, 400 (1934–35).

doubt quite similar as regards the energies of the emitted neutrons, it seems reasonable to assume that no serious difficulty exists in this respect.

It will be observed from Fig. 5 that the experimental points agree best with the theoretical values for C assumed zero. However, on the basis of the picture underlying these calculations $C \sim 0$ is hardly reasonable because of the stability of Li^6. In the final analysis, the disagreement between the present results and the work of Massey and Mohr is not to be regarded as serious, since it is now well known that calculations based on a simple potential well are not to be trusted.

In conclusion, it is a pleasure to thank Professor A. F. Kovarik for much helpful discussion and advice throughout the course of this work. The writer also wishes to express his appreciation to Dr. E. C. Pollard for discussion and technical assistance.

APRIL 15, 1938 PHYSICAL REVIEW VOLUME 53

The Gamma-Radiation from Boron Bombarded by Protons

W. A. FOWLER, E. R. GAERTTNER* AND C. C. LAURITSEN
W. K. Kellogg Radiation Laboratory, California Institute of Technology, Pasadena, California

(Received January 28, 1938)

Employing a Wilson cloud chamber we have determined the distribution in energy of pairs and recoil electrons ejected from lead and carbon laminae by the gamma-radiation from boron bombarded by protons. Both the pair and electron distributions indicate three prominent gamma-ray components at 4.3 ± 0.3 Mev, 11.8 ± 0.5 Mev, and 16.6 ± 0.6 Mev with relative intensities of 1 : 1 : 1/7, respectively. The radiation is believed to result from proton capture by B^{11} to form an excited state of C^{12} which radiates in a single transition to the ground state or in a double transition through the well-known intermediate state at 4.3 Mev. Resonance in the yield has been found only in the region 150→200 kv and the total yield of quanta per incident proton above resonance on a thick boron target is estimated to be $\geq 5 \times 10^{-10}$.

TWO previous communications from this laboratory[1] have described in some detail improvements in the method of determining the energy of gamma-rays from cloud chamber studies of the secondaries produced by these radiations. These improvements essentially involved the elimination as far as possible of secondaries of uncertain origin by proper collimation of the gamma-ray beam and by the use of stereoscopic photographs. Only those secondaries originating in a thin lamina placed within the cloud chamber were employed to determine the gamma-ray energies.[2] This improved method was first used in studies of the radiation from $Li^7 + H^1$ and $F^{19} + H^1$. We have recently extended the observations to the radiation from boron bombarded by protons. The original results concerning the radiation[3] had indicated a complex distribution of electrons extending up to 13 Mev with greatest intensity below 4 Mev and groups of electron-positron pairs near 10 and 14.5 Mev. It will be seen that these results are not in contradiction with those reported here if due allowance is made for the lower resolving power in the original experiments.

Because of the low intensity of the radiation from $B + H^1$ some slight modifications were made in the experimental arrangement described in the first reference. In order to have the target as close as possible to the secondary emitters the length of the lead collimator was reduced from 18 to 10 cm and the target tube was located adjacent to the Helmholtz coils surrounding the

---

* National Research Fellow.

[1] Delsasso, Fowler and Lauritsen, Phys. Rev. **51**, 391, 527 (1937).

[2] See also Richardson and Kurie, Phys. Rev. **50**, 999 (1936); Gaerttner and Crane, Phys. Rev. **51**, 49 (1937); **52**, 583 (1937); Kruger and Green, Phys. Rev. **52**, 773 (1937).

[3] Crane, Delsasso, Fowler and Lauritsen, Phys. Rev. **48**, 102 (1935).

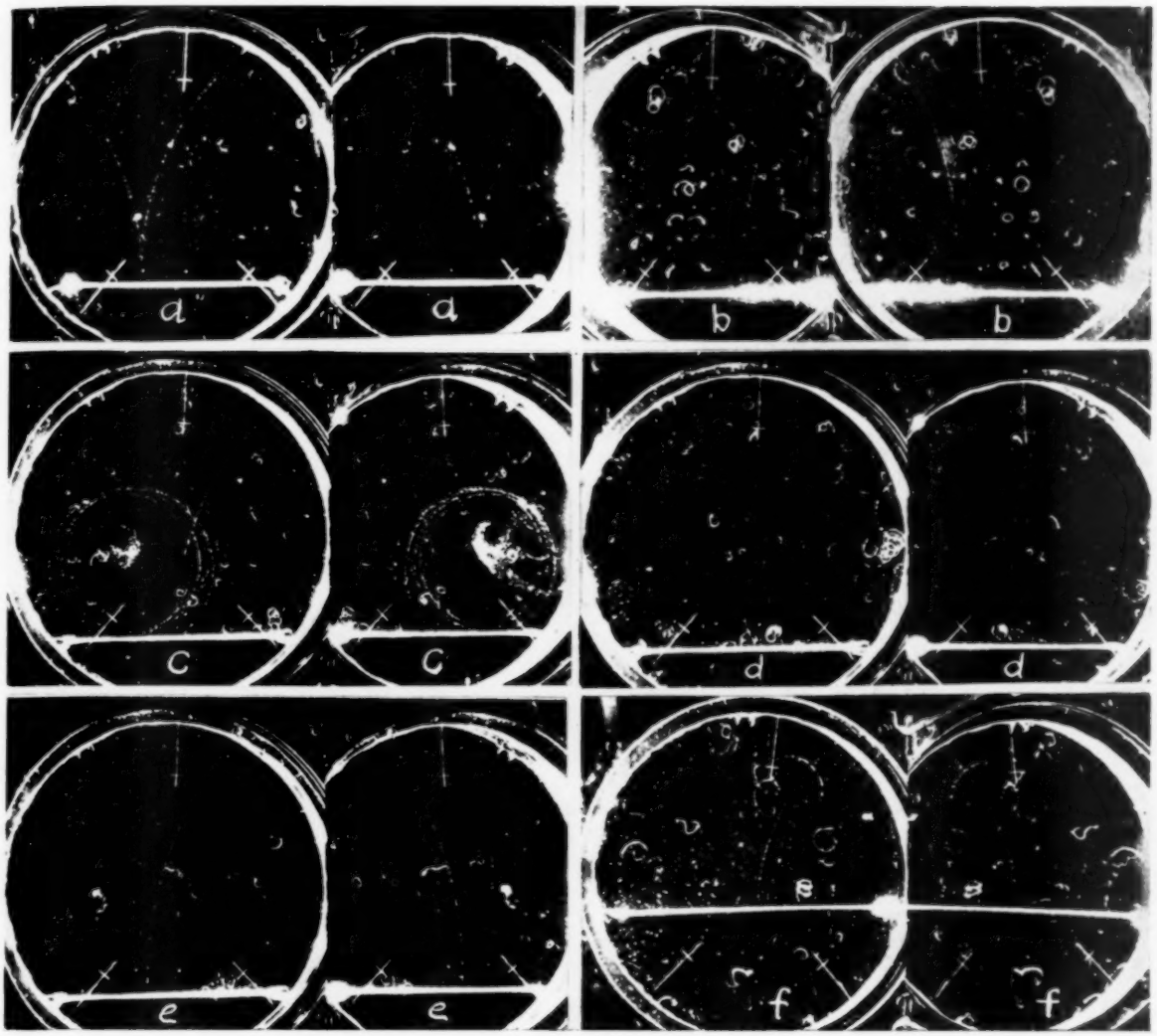

FIG. 1. Stereoscopic views. *a*, A 15.6 Mev pair ejected from a 1.00 mm lead foil by the gamma-radiation from $B+H^1$ (500 kv). The negative pair member bending toward the intersection of the two views has 7.0 Mev kinetic energy while the positive member has 7.6 Mev kinetic energy. Magnetic field = 2000 gauss. *b*, A 16.1 Mev pair (negative has 9.5 Mev, positive has 5.6 Mev) originating in the air-alcohol vapor within the cloud chamber. $B+H^1$ (900 kv). 2500 gauss. *c*, A 10.8 Mev pair (negative has 7.9 Mev, positive has 1.9 Mev) ejected from a 0.33 mm lead foil by the radiation from $B+H^1$ (900 kv). 2500 gauss. *d*, A 4.2 Mev pair (negative has 1.4 Mev, positive has 1.8 Mev) ejected from a 0.33 mm lead foil by the radiation from $B+H^1$ (900 kv). 2500 gauss. *e*, An 11.7 Mev electron ejected from a 0.33 lead foil by the radiation from $B+H^1$ (900 kv). 1500 gauss. *f*, A 4.0 Mev electron ejected from a 1.2 mm carbon lamina by the radiation from $B+H^1$ (900 kv). 1500 gauss.

chamber. The secondary emitters were a 0.33 mm lamina of lead (18,000 photographs) and a 1.2 mm lamina of carbon (4000 photographs). The theoretical average energy loss by collision for electrons of energy between 2 and 20 Mev is approximately 0.4 Mev for the lead and 0.5 Mev for the carbon lamina.

The accelerating tube was operated at 850 to 900 kilovolts peak voltage while the total current was about 20 microamperes during the chamber expansion. The ion beam was not magnetically analyzed and therefore some of the low energy radiation might be attributed to boron bombarded by deuterons. However, deuterium gas had not been used in the tube for several months previous to these observations and it is thus certain that the deuterium contamination did not exceed one part in several

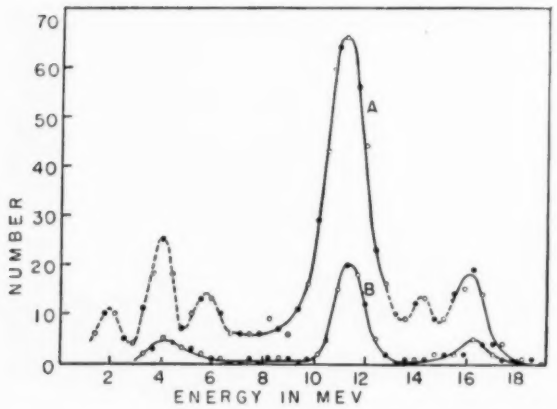

FIG. 2. Curve *A*, the distribution in energy (kinetic plus 2 mc^2) of 347 pairs ejected from a 0.33 lead foil by the radiation from B+H^1 (900 kv). The points have been connected by broken curves in regions where the nature of the curve is somewhat doubtful because of low resolving power and large statistical fluctuations. Curve *B*, the distribution in energy of the 68 most distinct and most accurately measured pairs from curve *A*. In both curves energy intervals of 0.77 Mev overlapping by one-half their width have been used.

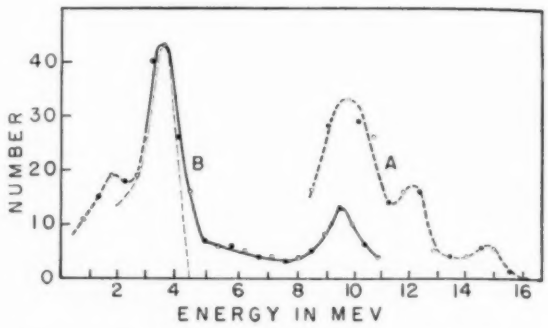

FIG. 3. Curve *A*, the distribution in kinetic energy of recoil electrons ("single" negative electron distribution minus "single" positive electron distribution) ejected from a 0.33 mm lead foil plotted in overlapping 1 Mev intervals. Curve *B*, the distribution in kinetic energy of 177 single electrons ejected from a 1.22 mm carbon lamina plotted in overlapping 0.9 Mev intervals. The superimposed dotted curve indicates the theoretical shape of the distribution in energy of electrons produced in a 1.2 mm carbon lamina by a gamma-ray of 4.3 Mev energy (same energy interval).

thousand. As the radiation is about one-fiftieth to one-tenth as intense as that from B+H^2, less than five percent of the observed tracks can be due to this source. Thick targets of pure amorphous boron (Eimer and Amend) were employed and were frequently replaced. Such targets have not been found to emit disintegration particles characteristic of transmutations involving lithium or fluorine, the only elements showing a greater yield of gamma-radiation under proton bombardment. We feel that practically all the radiation observed must be attributed to boron bombarded by protons.

The measurement of tracks on the cloud chamber photographs was carried out independently by two observers and the results presented represent the average of their separate data. In all cases the data have been plotted as the number of secondaries observed in equal energy intervals separated by one-half the interval width. The two sets of points so secured are indicated by open and full circles in the accompanying figures. The points have been connected by broken curves in regions where the nature of the curve is somewhat doubtful because of low resolving power and large statistical fluctuations. Examples of the cloud chamber photographs are shown in Fig. 1.

ENERGY OF THE GAMMA-RADIATION

Curve *A* of Fig. 2 shows the distribution in energy (kinetic plus 2 mc^2) of 347 pairs ejected from the 0.33 mm lead foil. Of these pairs 234 were secured with the foil located 2 cm from the center of the chamber and with a magnetic field of 1700 gauss while the remaining 113 were secured with the foil located 5 cm from the center of the chamber and with a field of 2580 gauss. Of the pairs secured under the latter conditions, 68 were selected for particular distinctness and as representing those most accurately measured, and have been plotted as curve *B* in Fig. 2. In both curves the energy interval is 0.77 Mev.

Curve *A* of Fig. 3 shows the distribution in kinetic energy of recoil electrons ejected from the 0.33 mm lead foil plotted in 1.0 Mev intervals. The magnetic field was 1700 gauss, and as the foil was located only 2 cm from the center of the 15 cm chamber, tracks originating in the scatterer could be distinguished from traversals originating in the chamber wall. The large angle subtended by the target at the foil made it possible to eliminate only those tracks making an angle greater than 30° with the incident radiation. This failure, however, seriously reduces the resolving power of the method only for radiation below 3 Mev energy.

To secure the distribution in energy of the recoil electrons the number of single positrons

observed in any interval has been subtracted from the number of observed single electrons. This procedure is based on the assumption that none of the "observed" positrons are electrons originating in the glass walls of the chamber and terminating in the lead lamina and that all are members of pairs, the negative member of which was stopped or greatly scattered in the lead lamina. It is further assumed that an equal number of single electrons is observed because of the stopping or scattering of positive members of some pairs. In the high energy region this is a feasible procedure as the number of single positrons is approximately 10 percent the number of single electrons and it is entirely reasonable that the low energy electrons associated in pairs with that number of positrons should have been completely absorbed in the lead foil. Even so, curve *A* of Fig. 3 is subject to the large statistical fluctuations in the number of single positrons and hence is represented by a broken line connecting the observed points. In the low energy region the number of single positrons was almost one-half the number of single electrons, and the difference curve was not considered to be at all trustworthy. It is well to point out in this connection that the number of single positrons observed seems to exceed somewhat the number for which the associated negative pair member should be completely absorbed in the lead foil or scattered at a very large angle, and that the origin of these low energy unassociated positrons is not entirely clear. When collimation is employed and stereoscopic photographs are taken few such single positrons appear to originate in carbon or aluminum laminae of equivalent stopping power and hence not all of those observed with lead laminae can be electrons terminating in the lead. It remains however for more definite experiments to clear up this difficulty. In order to investigate the low energy end of the spectrum more carefully we used the 1.2 mm carbon lamina and found 177 measurable tracks which are plotted as curve *B* of Fig. 3 in 0.90 Mev intervals.

From these curves the radiation can be seen to consist of at least three components at 16.6 ± 0.6, 11.8 ± 0.5, and 4.3 ± 0.3 Mev as tabulated in Table I. The energies of the two high energy components are determined most accurately from the pair distributions. The maxima in this distribution correspond to pairs originating in the center of the lead foil and as each member of the pair loses energy before emerging from the foil, the gamma-ray energy is given by adding the equivalent foil thickness in energy units, namely 0.4 Mev, to the energies at which the maxima occur. Only the ionization energy loss is added as the radiative loss will merely introduce a small increase in the lower energy side of a given group of pairs. The positions of the maxima were taken as an average of the positions given by curves *A* and *B*, Fig. 2. The component at 11.8 Mev has a width at half-maximum of 1.8 Mev all of which can be attributed quite reasonably to the sources of error inherent in this method.[1] From theoretical considerations the natural width of nuclear gamma-rays is very small and our results give no evidence that this is not true for the radiation discussed in this paper.

The existence of a component at 4.3 ± 0.3 Mev is most clearly demonstrated by Fig. 3, curve *B*, where the superimposed dotted curve indicates the theoretical shape[2] of the distribution in energy of electrons produced in a 1.2 mm carbon sheet by a gamma-ray of 4.3 Mev energy. The higher energy recoil electron distribution is as consistent with the pair curves as can be expected in view of the large radii of curvature of the tracks measured (20 to 30 cm).

It is apparent that neither the pair nor the

TABLE I. *Relative intensities of the three main components of the gamma-radiation from* $B+H^1$. *(π = pair formation cross section; σ = Klein-Nishina cross section).*

Gamma-Ray Energy	Relative Pair Intensities	Relative π	Corrected Values		Relative Recoil Intensities	Relative σ	Corrected Values	
			For π	Final			For σ	Final
16.6 ± 0.6	0.2	1.3	0.16	<0.16	0.1	0.85	0.12	>0.12
11.8 ± 0.5	1.0	1.0	1.0	1.0	1.0	1.0	1.0	1.0
4.3 ± 0.3	0.25	0.35	0.7	>0.7	3.5	2.25	1.5	<1.5

recoil electron curves are completely accounted for by the theoretical expectations based on the three components in Table I. To account completely for the curves with the calculated distributions it is necessary to assume the existence of weak components at roughly 2.5, 6.0 and 14.5 Mev. Much more extended observations will be necessary to establish definitely the existence and energy of these components. Indications of a 6.0 Mev component were not obtained consistently so that the pairs near this energy in curve *A*, Fig. 7, may be due to some contamination, possibly fluorine.

The Relative Intensities of the Gamma-Ray Components

Estimates of the relative intensities of the gamma-ray components made from both the pair and recoil electron curves are given in Table I. In estimates from the pair curve, the relative number of pairs thought to be due to the three main components has been computed and corrected for the variation in pair formation cross section with energy.[4] The relative intensity of the 4.3 Mev component must be greater than the value secured by making this simple correction because of the relatively greater loss of low energy members of pairs produced by this line by absorption and scattering in the lead lamina. A not unreasonable increase of 40 percent will make the intensity of this component equal to that of the 11.8 Mev component. In the case of recoil electrons a correction for the Klein-Nishina cross section[4] has been applied. As most of the recoils lie within a cone about the direction of the incident radiation which is smaller than the angle subtended at the secondary emitter by the target, the total cross section for the production of recoils has been employed. The relative loss of recoil electrons from 4.3 and 11.8 Mev radiation is not nearly as marked as the relative loss of pairs from such radiations. To make even fairly accurate measurements of the high energy recoils at 1500 gauss required very distinct and sharp tracks traversing the full length of the chamber. For this reason the relative intensity of the 4.3 Mev component must be somewhat lower than the result given by the simple Klein-Nishina correction. It is thus seen that the recoil electron and pair data agree to within a factor less than 2. The 16.6 Mev component is roughly 15 percent as intense as the 11.8 Mev component, while the 4.3 Mev component, neglecting the secondaries near 2.5 and 6.0 Mev, is approximately equal in intensity to this component.

The Origin of the Radiation

The only transmutation involving either of the two isotopes of boron under proton bombardment which on the basis of the conservation of energy can result in the production of the two high energy components of the observed radiation is

$$B^{11}+H^{1}\rightarrow(C^{12})\rightarrow C^{12}+h\nu. \qquad (1)$$

The difference between the doublet $B^{11}H^{1}-C^{12}$ is given by Bainbridge and Jordan[5] as 17.14 ± 0.10 thousandths of a mass unit corresponding to a difference on the energy scale of 16.0 ± 0.1 Mev.

Reasons will be advanced in a later section of this paper for believing that the excited state of C^{12} from which the observed radiation originates corresponds to the resonance at 180 kv observed in the excitation function for the gamma-rays from $B^{11}+H^{1}$ by Bothe and Gentner.[6] This excited state of C^{12} thus differs from the ground state by 16.2 ± 0.1 Mev.

The energy of the most energetic component of the observed radiation (16.6 ± 0.6 Mev) is in agreement with this difference and thus substantiates the existence of the capture process implied in reaction (1). The 11.8 ± 0.5 Mev component must result from at least a double radiative transition to the ground state of C^{12} and as the 4.3 ± 0.3 Mev component is of equal intensity within the experimental errors, it seems reasonable to associate the two lines in such a double transition yielding 16.1 ± 0.6 Mev as the total transition energy, again in agreement with the energy difference calculated from the masses. The position of the intermediate excited state of C^{12} is not uniquely determined but it is most reasonable to place the level at 4.3 Mev as the

[4] See *Quantum Theory of Radiation* by Heitler, pp. 158, 200.

[5] Bainbridge and Jordan, Phys. Rev. **51**, 385 (1937).
[6] Bothe and Gentner, Zeits. f. Physik **104**, 684 (1937).

existence of such a level has been established in the reactions

$$N^{14}+H^{2}\rightarrow C^{12}+He^{4}, \quad (2)$$

where alpha-particle groups differing by 4.3 Mev have been observed[7] and in

$$B^{11}+H^{2}\rightarrow C^{12}+n^{1}, \quad (3)$$

$$Be^{9}+He^{4}\rightarrow C^{12}+n^{1}, \quad (4)$$

where neutron groups differing by 4.4 Mev have been observed.[8] Gamma-radiation with energy from 4.3 to 4.4 Mev has been found to accompany these reactions.[9]

A reaction similar to (1) involving B^{10}

$$B^{10}+H^{1}\rightarrow(C^{11})\rightarrow C^{11}+h\nu \quad (5)$$
$$\downarrow$$
$$B^{11}+e^{+}$$

has been suggested by Crane and Lauritsen[10] to account for the production of positron active C^{11} (20 min.) when boron is bombarded with protons. The mass difference of the doublet $B^{10}H^{1}-B^{11}$ is given by Bainbridge and Jordan[5] as 11.60 ± 0.10 thousandths of a mass unit corresponding to 10.8 Mev and the positrons have been found[10] to have an observed maximum energy of 1.1 ± 0.1 Mev. The energy available for radiation is thus 8.7 Mev. The yield found by Crane and Lauritsen[10] at 900 kv peak corresponds to 10^{-11} to 10^{-10} positrons per incident proton while Allison[11] was unable to find any effect at 500 kv and set an upper limit for the yield at 10^{-12} positrons per proton on pure B^{10}. The resonance voltage for reaction (5) must thus be above 500 kv.

The absolute yield of the observed radiation will be shown in a later section to be at least 5×10^{-10} quanta per incident proton above resonance. Since the yield per proton at 900 kv for reaction (5) is less than this and since the resonance occurs above 500 kv as compared to 180 kv for the observed radiation it is not surprising that with alternating voltage and a beam containing molecular as well as atomic ions we do not obtain any definite indication of radiation near 8.7 Mev. Part of the observed radiation below 8.7 Mev may be attributed to (5) and it will remain for experiments with targets of the separated isotopes to solve this particular problem.

The Excitation Function

It is of primary importance in arriving at some understanding of capture reactions similar to (1) to determine the energy of the excited nuclear states from which the various components of the radiation arise. In the majority of cases the energy breadth of these states is small compared to the range of the bombarding voltages available and thus an excellent measure of the energy of the states is secured by the determination of the voltages at which resonance occurs in the excitation function for the radiation. To complete the observational details, the measurement of the resonance voltage and breadth must be supplemented by an analysis of the structure and absolute intensity of the radiation due to the resonance in question. In this way complete information concerning the energy values of the excited states of various nuclei and their transition probability for radiation to lower states will be secured. There can be little doubt that such information is necessary in reaching an understanding of nuclear structure.

In the case of the radiation from boron bombarded by protons the existence of two resonances in the excitation function has already been established. Using accelerating voltages up to 500 kv Bothe and Gentner[6] found a resonance effect at 180 kv and no effect of comparable magnitude at any other voltage except 360 kv where the molecular ions produced by their ion source became effective for the 180 kv resonance. The existence of resonance at 820 kv has been found by Herb, Kerst and McKibben.[12] The intensity of the radiation which they observed at voltages below 820 kv was so small that lower resonances would probably have escaped detection.

[7] Lawrence, McMillan and Henderson, Phys. Rev. **47**, 273 (1935); Cockcroft and Lewis, Proc. Roy. Soc. **154**, 261 (1936).

[8] Bonner and Brubaker, Phys. Rev. **50**, 308 (1936); Bernardini and Bocciarelli, Accad. Lincei, Atti. **24**, 132 (1936).

[9] Crane, Delsasso, Fowler and Lauritsen, Phys. Rev. **48**, 484 (1935); **46**, 1109 (1934); Bothe, Zeits. f. Physik **100**, 273 (1936).

[10] Crane and Lauritsen, Phys. Rev. **45**, 497 (1934); **48**, 103 (1935); Fowler, Delsasso, and Lauritsen, Phys. Rev. **49**, 561 (1936).

[11] Allison, Proc. Camb. Phil. Soc. **32**, 179 (1936).

[12] Herb, Kerst and McKibben, Phys. Rev. **51**, 691 (1937).

No completely satisfactory answer can be given to the question of which resonances contributed to the radiation discussed in this paper. The difficulties inherent in the interpretation of yield curves secured with alternating voltage tubes, with ion sources giving both atomic and molecular ions, and with thick targets are well known. Observations with the cloud chamber are further complicated by the fact that the ions are quite appreciably deflected by the external magnetic field of the Helmholtz coils. In the experiments described above in which the energy and relative intensity of the radiation was determined the ion tube was operated at its maximum steady peak voltage of from 850 to 900 kv (spark gap determinations) simply to get a large percentage of ions to the target through the magnetic field and to insure a reasonable yield of gamma-rays.

We have made additional observations to compare the variation of yield of the $B^{11}+H^1$ gamma-rays with excitation curves for Li^7+H^1 and for $F^{19}+H^1$ which are known to exhibit resonance effects at 440 and 330 kv, respectively. The radiation from metallic lithium previously exposed to air and calcium fluoride targets bombarded with protons was found to be intense enough to permit the use of a sensitive electroscope in determining the excitation curves. The electroscope was surrounded by 5 cm of lead except on the side toward the target where the thickness of lead was reduced to 1 cm. Readings of 50 to 100 times the background (background $=0.2$ divisions per minute) were secured at the maximum tube voltage available and with currents of 25 microamperes to the target. The yield curve for $F^{19}+H^1$ was found to rise linearly from about 370 to 750 kv peak. A second linear rise of increased slope was found between 750 and 850 kv peak. The excitation curve for Li^7+H^1 rose linearly from about 485 to 850 kv peak. The observed rise for atomic and molecular ions was thus found to occur at peak voltages approximately ten percent higher than the known resonance voltages. A similar yield curve for the Li^7+H^1 radiation was secured by counting the number of high energy secondaries observed per cloud chamber expansion. The radiation from $B^{11}+H^1$ was so weak in intensity that it was not practical to determine its yield curve with the electroscope but data secured from 1500 cloud chamber photographs taken with a magnetic field of 400 gauss revealed no other resonance effects than the expected ones at peak voltages near 200 and 400 kv. Above 700 kv peak the yield was found to increase only slightly, indicating that the resonance effect at 820 kv was not reached at the maximum peak voltage used.

Even before the experiments described above dealing with the yield curves were carried out, it was realized that some information concerning the resonances entering into the production of the radiation from $B^{11}+H^1$ could be gained by determining the energy distribution of the radiation at a lower bombarding voltage than 900 kv peak. Since Bothe and Gentner's investigations extended to 500 kv it was deemed sufficient to repeat the original experiments with voltages of 500 kv and 700 kv peak. On 1500 photographs taken at 500 kv peak and 500 photographs at 700 kv peak, pairs corresponding to all three of the main components in practically the same relative proportions as given in Table I were found. The results of Bothe and Gentner are consistent with these results as they found the recoil electrons produced when their tube was operated at 410 kv to have a "range" corresponding to an energy of 14 Mev in good agreement with intense radiation at 11.8 Mev and weaker radiation at 16.6 Mev.

From the evidence yielded by the excitation curves and from the fact that the energy distribution of the radiation is independent of the voltage it is reasonable to conclude that only the resonance at 180 kv or possibly a weak but so far undetected resonance between 180–500 kv enters into the production of any of the three main components of the observed radiation.

The Absolute Intensity of the Radiation

The importance of determining the absolute intensity of the radiation from capture reactions has been indicated in the beginning of the previous section. One attempt in this direction has been made by Hafstad, Heydenburg and Tuve[13] who concluded from their electroscope determinations that the cross section for the

[13] Hafstad, Heydenburg and Tuve, Phys. Rev. **50**, 504 (1936); Bethe, Rev. Mod. Phys. **9**, 207 (1937); Hafstad and Tuve, Phys. Rev. **48**, 306 (1935).

resonance capture of protons by Li^7 at 440 kv was roughly 10^{-27} cm^2 corresponding to a yield of 7×10^{-10} quanta per incident proton on LiOH (Bethe). The measurements of Bothe and Gentner[6] on the relative yields of the radiation from $B^{11}+H^1$ and Li^7+H^1 then make it possible to determine the absolute yield of that from $B^{11}+H^1$. However, we have felt that a more direct estimate would make it possible to determine the absolute yield somewhat more closely.

On the basis that the only resonance is at a voltage low compared to the peak voltage used in our observations, a fairly reliable estimate of the yield can be made from the number of secondaries observed per cloud chamber expansion for a given target current. Assuming for simplicity that the radiation is emitted isotropically in all directions the number of secondaries (N) is related to the yield of quanta by the relation

$$N=IY_cTC\Omega/4\pi,$$

where I=current to the target, Y_c=yield of quanta per unit current, T=sensitive time of chamber, Ω=solid angle subtended at the target by the secondary emitter, and C=number of secondaries produced per quantum falling on the secondary emitter.

The yield per incident ion in the beam is thus

$$Y_i=2N/ITC\Omega\times10^{-12}$$

if I is measured in microamperes. The integrated yield above resonance per incident proton (Y_p) then can be determined if the atomic and molecular constitution of the beam is known and if the fractions of atomic and molecular ions above their respective resonance voltages are known.

Magnetic analysis of the ion beam revealed that it is composed chiefly of approximately equal numbers of ions corresponding to m/e ratios of $+1$ and $+2$. These components of the beam have been identified as being responsible for the yield increases at 370 and 750 kv peak in the excitation curve for $F^{19}+H^1$. Weak components corresponding to m/e ratios of -1 and $+3$ have also been found. The mass 1 component of negative charge is due to the acceleration during one-half of the alternating voltage cycle of hydrogen atoms which have captured an additional electron. The bands found on the photographic plates secured in the magnetic analysis indicated that the components corresponding to various m/e ratios were composed of ions of all energies with a definite concentration near the maximum voltages (at least 80 percent above one-half the maximum voltage). On the basis that the beam is composed equally of atomic and diatomic ions all of which are above the resonance voltage, a minimum value for Y_p can be secured which is given by $Y_p\geq 2/3Y_i$. In the case of the $B^{11}+H^1$ radiation this minimum value will not be far wrong if the only resonance is at 180 kv as the measurements were made at 900 kv peak. If resonances above 500 kv enter in, contrary to our present belief, then only atomic ions will be effective and the above expression will yield too low an estimate of the yield for all resonances involved.

With a total current of 20 microamperes to the target we have found 0.04 pairs per photograph in the region near 11.8 Mev on the best twenty-five percent of the films taken at 900 kv peak. Although this figure is larger than the average number of pairs found on all films, it probably approaches very closely the actual yield when both the ion tube and cloud chamber were simultaneously operating in the most satisfactory manner. The effective solid angle subtended by the secondary emitter at the target was $\Omega=0.013$ steradians. The number of pairs produced by an 11.8 Mev quantum in passing through the secondary emitter of 0.33 mm of lead is $C=0.015$. The sensitive time of the chamber was found by varying the time of bombardment with respect to the time of chamber expansion. The time from the first appearance of sharp tracks until no tracks appeared was found to be $T=0.06$ seconds. From these data we find $Y_i=3.4\times10^{-10}$ quanta per ion and thus $Y_p\geq 2.3\times10^{-10}$ quanta (11.8 Mev) per proton. The yield for the 4.3 Mev component is also at least 2.3×10^{-10} quanta per proton and that for the 16.6 Mev component at least 0.4×10^{-10} quanta per proton. The total yield of the three main components is thus $Y_p\geq 5.0\times10^{-10}$ quanta per proton.

It is interesting to compare the yields of gamma-rays from $B+H^1$ with the yields of those from Li^7+H^1 and $F^{19}+H^1$. Using a Geiger counter surrounded by 1.5 cm of lead Bothe and Gentner[5] secured 600, 100 and 20 counts per

minute from $LiOH+H^1$, CaF_2+H^1, and $B+H^1$, respectively. These results were secured under different experimental conditions for each target and indicate only the order of magnitude of the relative yields. Using an electroscope surrounded by 1 inch of lead, Hafstad and Tuve[13] found a ratio of ionizations of 0.13 for CaF_2+H^1 and $LiOH+H^1$. Observations made in this laboratory indicate a higher yield from CaF_2+H^1 relative to $B+H^1$ than the ratio of five to one indicated roughly by Bothe and Gentner's results. The yields found for $Li+H^1$ in this laboratory are not trustworthy as the composition of the surface of the target employed was uncertain. In all cases the observed yields must be corrected for the relative response of a counter or electroscope to incident quanta of different energies. In case the secondaries are produced in lead it can be shown that the response is roughly proportional to the energy of the quantum. The theoretical cross sections for pair formation and recoil electron production must be taken into account as well as the range of the pair and recoil secondaries. On this basis the yields from $LiOH+H^1$ and CaF_2+H^1 must be corrected by factors of ~ 2 and ~ 0.5 relative to that from $B+H^1$. The corrected yields are, respectively, 7×10^{-9} and 5×10^{-9} quanta per incident proton.

The yield for $LiOH+H^1$ is much larger than that given by the results of Hafstad, Heydenburg and Tuve, and the source of the discrepancy is not entirely clear. More direct evidence is obviously needed. Our results indicate a gamma-ray breadth of 40 volts for the 440 kv resonance for Li^7+H^1.

In conclusion it is well to point out that the radiative capture of protons by B^{11} is intimately connected with the alpha-particle transmutations occurring when boron is bombarded by protons. The $B^{11}+H^1$ reactions have been discussed by Kalckar, Oppenheimer and Serber,[14] but it is difficult to reconcile their conclusions simultaneously with the energy distribution of the gamma-radiation, with the large yield which we find and with other recent experimental results on these reactions. Further discussion of these difficulties will be found in this issue in an article by Professor Oppenheimer and Dr. Serber.

[14] Kalckar, Oppenheimer and Serber, Phys. Rev. **52**, 279 (1937).

APRIL 15, 1938 PHYSICAL REVIEW VOLUME 53

Note on Boron Plus Proton Reactions

J. R. OPPENHEIMER AND R. SERBER
University of California, Berkeley, California

(Received February 1, 1938)

A discussion of the experimental evidence on the $B^{11}+H^1$ reactions and of the selection rules available for their interpretations shows that it is not possible to obtain a satisfactory description on the assumption that the same resonance level of C^{12} is responsible, both for the 16 Mev γ-ray observed by Fowler, Gaerttner and Lauritsen, and the long range alpha-particles whose angular distribution was determined by Neuert.

THE disintegrations induced when B^{11} is bombarded with protons exhibit certain striking peculiarities. We wish to return to their interpretation in the light of new experimental evidence[1] on the yield and spectrum of the γ-rays observed in these reactions.

The essential findings may be briefly summarized. The most probable reaction involves[2] the emission of short range α-particles, leaving the Be^8 in an excited unstable state (probably ^1D). This reaction shows no resonance,[3] and is accompanied by no observable γ-rays or long range α's. Both the long range α's and the

[1] Fowler, Gaerttner and Lauritsen, Phys. Rev. **53**, 628 (1938).

[2] Dee and Gilbert, Proc. Roy. Soc. **154**, 279 (1936).

[3] Williams, Wells, Tate and Hill, Phys. Rev. **51**, 434 (1937).

γ-rays come from a resonance reaction.[4, 5] The resonance occurs at about 160 kv, and the resonance energy agrees within the experimental uncertainty of 2–3 kv for the two reactions.[6, 7]

Since for neither reaction has another resonance level been observed in the range up to 500 kv, it is natural to ascribe both reactions to the same level of the excited compound C^{12}. The resonance yield of α's from a pure B target is roughly 5×10^{-10};[8] the total yield of γ-rays determined by Fowler and Lauritsen[1] is also 5×10^{-10}.[8]

The long range α-particles are anisotropically distributed,[9] roughly according to a $1+\cos^2\theta$ law (with θ the angle between the direction of emission and the direction of bombardment). The γ-ray spectrum[1] shows three resoluble lines, at 4, 12 and 16 Mev. The first two have equal intensity; the 16 Mev line, which corresponds to transitions to normal C^{12}, is about six times as weak. Fowler and Lauritsen give arguments based on the excitation curves of Bothe and Gentner and their own work to make it plausible that all three γ-rays come from the 160 kv resonance.[1]

It is clear that for the interpretation of these findings selection rules will be essential. The known selection rules which could be invoked are these:

1. A compound nucleus cannot decay into products with vanishing intrinsic angular momentum if it has odd parity and even angular momentum, or even parity and odd angular momentum. This rule offers at first sight a natural explanation[10] of the absence of long range α's in the nonresonance reaction.

2. An odd C^{12} level of vanishing angular momentum can never give three α-particles. These rules, 1 and 2, are strict.

3. A triplet compound state will disintegrate to singlet products at a rate roughly 10^4 slower than a corresponding singlet, because the forces converting spin into orbital angular momentum are small. This argument is naturally invoked[10] to account for the great but not complete stability of the C^{12} resonance level to α-decay. Only singlet and triplet states may be expected when B^{11} is bombarded by protons.[11]

4. Since the Coulomb forces are still small for C, the isotopic spin[12] T may also be a fairly good quantum number, and a level of C^{12} with $T=1$ will disintegrate into products with $T=0$ at a rate reduced by a factor which may be of the order of 10^4 from that of levels with $T=0$. Only levels with $T=0, 1$ will be formed in the reactions considered.

No further relevant selection rules of comparable rigor would seem to follow from known invariance properties of the nuclear system.

The relatively large yield of short range α's shows that this reaction must come predominantly from the capture of s-protons, and the absence of observable resonance indicates that

[4] Bothe and Gentner, Zeits. f. Physik **104**, 685 (1937).
[5] Allen, Haxby and Williams, Phys. Rev. **53**, 325(A) (1938).
[6] We are indebted to Dr. Williams for a further discussion of the experimental results reported in reference 5.
[7] Allen, Haxby and Williams give 10 kv as the observed breadth of the resonance, but it seems (reference 6) not impossible that this is entirely instrumental, and comes primarily from the ripple and unsteadiness of the accelerating voltage of the protons. If one were to accept the observed breadth as real, it would add further serious difficulties to the interpretation; for since the proton breadth of the level must be very small compared to 10 kv, and since γ-radiation competes successfully with α-emission, this would necessitate a γ-ray breadth of the order of several kilovolts. This is larger than any value heretofore observed, and seems particularly implausible for radiation of magnetic dipole or electric quadripole type which, as we shall see, is probably involved in these reactions.
[8] The γ-ray yield is smaller than that from the Li^7+H^1 reaction by a factor of 10–20. If one accepts the absolute radiative field for the Li reaction given by Hafstad, Heydenburg and Tuve (Phys. Rev. **50**, 504 (1936)), one is led to γ-ray yields from the B reaction here considered which are about a tenth of those given by Fowler and Lauritsen. The precise value of the yield will not be important for our argument. In fact the γ-ray breadths of highly excited light nuclei are so difficult to estimate theoretically that our information about them must depend on just such absolute yield measurements as are here involved.
[9] Neuert, Physik. Zeits. **38**, 122 (1937).
[10] Kalckar, Oppenheimer and Serber, Phys. Rev. **52**, 279 (1937).
[11] In a recent letter Landau (Phys. Rev. **52**, 1251 (1937)) has objected to this argument, on the ground that the spin-orbit off-diagonal perturbation energy is not small compared to the spacing of the levels of a sufficiently highly excited sufficiently heavy nucleus. Quite apart from the fact that the "combining" resonance levels of C^{12} would seem to be spaced by several hundred kilovolts, this argument appears to involve a misapprehension, in that it uses an estimate of the magnitude of the matrix elements of the spin-orbit coupling energy based on a "one-body" model, of the level spacing based on a "many-body" model. It would in fact seem that the "average energy denominator" occurring in the perturbation theoretic treatment can hardly be essentially smaller than $\hbar$/collision time, and that the triplet contamination of a singlet wave function can hardly exceed a few percent. Analogous arguments apply to the selection rule 4.
[12] Wigner, Phys. Rev. **51**, 106 (1937). We are indebted to Professor Breit, who in private communications has emphasized the role which might be played by the so-called "partition quantum numbers."

singlet levels, with rapid α-decay rate and Γ_α breadths of the order of hundreds of kilovolts, must be involved. Since normal B^{11} is pretty certainly odd, 1 can be used to explain the absence of long range α's only if the C^{12} involved has even angular momentum; this cannot be zero by 2. We are thus led to assign for the normal state of B^{11} an odd D, G term. The most plausible state seems to be a $^2D_{3/2}$.

The angular dependence of the long range α's shows that the resonance level is formed not by s, but by p or d proton capture. Estimates of the proton breadth, based on correcting the observed breadth of the 440 kv resonance level in the Li^7+H^1 reaction for altered barrier penetrability, give $\Gamma_p \sim 5$ v for p-protons, and about 1/100 of that for d-protons. The observed resonance yields thus show that we have to do with p-capture, and that the minimum possible value for γ-ray and long range α breadth is of the same order as the proton breadth. Since $\Gamma_\alpha < 10\Gamma_\gamma$, it is hard to accept the "observed" breadth of the resonance level, $\sim$10 kv, as real.

The resonance level is then even; its angular momentum i must be 1 or 2, since it gives γ-rays to ^1S of normal C^{12}; and since it gives long range α's we must have $i=2$. The resonance level must therefore be a ^1D, or a $^3P_2$, $^3D_2$, or $^3F_2$. Now the energy[13] of the resonance level differs from that of normal B^{12} by just about what we should expect for the Coulomb energy difference ($\sim$0.002 mu). Since the normal state of B^{12} is the lowest lying term of isotopic spin $T=1$, we should expect[14] the resonance level to be a singlet or triplet P, D or F with $T=1$. The great stability of the level to α-decay would suggest that it is a triplet, so that selection rules 3 and 4 could both be invoked to explain this stability. Since however an even pure triplet $^3P_2$, $^3D_2$, $^3F_2$, cannot combine with the ^1S normal state of C^{12} by γ-radiation, this possibility is excluded. In fact the only triplet which could give the high energy γ-ray with the observed intensity is an even ^3S, which can neither give long range α's nor be formed from a parent B^{11} in a ^2D state by p capture.

The only remaining possibility is that the resonance level is an even ^1D with $T=1$, and that its stability must be understood in terms of the approximate conservation law for isotopic spin. However the angular distribution to be expected for the long range α's, for p capture to ^1D from a $^2D_{3/2,\,5/2}$ parent term of B^{11}, is $\sin^2\theta$, which cannot be reconciled with the observed $1+\cos^2\theta$. It will be seen from Table I that, to obtain an anisotropy even qualitatively in agreement with experiment, we would be forced either to make the resonance level a ^3F, or to make the parent term one of odd L and thus to give up the explanation, in terms of the parity angular momentum selection rule, of the striking absence of long range α's in the dominant s capture reaction.

We have been led to this very unsatisfactory conclusion by the supposition that both the long range α-particles and the 16 Mev γ-rays come from the same resonance level. In this connection it should be emphasized that the yields of long range α-particles and γ-rays have not been adequately investigated in the range above 250 kv. If one assumes, as our arguments perhaps suggest, that the high energy γ-ray comes from a resonance level in this range, and other than that for which the angular distribution of the long range α's has been determined, no unique assignment of the resonance level is possible at present. If this should turn out to be true, one would probably still have some difficulty in reconciling a ^2D parent B with a triplet character for the resonance level.

TABLE I. *Angular distribution of long range α-particles. $c=\cos\theta$, $s=\sin\theta$.*

Resonance State of C^{12}	Normal State of B^{11}				
	$^2P_{1/2}$	$^2P_{3/2}$	$^2D_{3/2}$	$^2D_{5/2}$	$^2F_{5/2,\,7/2}$
^1D	$1+3c^2$	$1+3c^2$	s^2	s^2	$2+c^2$
$^3P_2$	$1+3c^2$	$1+6s^2$	$1+6s^2$	$3+c^2$	
$^3D_2$	$1+3c^2$	1	$3+4s^2$	$4+7s^2$	
$^3F_2$			$1+2c^2$	$1+16s^2$	
$^3F_4$				$3+5c^2$	

[13] We wish to thank Professor Breit for pointing out to us the possible homology of the resonance level and normal B^{12}.

[14] Feenberg and Phillips, Phys. Rev. **51**, 597 (1937).

Spectra of the Monoxides of Cerium and Praseodymium

WILLIAM W. WATSON
Sloane Physics Laboratory, Yale University, New Haven, Connecticut
(Received February 21, 1938)

Vibrational quantum assignments are presented for five sparsely developed emission band systems of CeO and one of PrO. Comparison is made with two known GdO systems (Piccardi) and one LuO system (Watson and Meggers). Nd has no evident oxide spectrum in the flame of the arc, and Meggers and Scribner report none for Yb and Tm. Reasons for the general poor development or complete lack of oxide band systems for a number of the rare earths are discussed. Fairly intense band systems seem to exist only for those rare earths having a *d* electron in their normal configuration.

LITTLE is known about the band spectra of the group of elements from cerium to lutecium, although evidence for the existence of spectra associated with oxide molecules of some of these rare earths has existed for years. Piccardi[1] has given a vibrational quantum analysis of two GdO systems in the blue region of the visible spectrum plus a few isolated band sequences in the orange and red regions. Some of the latter are surely due to impurities such as CaCl. Recently W. F. Meggers and the writer[2] have made an analysis, based on the data of Meggers and Scribner,[3] of a LuO band system. No other analyses of band spectra from rare earth molecules have as yet been reported.

This paucity of data on rare earth molecular spectra is of course in part due to the same difficulties which hinder the analyses of their atomic spectra; impurity of materials, complexity of the term schemes, high multiplicities, etc. In addition there is the probable prevalence of predissociation and the operation of the Franck-Condon principle, both tending to severely delimit the extent of existing band systems. Furthermore, the existence of fairly intense band systems seems to be correlated with the presence of a *d* electron in the normal configuration of the rare earth atom. The rare earths fulfilling this condition are to be found at the beginning, middle (Gd) and end (Lu) of the group.[4] We return to these points below after a brief description of a few regularities in the spectra of CeO and PrO.

Oxide spectra of cerium, praseodymium and neodymium were produced by using as the source a 220-volt d.c. arc between pure silver electrodes on to which appropriate salts were fused. Chlorides of all these elements were used, together with anhydrous CeO_2. Light was taken mostly from the flame of the arc, with constant renewal of the rare earth material during the exposure. Spectrograms covering the range 3500A–8700A were obtained in the first and second orders of a 21-foot grating. The spectrum of the cerium arc contains a large number of bands in the near infra-red from 6600A to 8700A, some of which are quite intense, sharp, single-headed bands degraded to the red. There are in addition some band groups in the blue for which CeO is the indicated emitter. In the praseodymium spectrum there are several fairly prominent band sequences in the interval from 5000A to 6000A, similar in arrangement to the blue CeO systems, but of a doublet character.[5] Both of these, the short wave-length CeO systems and the PrO systems, in turn resemble the GdO band systems described by Piccardi. All of these may represent corresponding transitions in the respective molecules.

The spectrum of the neodymium arc contains no conspicuous bands not assignable to impurities. A background of faint lines, probably molecular in origin, exists in some regions, but a quantum description of these bands is impossible.

[1] G. Piccardi, Gazz. chim. ital. **63**, 887 (1933).
[2] W. W. Watson and W. F. Meggers, Nat. Bur. Stand. J. Research **20**, 125 (1938).
[3] W. F. Meggers and B. F. Scribner, Nat. Bur. Stand. J. Research **19**, 31 (1937).
[4] W. Albertson, Phys. Rev. **47**, 370 (1935).
[5] G. Piccardi, Accad. Lincei Atti **23**, 358 (1936) has reported praseodymium oxide bands in the flame spectrum in this same wave-length range. His dispersion was low, however, and no quantum analysis was presented.

TABLE I. *A system of* CeO *emission bands. cm⁻¹ units.*

v′ \ v″	0	1	2	3	4	5	6
0	12764.9	11906.9					
1	13546.0	12687.9	11830.0				
2	14320.6	13464.6	12611.7	11768.1			
3		14243.1	13388.2	12536.3			
4				13312.7	12463.7	11626.5	
5					13229.2	12393.3	
6							12321.1

TABLE II. *B and C systems of* CeO *bands.*

v′ \ v″	0	1	2	3	v′ \ v″	0	1	2
0	13816.4 13805.1	12957.0			0	13700.1		
1	14601.8	13741.0 13736.5			1	14467.8	13607.5	
2		14522.0	13668.5 13664.6		2		14368.0	13514.0
3			14447.3	13600.4				

CaCl bands in the red are present on all spectrograms when chloride compounds are used in the source, and LaO bands occur in the Pr and Nd spectra. The cerous chloride and ceric oxide (Eimer and Amend) proved to be practically free of the usual lanthanum impurity.

CeO SPECTRUM

Clearly visible among the large number of bands in the near infra-red spectrum of the cerium arc are two sequences, one composed of intense single-headed bands degrading to the red from 7832A, the other a short group of prominent double-headed bands beginning at 7236A and also degrading to the red. At about the proper interval for a monoxide vibrational frequency on both sides of the first sequence there are similar but less intense sequences. This stronger sequence must therefore represent $\Delta v=0$ transitions, and the resulting frequency assignments of all the observed band heads in this *A* system are given in Table I. The restriction of vibrational transitions to two or three sequences about an intense $\Delta v=0$ sequence holds for all the rare earth oxide band systems so far investigated. It is associated with the small percentage change in the vibrational frequency in the two electronic states involved, and indicates an approximate equality of the stability of the various electronic energy levels of any one of these molecules.

Since odd multiplicities are demanded for CeO, the two heads in each of the bands starting at 7236A might be, say, *R* and *Q* heads of a $^1\Pi\rightarrow{}^1\Sigma$ transition. There are no very evident $+1$ or -1 sequences accompanying this group of bands which we designate system *B*. The best possible assignments are listed in Table II, together with the frequencies of another fragmentary system of single-headed bands starting at 7297A (13700.1 cm^{-1}). From the $\Delta G_v''$ intervals the lower state of this *C* system apparently is the same as that of the *B* system, but the intervals are too few in number to justify giving the usual vibrational energy equation.

Some rather prominent red-degrading band groups also occur in the blue region of the Ce arc spectrum. They are produced when either cerium chloride or oxide is placed in the arc but are not found in the praseodymium or neodymium spectra. Some of these heads occur at almost the same frequencies as given by Piccardi for GdO, but the spacing of bands in the sequences is only about half that for GdO. We therefore conclude that these bands are really due to CeO. The vibrational quantum assignments of two principal systems are given in Table III. Each system consists of but two sequences, the $\Delta v=0$ sequence being the more intense in each case. There is probably a third system some 300 cm^{-1} to the red of the *D* system but since only a single

TABLE III. *D and E systems of* CeO *bands. cm⁻¹ units.*

	E						*D*					
v′ \ v″	0	1	2	3	4		v′ \ v″	0	1	2	3	4
0	20863.6						0	20556.9				
1	21667.5	20830.6					1	21344.9	20511.6			
2		21632.3	20798.5				2		21295.9	20469.8		
3			21590.8	20763.3			3			21253.4	20432.4	
4				21555.3	20732.0		4				21209.2	20392.6

sequence is evident we do not enumerate its frequencies. The constants of the usual vibrational energy equations for all these CeO systems are displayed in Table V.

PrO Spectrum

Bands apparently characteristic of PrO occur in the range 5000–6000A. CeO, NdO, LaO and GdO have definitely been eliminated as their source, they have good intensity in the arc fed with Pr compounds, and some of them show the doublet structure expected for PrO whose atoms have normal terms ^4K and ^3P, respectively. In Table IV is displayed the one system that can be organized for these bands. Again there are principally just the two main sequences. There are also two rather prominent sequences 17614.9, 17566.9, 17523.7, 17479.1 and 17390.7, 17346.0, 17305.4, 17262.6 which are probably associated with others some 800 cm^{-1} to the violet in a region so replete with diffuse bands that accurate assignments are impossible. It is conceivable that the two sequences enumerated together form a system with vibrational intervals of plausible values for a PrCl molecule, but the evidence is rather in favor of the monoxide molecule as the emitter. The constants of the usual vibrational energy equation fitting this one PrO system are given in Table V.

Discussion

Although the oxide spectra of only a minority of the rare earths have been examined, it is already evident that well-developed systems of sharp bands are practically nonexistent for this group of elements. The band systems that do occur are usually abbreviated, the bands are often diffuse, and a background of uneven continua or large numbers of low intensity molecular lines with no apparent heads is frequently present. Admittedly this is not a particularly attractive field for band spectra research! These characteristic features of rare earth band spectra are undoubtedly due to a combination of circumstances. There is a rather large density of energy levels for most of these atoms, the multiplicities are high and the ionization potentials are low. Under such conditions the vast majority of possible molecular states are probably repulsion states, with resulting great prevalence of predissociation. These radiationless transitions must either eliminate completely or severely limit the extent of most of the possible band systems, and transitions to repulsion states could account for some of the continuous spectrum often present. Also the fact that the percentage difference between the vibrational frequencies of the two states of all the rare earth oxide band systems analyzed is always quite small leads to a Franck-Condon parabola so narrow as to have both its branches fall close to the main diagonal of the $v'v''$ array. One may then too predict from the Mecke rule that for many transitions the rotational B constants should be nearly identical in the two states concerned so that the resulting bands are practically headless.

The vibrational frequencies listed in Table V, together with those found for GdO[1] and LuO,[2] indicate but a small variation in the vibrational frequencies of the lower states of corresponding molecules of all the rare earths. As pointed out in

TABLE IV. PrO *system of emission bands.* cm^{-1} *units.*

v' \ v''	0	1	2	3	4	5
0	18679.4	17863.0				
1		18628.2	17813.8			
2		19387.0	18574.6	17762.9		
3					17710.6	
4					18464.5	17657.9

TABLE V. *Molecular constants for* CeO *and* PrO *bands.* cm^{-1} *units.*

System	ν_e	ω_e'	$\chi_e'\omega_e'$	ω_e''	$\chi_e''\omega_e''$
CeO *A*	12803.9	785.3	2.13	863.4	2.68
B	13855.2	788.3	1.76	866.7	3.30
D	20580.3	791.7	1.72	838.9	2.92
E	20880.3	807.9	2.04	841.4	2.24
PrO	18704.5	769.0	1.92	818.9	1.20

TABLE VI. *Wave-lengths of most intense band heads. Angstrom units. All bands degrade to the red.*

CeO	PrO	GdO	LuO
7926.96	5763.42	4892.2	4708.00
7879.34	5690.95	4615.6	4695.46
7831.78	5596.63		4684.16
7297.18	5352.00		4672.31
7275.51			4661.75
7235.78			
4863.20			
4791.70			

reference 2, only a 1 percent decrease in vibrational frequency is to be expected in going from CeO to LuO due to change in reduced mass, while approximate equality of the force constants governing the vibrations should exist because of the similarity in the outer electron configurations of these fourteen elements.

For qualitative chemical analysis the most intense bands for each of these molecules should prove more convenient than atomic lines for identifying the rare earths present in a mixture. This is especially true if the available spectrograph has not large dispersion. The wave-lengths of the heads of the most intense bands are listed in Table VI for all of the rare earth monoxide spectra so far analyzed. All bands degrade to the red.

Some of the rare earth elements apparently do not have any conspicuous band systems in the spectrum of the arc in air. In addition to the present search of the Nd spectrum, Meggers and Scribner report no characteristic bands for Yb[6] or from Tm[7] such as those found for Lu under identical conditions. Observations on the spectra of a number of the rare earths are lacking, of course, but it is apparent that for some of the atoms in this group oxide band systems of good intensity are missing. We venture to suggest that for such band systems to exist, a d electron must be present in the normal configuration of the rare earth atom. Lanthanum with its ds^2 configuration, together with a simple term scheme, has some seven well-developed monoxide band systems. Ce, Pr, Gd and Lu also have that same configuration in addition to 1, 2, 7 and 14 $4f$ electrons, respectively. Sm, Eu, Tm and Yb, on the other hand, have $4f^n6s^2$ normal configurations.

[6] W. F. Meggers and B. F. Scribner, Nat. Bur. Stand. J. Research **19**, 651 (1937).
[7] W. F. Meggers, private communication.

APRIL 15, 1938 PHYSICAL REVIEW VOLUME 53

Electrostatic Generator Operating Under High Air Pressure—Operational Experience and Accessory Apparatus

D. B. PARKINSON, R. G. HERB, E. J. BERNET AND J. L. McKIBBEN
Department of Physics, University of Wisconsin, Madison, Wisconsin

(Received February 11, 1938)

A description is given of experience gained in operation of the Wisconsin electrostatic generator with particular reference to the use of CCl_4 and CCl_2F_2 and to the problem of the fire hazard. Improvements in the charging belt system and the accelerating tube are discussed; and generator equipment, including the generating voltmeter, the voltage stabilizer and the ion source, is described.

INTRODUCTION

IN general design the Wisconsin electrostatic generator (Fig. 1) has not been changed since described in the first publication.[1] Although the generator has been in operation for almost two years all the original Textolite supports and the aluminum hoops are still in good condition. Corona points for the distribution of potential along the hoop system and accelerating tube are still satisfactory, although the points appear to be very dull. Additional operational experience has been acquired, however, and improvements have been made in the charging belts and in the accelerating tube. With (CCl_4 air and CCl_2F_2 air mixtures) the generator has been operated at 2.4 Mv for data on proton-proton scattering. Trouble has been experienced due to fires, and alterations have been made to reduce the fire hazard. These experiences and improvements are described in the present paper, and in addition a description is given of certain accessory apparatus, including the generating voltmeter, the voltage stabilizer, and the ion source.

[1] R. G. Herb, D. B. Parkinson, D. W. Kerst, Phys. Rev. **51**, 75 (1937).

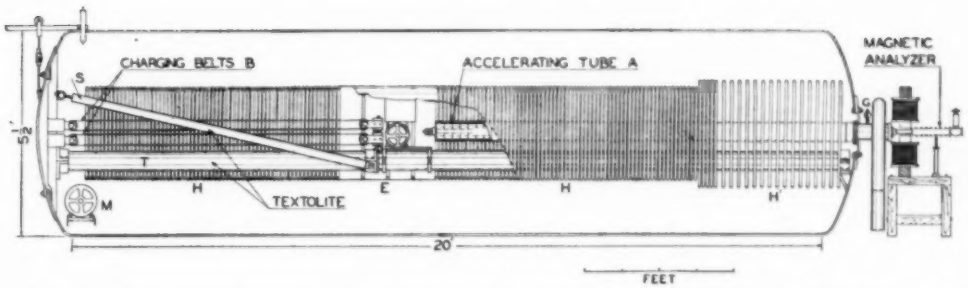

FIG. 1. Electrostatic generator. The steel tank enclosing the generator can be filled with air up to a pressure of 8 atmospheres. Charging belts B are made of rubberized fabric, 13 inches wide. Pulleys for the charging belts are 3 inches in diameter and run at a speed of 3600 r.p.m. Electrode E, made of galvanized iron, is at the highest generator potential. Aluminum hoops H and H' are mounted on small Textolite tubes so as to be insulated from one another. Corona current along the hoop system serves to maintain a uniform potential gradient from the maximum voltage at the electrode to ground at each end of the tank. Textolite tubes T and S support the entire structure inside the tank. Ions from a source in electrode E are shot through accelerating tube A to the end of the tank. Outside the tank the ion beam is deflected by a magnet and is directed into a target chamber.

CHARGING BELTS AND PULLEYS

The charging belts originally used were made of rubberized sheeting of the type used in hospitals. They were fairly satisfactory, but were ripped by sparks unless very thoroughly dried. The belts now being used are made of balloon fabric[3] which although light in weight, is tough and serviceable, and is unaffected by sparks. When these belts were first used, however, the pulley alignment was found to be rather critical. The pulleys then had no crowning except for a 1° taper at each end over a distance of $\frac{1}{2}$ inch. Recently this taper was changed to 2° along a distance of $\frac{3}{4}$ of an inch at each end, and since this change the belts have remained centered and have required very little attention.

ACCELERATING TUBE

Improvement of focus

The accelerating tube has been modified in certain details since it was first described. It is made up of 53 porcelain cylinders separated by metal electrodes with joints sealed by wax. The porcelain cylinders which were installed when the generator was constructed have given no trouble and are still in use. All of these cylinders are the same as the end cylinder shown in Fig. 4. Most of the metal focusing electrodes have been unchanged since construction of the generator, but the first five electrodes nearest the ion source were modified several times during the first year the generator was in operation, and the design finally adopted has a telescoping construction as shown in Fig. 4. The inner cylinders which are responsible for the focusing are made with a small diameter since tests had indicated that for good focus the cylinders must have diameters small compared to their lengths. The large outer cylinders serve to shield the gaps from charge collected on the inner wall of the porcelains.

A corona gap system is provided for the tube to give proper potential distribution. Sections one and three, counting from the high potential end of the tube, have variable corona gaps which can be individually controlled from outside the tank, and section two is permanently shorted. Until recently other sections of the tube were each equipped with three fixed corona gaps (Fig. 2) spaced evenly around the tube. With this arrangement the ion beam could usually be brought to a good focus by adjustment of the variable corona gaps.

Some trouble was experienced, however, with control of the ion beam over a wide voltage range. The fixed gaps had to be set at about 2 cm for operation in the region of 2 Mv, since for shorter gaps the large current drain required high charging currents which caused sparking down the belts. However, with the gaps at 2 cm and a pressure of 8 atmospheres in the tank, corona current at voltages below 1200 kv was too small to maintain a uniform potential

[3] This belting was first used by Dr. Tuve and his associates at Washington, D. C. It is obtained from the Goodyear Rubber Company, Akron, Ohio.

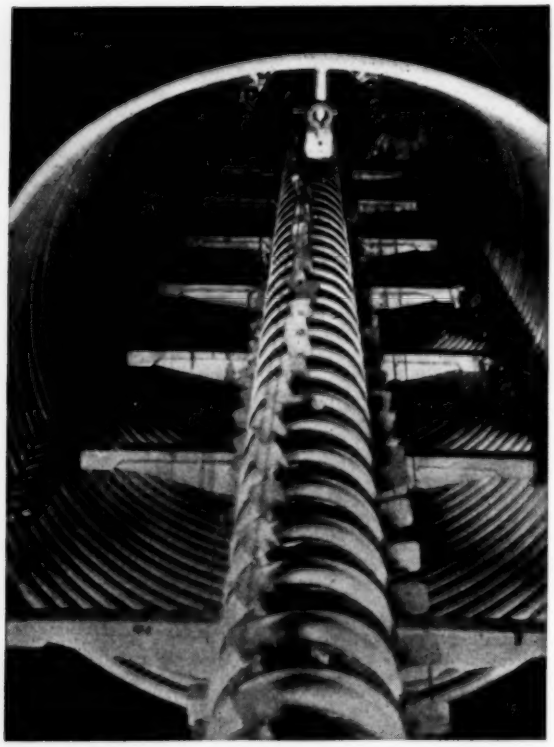

FIG. 2. View showing accelerating tube and hoop system. This photograph was taken before installation of the adjustable corona gap system along the tube.

distribution along the tube, and consequently difficulty was experienced in focusing the ion beam. This difficulty with focus has been eliminated by the installation of an adjustable corona gap system which can be controlled from outside the tank. Only one gap on each section of the tube has been made adjustable, the other two being permanently set at 2.5 cm. Needles of the adjustable gaps are mounted on a glass tube,* diameter ½ inch, running parallel to the accelerating tube as shown in Fig. 3. The glass tube can be moved along its axis so as to vary the gaps from zero up to about 3 cm. This adjustable system is common to all sections of the tube with the exception of the first three, which are arranged exactly as before. The ion beam can now be well focused at any voltage above about 800 kv with 8 atmospheres pressure in the tank. Thus by using the diatomic beam it is possible to

* Note added in proof:—This glass tube (Pyrex) behaved satisfactorily for about three months and then shattered because of flash-over at high voltage. New tubing was installed twice but it failed almost immediately. Failure of the glass tubing was probably caused by small capillaries which are generally present in drawn Pyrex. The glass tube was replaced by a Dilecto rod grade XX of ½ inch diameter which has given no trouble during a month of operation at potentials up to 2.2 Mv.

FIG. 3. View showing the accelerating tube and the adjustable corona gap system. The glass tube which supports the adjustable needles is indicated by the arrow.

work with ions having an energy as low as 400 Kev without releasing air from the tank.

Leaks

During the summer of 1937 the wax joints of the accelerating tube caused considerable trouble due to leaks which frequently developed when air pressure in the tank was increased above about 6 atmospheres. Red sealing wax (American Express No. 2) had been used for the joints. This wax is strong, but rather brittle, and apparently as the compressional force on the tube was increased, the strains developed due to uneven seating of the porcelain cylinders on the aluminum disks were sufficient to cause minute cracks to form. Practically all the trouble due to leaks in the tube was eliminated by covering the red wax with a coat of Picein wax (melting point 80°C) which is sufficiently plastic at room temperatures to take small deformations without cracking.

Performance at high voltage

When the generator is operated at its maximum steady voltage of 2.4 Mv the accelerating tube gives no trouble. However, during test work with CCl_4 and CCl_2F_2 in the tank, discharges sometimes took place in the tube causing the vacuum to go bad when the voltage was held at 2.5 Mv for periods of more than about one-half minute. It therefore seems that the maximum operating voltage of the generator is very near the maximum voltage which the tube will withstand continuously. For short periods of time the tube will withstand somewhat higher voltage, and when the generator voltage was held above 2.7 Mv for a few seconds, the tube did not break down.

Ion Source

After some experimentation with various kinds of ion sources the arrangement shown in Fig. 4 was adopted and has now been in use for about one year. High yields of ion current cannot be claimed for this source, but it has been almost entirely free of trouble since it was installed, and for use with a generator of the Wisconsin type reliability is of considerable importance.

A hairpin type filament is used, made of 16 mil tungsten wrapped with 5 mil nickel, and coated with a barium oxide-strontium oxide mixture. The filament has never burned out and has been

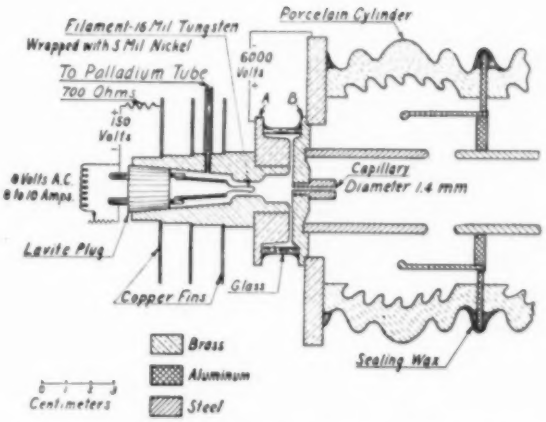

FIG. 4. Ion source and first section of accelerating tube.

recoated only once. Filament heating current is generally set at about 9 amperes, and the filament emission is usually between 100 and 200 milliamperes. The positive ion current to plate B has never been measured but judging from the behavior of similar sources tried at this laboratory, it is estimated that this current is never greater than 5 milliamperes.

Hydrogen from a supply tank in electrode E, Fig. 1, is admitted to the ion source through a palladium regulator tube which is electrically heated by current from the power supply in electrode E. By means of a string control the temperature of the palladium tube, and consequently the hydrogen flow, can be regulated from outside the tank. Pressure in the vacuum system is measured by means of a Western Electric ionization gauge (G, Fig. 1) mounted on the system near the end of the tank, but pressure in the ion source has never been measured. Data regarding yields from the ion source have all been obtained with the source installed on the generator and with the magnetically resolved ion beam passing through a $\frac{3}{16}$-inch hole into a target chamber. Ion current yields increase rapidly as hydrogen flow is increased, but the maximum proton current through the $\frac{3}{16}$-inch hole is limited to about three microamperes, since any further increase in hydrogen flow causes defocusing of the ion beam. With the hydrogen flow at its optimum, the pressure indicated by the ionization gauge is about 1.5×10^{-5} mm Hg. The hydrogen diatomic ion current is then somewhat less than the proton current, but as hydrogen

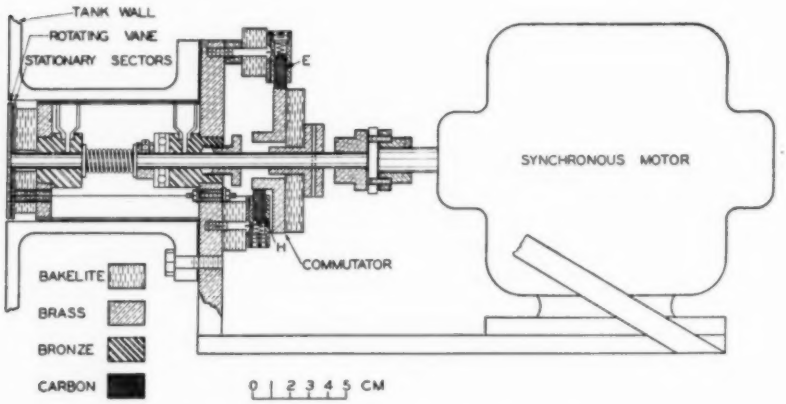

FIG. 5. Cross-sectional view of generating voltmeter.

flow is decreased the proportion of diatomic ion current to proton current increases, and when the pressure indicated by the ionization gauge is less than 5×10^{-6} mm Hg the diatomic ion current is approximately twice as great as the proton current. Ions of greater mass than the hydrogen diatomic ions are never present in appreciable quantities.

FIRE HAZARD

As many inquiries have been received regarding the fire hazard in the Wisconsin generator a description will be given of all fires that have occurred since construction of the generator. Provision was made for fire protection before the generator was put into operation. The tank was equipped with a two-inch gate valve for rapid release of high pressure air in case of fire, and a cylinder of CO_2 was left permanently connected so that the tank could be flushed with this gas after the air pressure had dropped close to atmospheric pressure.

The first fire occurred soon after completion of the generator when sparking tests were being run at high voltage with the tank at a pressure of 8 atmospheres. A Textolite tube of $\frac{1}{2}$-inch diameter and $\frac{1}{32}$-inch wall thickness was used to adjust corona gaps on the hoop system. This had become frayed by sparks and fire caught on a section that had been wrapped with friction tape. The fire was noticed soon after starting (probably less than one minute) because of a rapid drop in voltage, and when air pressure was released from the tank the fire went out. CO_2 was let into the tank but was probably not necessary. About 10 inches of the Textolite tube was burned, but no other damage was done. Tests had shown that the setting of the corona gaps on the hoops was not critical; the adjustable system with its Textolite tube was therefore discarded and stationary gaps set at about 2 cm were installed.

Fire number two was also caused by a spark at high voltage with 8 atmospheres pressure in the tank. It caught on a light pasteboard tube which served as an air line from a blower at one end of the tank up to the ion source. This fire also went out when pressure was released and nothing was damaged except the pasteboard tube. This tube was discarded and the main Textolite support (T, Fig. 1) was equipped to serve as an air line.

Fire number three was caused by a short circuit in the power supply for the ion source when tests were being made with the tank at atmospheric pressure. Considerable damage was done both to the power unit and to the high potential electrode. In rewiring the power supply, rubber and fabric insulation was reduced to a minimum, and bus bar wiring was installed wherever possible.

Another fire, which ruined a set of charging belts, occurred when the generator was not running. Voltage was accidently thrown onto the needles for the charging belts and was raised so high that intense sparking from the needles caused the belts to ignite. As the tank was then open the fire was put out with an extinguisher.

After these experiences with fires it was thought that all fire hazards had been eliminated, but recently, when running at 2.4 Mv, a wooden

board under a driving motor (M, Fig. 1) caught fire. Although the motor frame was well grounded, apparently a surge due to a high voltage spark caused a discharge along the wood. This fire, like the others, went out when the air pressure was released, and nothing was damaged excepting the board. The motor support was then modified to eliminate all danger of fire.

When the generator was in its early developmental stage hundreds of sparks passed down the Textolite tension members without causing the slightest charring or fraying. The charging belts originally used (hospital sheeting) were sometimes ripped by sparks but were never set on fire, and the balloon fabric belts now used are unaffected by sparks.

These experiences indicate that textolite, unless extremely thin and fragile, can be safely used, and that rubberized charging belts, under ordinary circumstances, do not constitute a fire hazard. It does seem essential, however, to avoid the use of inflammable material as much as possible.

Use of CCl_4 and CCl_2F_2

With pure air at 8 atmospheres pressure in the generator the maximum usuable potential is limited to about 2.1 Mv by radial sparking from the high potential electrode. Humidity has no noticeable effect on sparking potential, but to avoid loss of charge due to conduction along insulators the relative humidity must be kept below about 35 per cent.

Investigations conducted at this laboratory[3, 4] showed that the dielectric strength of mixtures of air with a small percentage of CCl_4 or CCl_2F_2 is considerably greater than the dielectric strength of pure air. Pure CCl_2F_2 was found to have a dielectric strength of about three times that of air, and the dielectric strength of a CCl_2F_2 air mixture was found to increase very rapidly with concentration of CCl_2F_2 in the region of small concentrations.

Recently with CCl_4 and later CCl_2F_2 in the generator reliable data on proton-proton scattering was obtained at 2.4 Mv. With the tank at 8 atmospheres pressure, 4 kg of CCl_4 evaporated into the generator increased the direct spark-over voltage from about 2.1 Mv to 2.4 Mv. This amount of CCl_4 in the tank gives a vapor pressure of 33 mm of Hg which is approximately 33 percent of the pressure for saturation. When higher concentrations of CCl_4 were tried sparking along the charging belts limited the usable potential to a value considerably below 2.4 Mv. In our work at 2.4 Mv considerable trouble was experienced because of sparking down the control strings which run from the end of the generator up into the high potential electrode. Untreated cotton and silk lines were satisfactory in pure air but were torn to pieces by sparks when CCl_4 was used. These lines withstood the voltage satisfactorily when impregnated with paraffin, but stretched to such an extent in the CCl_4 atmosphere that they became useless as controls. Cuttyhunk fishlines (linen impregnated with tar) were then installed and have been entirely free of trouble at the highest potentials obtainable, using either CCl_4 or CCl_2F_2 in the tank.

During the test work with CCl_4 none of the materials in the generator were affected except the control strings, but later when 8 kg of CCl_4 was allowed to remain in the tank for several days the behavior of the generator indicated that either the belts or the Textolite supports had become conducting. It is possible, however, that this behavior of the generator was due to other conditions, and because CCl_4 has not been tried since then the effect cannot be considered as established.

For most of the work at 2.4 Mv, CCl_2F_2 was used in the generator. Five kg of CCl_2F_2 in the tank, giving a vapor pressure of 55 mm Hg (1.4 percent of saturation) increased the usable potential from 2.1 Mv to 2.4 Mv, and when greater concentrations were tried failure along the charging belts caused a decrease in the usable voltage. CCl_2F_2 appeared to have no effect on materials in the generator.

Experience with the use of CCl_4 and CCl_2F_2

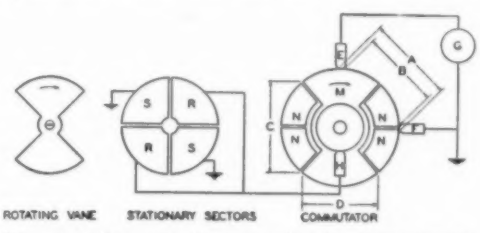

FIG. 6. Schematic diagram of voltmeter circuit.

[3] M. T. Rodine and R. G. Herb, Phys. Rev. **51**, 508 (1937).
[4] C. M. Hudson, L. E. Hoisington and L. E. Royt, Phys. Rev. **52**, 664 (1937).

and also with pure air at high pressure has shown that the voltage for flash-over along long insulators does not increase linearly with the dielectric strength of the gas or vapor surrounding the insulator, and that under certain circumstances the flash-over voltage may actually decrease when the dielectric strength of the gas is increased.

This effect puts a serious limitation on the maximum generator voltage since measurements on the dielectric strength of CCl_2F_2 indicate that by using a high pressure of this vapor in the generator its radial sparking potential could be increased to over 4 Mv.

The Generating Voltmeter

Construction

Generating voltmeters are now in common use and many have been described in the literature. It is believed however that the instrument to be described represents some improvement over others, both in simplicity and in reliability, and that a description of its performance on the Wisconsin electrostatic generator will be of value.

Figure 5 shows the construction of the voltmeter, and in Fig. 6 a diagram is given of the electrical circuit. The assembly is mounted on a flanged fitting which extends radially from the cylindrical wall of the tank opposite the high voltage electrode. The rotating vane, of $\frac{1}{16}$-inch brass, is mounted flush with the inner surface of the tank and is spun by direct drive from a synchronous motor. Stationary sectors R and S, also of $\frac{1}{16}$-inch brass, are screwed onto a heavy Bakelite disk with a clearance of about $\frac{1}{64}$-inch from the rotating vane. The rotating vane and stationary sectors S are grounded, and the sectors R are periodically connected through the commutator to a Leeds and Northrup galvanometer of sensitivity 2.99×10^{-9} amperes per mm. As the rotating vane turns, a charge which is proportional to the potential of the generator flows onto and off the sectors R, and feeds an alternating current into the commutator. Sectors N of the commutator are made of $\frac{1}{4}$-inch brass, fastened with screws to a Bakelite disk and are all insulated from one another and from ground. Carbon brush H makes permanent contact with sector M. An examination of the diagram will show that with orientations as given in Fig. 6 only those pulses are measured which are caused by sectors R being covered, the reverse pulses due to the uncovering of R being sent to ground. During development of the commutator it became evident that the galvanometer circuit must never be shorted by a sector of the commutator since if the circuit is shorted thermal e.m.f.'s at the brushes produce a current through the galvanometer. Thus in constructing the commutator the relative size of sectors M and N for a given arrangement of brushes E and F must be such that $B>D$ and $C>A$. Since the sectors N are all floating and are separate from one another and sector M is connected only to sectors R, the conditions given above establish the essential requirement that the circuit through the galvanometer never be closed, and thus trouble due to thermal e.m.f.'s is eliminated. If the voltmeter is turned on with the generator potential zero there is no noticeable deflection of the galvanometer G, and when measuring a high steady potential the galvanometer behaves as well as if a steady direct current were being measured.

It is possible that a commutator of the ordinary type could be used providing a high resistance were put in the galvanometer circuit to suppress thermal currents. This arrangement has not been investigated thoroughly, but when a resistance of 200,000 ohms was put in the galvanometer circuit the voltmeter sensitivity was changed by about 2 percent. There seemed to be a possibility that this change in sensitivity would depend on the capacity of the system, and that a change in the clearance between rotating and stationary sectors would therefore change the sensitivity. Another possible objection to a high resistance in the galvanometer circuit is that this arrangement would make insulation requirements from commutator and sectors R to ground more exacting.

To obtain reliable operation of the voltmeter the commutator must be provided with a grounded shield (not shown in drawings) since if the commutator can "see" a charged surface, such as an insulator which has picked up a charge, a current will be generated which will be superimposed on the current from the sectors and thus readings will be inaccurate.

Calibration

For calibration of the voltmeter, use was made of the gamma-ray resonance from lithium bom-

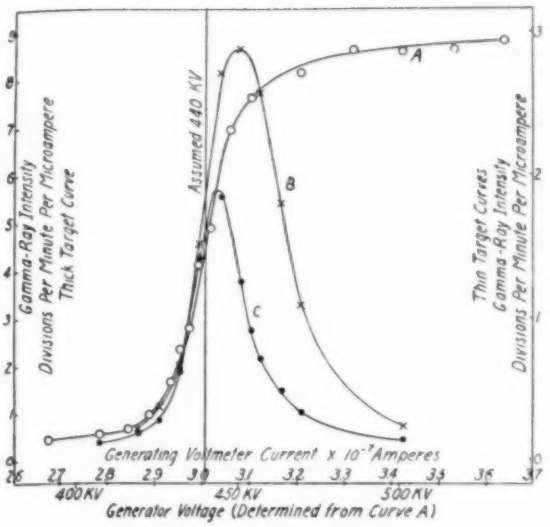

FIG. 7. Gamma-ray yield curves from lithium bombarded by protons. A Lauritsen type electroscope was used for measurement of gamma-ray intensity. Curve *A* was used for calibration of the generating voltmeter.

barded by protons. Hafstad, Heydenburg, and Tuve[5] studied this resonance by the use of a high resistance voltmeter and found a value of 440 kv for the resonance peak. At Wisconsin, an entirely independent determination was made of this resonance voltage by the use of a small electrostatic generator and results agreed well with those obtained at Washington. Several runs on the lithium gamma-ray resonance were then made with the large generator and when a potential of 440 kv was assumed for the resonance peak, the output of the voltmeter was determined to be 6.90×10^{-10} amperes per kilovolt.

During regular experimental work with high energy protons several checks have been made on the linearity of the voltmeter by changing from use of monatomic ions to the use of diatomic ions for bombardment. At a generator voltage V each proton of a diatomic hydrogen ion has an energy of $\frac{1}{2}\ eV$ and thus if the voltmeter is linear, monatomic ions at a voltmeter reading of V should give the same result as diatomic ions at a voltmeter reading of $2V$. This condition was found to be satisfied in all experiments within the limits of experimental error which were probably never better than 1 percent.

Recently the sensitivity of the voltmeter was rechecked by running yield curves for gamma-rays from both thick and thin lithium targets. Results are shown in Fig. 7. The position of maximum slope of curve *A* is assumed to be at 440 kv, and the voltmeter current at this position is 3.01×10^{-7} amperes, from which one obtains a sensitivity of 6.85×10^{-10} amperes per kilovolt. This sensitivity is approximately 0.7 percent lower than the value determined 18 months previous when the voltmeter was first calibrated. The peaks of the thin film curves *C* and *B* are shifted from the resonance peak indicated by curve *A* in the direction of higher voltage. This shift is caused by the finite thickness of the films and is greater for curve *B* since the film used for this curve was of greater thickness than the film used for curve *C*. Because of this shift in resonance peaks it seems that thin target yield curves are not satisfactory for calibration of voltage.

[5] L. R. Hafstad, N. P. Heydenburg and M. A. Tuve, Phys. Rev. **50**, 504 (1936).

AUTOMATIC VOLTAGE STABILIZER

For most experimental work with the high voltage generator the voltage is set at some definite value and must be held to this value very closely while determining a reaction or scattering yield. Generator voltage depends upon the amount of corona current fed from needle points to the in-going sides of the charging belts. High voltage for the charging needles is supplied by a transformer and kenotron rectifier set, and consequently the potential of the electrostatic generator can be varied by changing the voltage applied to the transformer.

Comparatively long period drifts in generator voltage are easily corrected by manually operated rheostats in series with the primary of the transformer supplying the rectifier set. However, small short period fluctuations of the order of a second or two cannot be followed accurately by the manually operated rheostats.

For this reason an automatic voltage stabilizer was designed by one of the authors (JLM) to keep the voltage more closely to a given value than was possible with manual control. The stabilizer consists of a two-stage direct coupled amplifier whose input is a voltage derived from corona current to a needle projecting into the tank opposite the high voltage electrode Needle setting can be changed from 0 to 2 cm projection by means of a small reversible motor controlled by a switch which is placed so as to be convenient

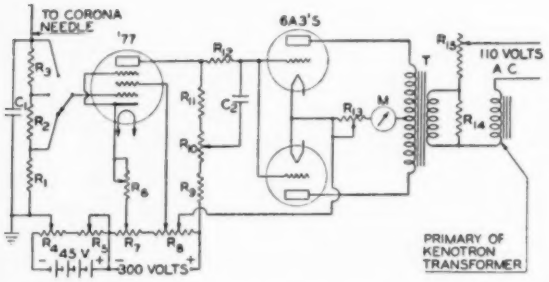

FIG. 8. Circuit diagram of voltage stabilizer. $R_1 = 1$ megohm wire wound. $R_2 = 0.5$ megohm wire wound. $R_3 = 0.5$ megohm wire wound. $R_4 = 25{,}000$ ohm potentiometer for voltage control. $R_5 = 5000$ ohm variable for fine adjustment of voltage. $R_6 = 5000$ ohm variable gain control. $R_7 = 1000$ ohm potentiometer for mu balance. $R_8 = 50{,}000$ ohm resistor with taps. $R_9 = 0.5$ megohm. $R_{10} = 9$ resistors of 50,000 ohms mounted on a selector switch. $R_{11} = 1$ megohm. $R_{12} = 4$ megohm. $R_{13} = 2500$ ohm resistor with taps. R_{14} and R_{15} = rheostats for control of high voltage. $C_1 = 0.5$ microfarad. $C_2 = 1.5$ microfarad. T = Thordarson T5604 radio power transformer. M = milliameter : 0–100 milliamperes.

for the operator. The output of the amplifier controls the current in the primary of the transformer supplying the kenotrons.

The circuit diagram is given in Fig. 8. A corona current of 10 to 40 microamperes flows to ground through the resistors R_1, R_2, and R_3. The voltage drop across a selected number of these resistors is amplified by a type 77 screen grid tube, and the plate circuit is direct coupled to the grids of two 6A3 power tubes. Resistor R_8 is set to maintain a potential of 100 volts on the screen of the 77 tube, and to give suitable bias to the grids of the 6A3's. R_7 provides a mu balance to counteract line voltage fluctuations entering through the power supply, and R_{13} is set to limit the maximum value of plate current of the 6A3's to about 80 milliamperes. No d.c. potential is applied to the plates of the 6A3's; their voltage supply is the transformer T, and thus the amount of power drawn from the secondary of T is determined by the grid potential of the 6A3 tubes. The primary of T parallels part of the manually operated rheostats which control the potential of the kenotron rectifier set. Since the impedance of the primary of T depends on secondary load, a variation in load will cause a variation in the voltage of the kenotron set. Generator voltage will not respond immediately, however, because of the finite speed of the charging belts and the generator capacity. This time lag causes troublesome hunting of the stabilizer unless suitable time constants are introduced into the circuit. If condenser C_2 is not used hunting occurs with a period of about $\frac{1}{2}$ second. It can be eliminated by using the maximum value of R_6 and by sufficient reduction of the plate load resistor of the 77 tube, but the gain of the amplifier is then insufficient for good regulation. A condenser across the entire plate load resistor increases the period of the hunting action but gives little improvement in performance.

Trouble due to hunting has been practically eliminated by the introduction of two different time constants into the circuit. Condenser C_2 is placed across only a selected fraction of the plate load resistor, as shown in Fig. 8, making amplifier response partially fast and partially slow. The ratio of rapid to slow speeds of correction is not critical over a certain range and can be easily adjusted to eliminate hunting with the amplifier gain set sufficiently high for good regulation.

Because of small rapid fluctuations in corona current which sometimes occur when the generator voltage is constant, a smoothing condenser C_1 is placed across the input resistance. The size chosen gives satisfactory smoothing action and is not large enough to cause hunting of the stabilizer.

Best operation is obtained if the time constants of all other portions of the circuit are kept as small as possible. No condenser is used to smooth the voltage applied to the charging needles by the kenotron rectifier set.

To set the stabilizer into operation the generator voltage is adjusted to approximately the desired value by means of R_{15}, and the distance which the corona needle projects into the tank is adjusted to give the best performance of the stabilizer. By means of R_4 or the fine control R_5 the generator voltage is then set accurately at the desired value.

When the generator is in good condition and the stabilizer has been properly adjusted the voltage is held constant to within approximately 0.5 percent.

We wish to express our indebtedness to Dr. D. W. Kerst for help in this research and to Professor G. Breit, Professor H. B. Wahlin, and Professor L. R. Ingersoll for advice and support. We also wish to express our thanks to the Wisconsin Alumni Research Foundation for generous financial assistance.

On the Electromagnetic Properties of Nuclear Systems

W. E. LAMB, JR. AND L. I. SCHIFF*
University of California, Berkeley, California
(Received February 8, 1938)

If one supposes that a charge bearing field is responsible for nuclear forces, the charge and current of this field must be considered in describing the electromagnetic properties of nuclei. In this paper we discuss the extent to which these electromagnetic anomalies permit phenomenological description in terms of the charges and magnetic moments of the single heavy particles and the forces acting on them. We are guided in this discussion by the formalism of the electron neutrino field theory and that of the dynaton theory proposed by Yukawa. Apart from the known effect of exchange currents on electric dipole radiation, the most marked differences from the phenomenological treatment appear in the estimates of magnetic dipole radiation and magnetic spin dependent forces. The formalism used is developed in the Appendices. Appendix I gives the proof of Serber's result on the repulsive nature of the field theoretic interaction between neutron and proton in the deuteron. Appendix II considers the electric properties of heavy particles in more detail, and shows that Siegert's theorem, which connects the exchange current with the exchange interaction, is valid for the dynaton theory. Appendix III discusses more completely the magnetic properties of heavy particles.

IT has been suggested that the finer features of the forces between neutrons and protons might be discovered if one were to study processes involving the interaction of these particles with the electromagnetic field, such as the photodisintegration of the deuteron[1] or the radiative capture of neutrons in hydrogen. The assumption has generally been made that it is possible to assign the various electromagnetic properties, such as charge and magnetic moment, to the individual heavy particles in a purely phenomenological manner. Thus the charge and all of the electric moments of the neutron were taken to be zero, while a magnetic moment of $\mu_N \sim -2.0$ n.m. (nuclear magnetons) was assumed. The proton was described by its charge $+e$ and a magnetic moment $\mu_P \sim 2.5$–2.8 n.m. It was then assumed that when two such particles were brought close together, as in the bound states of the deuteron or in heavier nuclei, these properties would remain the same as for the isolated particles; it was also assumed that radiative transitions could be calculated by the use of the electromagnetic moments characteristic of the single heavy particles, independently of the states of the nucleus involved. Again, it was thought that the total nuclear magnetic moment could be calculated additively from contributions of the constituent single particles. There is, of course, no *a priori* reason why these things should not be so. One has, however, been led to believe that a field theory of some sort might be found which would afford a description not only of the nuclear forces, but also of the magnetic properties of the single heavy particles. With such a view, one would be quite prepared to expect a "distortion" of these properties by the presence of other heavy particles. In this paper, we shall discuss a number of these questions in order to see in how far such field theories permit of a phenomenological development of nuclear physics in terms of the properties of particles with forces acting between them.

No consistent and satisfactory example of a field theory of nuclear forces exists at present. Several attempts[2] at one were made using modifications of the electron-neutrino field which was introduced by Fermi[3] to describe beta-decay. In order to obtain strong short range forces, and to have a convergent theory, it is here necessary to use a coupling energy between the heavy and light particles which contains a

* National Research Fellow.

[1] G. Breit and E. U. Condon, Phys. Rev. **49**, 904 (1936).

[2] A. Nordsieck, Phys. Rev. **46**, 234 (1934); I. Tamm, Nature **133**, 981 (1934); D. Iwanenko, ibid.; C. F. v. Weizsäcker, Zeits. f. Physik **102**, 572 (1936); M. Fierz, Zeits. f. Physik **104**, 553 (1937); J. Solomon, J. de phys. et rad. **8**, 179 (1937); N. Kemmer, Phys. Rev. **52**, 906 (1937); H. Primakoff, Phys. Rev. **51**, 990 (1937).

[3] E. Fermi, Zeits. f. Physik **88**, 161 (1934).

finite distance operator,[4] and this makes it impossible to set up a quantum theory of the field which is covariant, Hamiltonian and gauge invariant. The presence of a finite distance operator is particularly inconvenient for our purposes, because the differential conservation laws of charge and current are rendered invalid, thus destroying the consistency of the electromagnetic calculations. If one allows convergence factors (as is necessary to obtain finite results), the interaction between a neutron and a proton in a symmetric state is found to be repulsive,[5] in disagreement with the known stability of the triplet state of the deuteron (see Appendix I). Then also, since like particle forces arise only in a higher order than do unlike particle forces, they turn out to be far too small to agree with the experiments on proton-proton scattering. The theory can, however, be made to assign reasonable magnetic moments to the heavy particles without too much artificiality.

Another attempt at a field theory of the interaction of nuclear particles was made by Yukawa.[6] He introduced spinless particles obeying Bose-Einstein statistics, possessing a mass m between the masses of electron and proton and a charge $\pm e$, the charge of the proton. These "dynatons" were assumed to obey the scalar relativistic wave equation which has been investigated by Pauli and Weisskopf.[7] Evidence has recently been found[8] for the presence in cosmic radiation of particles with masses of this order of magnitude. This field theory is more nearly convergent than the electron-neutrino field theory, and for its interpretation, no finite distance operators are needed. However, the difficulties of the repulsive neutron-proton forces and the small like particle forces remain; furthermore, one is driven to very artificial devices in order to obtain magnetic moments for the heavy particles from the light particle field.

More promising is the recent proposal of Teller[9] in which like and unlike particle forces arise in the same order. This suggestion derives nuclear forces from a neutral electron-positron field, coupled to the heavy particles by an energy large compared to the kinetic energy of the pairs, and involving a finite distance operator. On this theory, even the dynamical problem of the heavy particles cannot in general be formulated phenomenologically, i.e., without the explicit consideration of the light particles; this will be so *a fortiori* for the radiative properties of the system.

Because of the very many difficulties involved in the formulation of such field theories, we shall not regard their predictions too seriously. At best they can indicate in what situations caution may be necessary in the phenomenological description of nuclear processes. We shall begin with a qualitative discussion of the various questions raised, occasionally quoting the results of field theoretic calculations, some details of which may be found by the interested reader in the Appendices.

Let us first discuss the electromagnetic properties of a single heavy particle, say a neutron, according to such a field theory. On either field theory one may introduce a dimensionless parameter g to measure the strength of the coupling between heavy and light particles. The neutron-proton forces arise in order g^2, and we will always adjust the value of g to give forces of the observed order of magnitude. The existence of this coupling means that there is a certain probability of finding the neutron dissociated into a proton and a negative light particle. If we restrict our consideration to the expectation values of the charge and current for states of the neutron involving periods long compared to the relaxation time $\tau \sim a/c$ of the light particle cloud, where a is the range of nuclear forces, the charge density is spherically symmetric and all of its electric moments about the heavy particle vanish. The expressions for charge density and total charge may be found in Appendix II. As long as the coupling used does not involve the heavy particle spin, the low frequency components of

[4] By a finite distance operator or convergence factor in a coupling, it is meant that values of the light particle wave functions at finite distances from the heavy particles are involved in the interaction energy.

[5] R. Serber, Phys. Rev. **53**, 211 (1938).

[6] H. Yukawa, Proc. Phys.-Math. Soc. Japan **17**, 48 (1935); J. R. Oppenheimer and R. Serber, Phys. Rev. **51**, 884 (1937).

[7] W. Pauli and V. Weisskopf, Helv. Phys. Acta **7**, 709 (1934).

[8] S. H. Neddermeyer and C. D. Anderson, Phys. Rev. **51**, 884 (1937); J. C. Street and E. C. Stevenson, Phys. Rev. **52**, 1003 (1937); D. R. Corson and R. B. Brode, Phys. Rev. **53**, 215 (1938).

[9] We are indebted to Professor Teller and Professor Oppenheimer for opportunity to see the paper of Critchfield and Teller prior to publication.

the current density also vanish, and therefore fail to give any supplementary magnetic moments to the heavy particles.

If now we consider frequencies ν which although still small compared to the reciprocal of the relaxation time, a/c, are not negligible, the spherical symmetry of the charge distribution will be destroyed and the neutron may emit electric quadrupole radiation. The quadrupole moment will be small. For in the first place, the total charge involved is small, of the order $e\hbar/(Mca)$; this is true even on the dynaton theory, as only dynatons of relatively low energy and consequent long relaxation time can contribute to the distortion of the charge distribution. In the second place, the separation of positive and negative charge in the neutron will be of the order $a(\nu a/c)$, and the ratio of this distance to the wave-length of the radiation is $(a/\lambda)^2$ which will be small unless one considers radiation of frequency comparable to that necessary to produce photodisintegration of the neutron.

It is true that in a nucleus, the forces may be great enough to induce dipoles of the order $a(e\hbar/Mca) \sim e\hbar/(Mc)$. Even these, however, for wave-lengths large compared to a will give completely negligible corrections to the radiative moments. Far more important are the distortions of the charge distribution induced by the presence of neighboring heavy particles.

Let us turn now to the question of the origin of the magnetic moments of the heavy particles. As is well known, the Dirac equation does not describe these correctly. One can, of course, modify this equation by the inclusion of the so-called neutrino terms[10]

$$\eta\sigma_{\mu\nu}F_{\mu\nu}\psi,$$

where ψ is the wave function of the particle, $F_{\mu\nu}$ is the electromagnetic field tensor, $\sigma_{\mu\nu}$ is the six vector spin matrix, and η is a constant which determines the value of the extra magnetic moment. The consequences of this for the singlet-triplet splitting in the deuteron are discussed below. Another possibility, first pointed out by Wick,[11] is that the light particle cloud which surrounds a heavy particle may have a resultant magnetic moment. For this to be possible, it is clearly necessary to couple the magnetic moment of the light particles with the spin of the neutron or proton. In the electron-neutrino field theory, this can easily be done, and one can use such a coupling to calculate the charge and current density about a heavy particle. The current density of course no longer vanishes, although it is divergence-free, and if the heavy particle is at rest, there is a current distribution that is symmetric about its spin axis. By suitably choosing the coupling, the neutron and proton may be given magnetic moments quite independent of one another; in particular the moments may be equal in magnitude and opposite in sign. (See Appendix III.) On the other hand, the scalar dynaton which we have considered till now cannot be coupled to the spin of the heavy particles so as to give them a magnetic moment, unless one introduces a finite distance operator. This is so because the scalar dynaton has no spin magnetic moment, and for there to be an orbital magnetic moment,[12] the dynatons would have to be created at a finite distance from the heavy particle. However, one can introduce in addition to the scalar dynaton another kind of dynaton possessing unit spin and described by a six vector wave function.[5, 13] Alternatively, one may think of a single particle existing in both scalar and six vector states. Both types of dynatons are coupled to the heavy particles and to one another through the electromagnetic field so as to give them an intrinsic magnetic moment of arbitrary magnitude and sign. (Appendix III.) This coupling scheme gives mixed Heisenberg and Majorana forces between neutron and proton, and when the constants are properly adjusted, gives the anomalous magnetic moment of the proton. On this theory, the neutron is given the same magnetic moment as the proton in contradiction with some direct experimental evidence which indicates that μ_N and μ_P have opposite sign. Because, however, of the interference terms which appear, the magnetic moment of the

[10] W. Pauli, *Handbuch der Physik*, Vol. 24/1, p. 233.
[11] G. C. Wick, Accad. Lincei **21**, 170 (1935).

[12] H. Frölich and W. Heitler, Nature **141**, 37 (1938).
[13] H. J. Bhabha, Nature **141**, 117 (1938), has proposed a formalism involving a four vector dynaton; however, in the nonrelativistic limit for the heavy particles, this is completely indistinguishable from the scalar dynaton formalism of Yukawa. Similar considerations apply to the suggestion of N. Kemmer, Nature **141**, 116 (1938).

deuteron could still be brought into agreement with the observed ~ 0.85 n.m. The equality of the field theoretically calculated anomalous magnetic moments for neutron and proton is a consequence of the fact that positive and negative dynatons are given the *same* magnetic moment in spite of their opposite charges; this in turn follows from the fact that the magnetic coupling terms of Eq. (17) in the Lagrangian involve a second rank tensor, unaltered by mirroring.

We now turn to a consideration of the deuteron, where we have to do with two heavy particles which are not very far apart in comparison to the range of nuclear forces. If we deduce the nuclear forces from a charge bearing field theory, there will be currents between the two heavy particles. These exchange currents will give rise to radiation and must be taken into consideration when calculating the probability of electric dipole radiation; i.e., it will not suffice to know only the currents that are due to the motion of the heavy particles. For the interaction of the system with the radiation field, in the limit of wave-lengths large compared to the size of the deuteron, is determined by

$$-(\mathbf{A}/c)\cdot\int \mathbf{s}(x)d\tau,$$

where $\mathbf{A}$ is the vector potential of the radiation field, and $\mathbf{s}(x)$ is the current density. There are contributions to $\mathbf{s}(x)$ from both heavy and light particles, and one might suppose that a detailed knowledge of the light particle current would be necessary to determine this interaction energy. However, as Siegert[14] has shown, one may avoid this by use of the conservation laws of charge and current. By their help, the above interaction energy may be transformed into the form

$$-(\mathbf{A}/c)\cdot\int \mathbf{x}\partial\rho(x)/\partial t d\tau = -(\mathbf{A}\cdot\partial\mathbf{D}/\partial t)/c, \quad (1)$$

where $\mathbf{D}$ is the dipole moment of the system. The advantage of this form is that one would expect the matrix elements of the light particle charge density to vanish identically, since particles of both signs contribute to the exchange current. This point may be verified on either electron-neutrino or dynaton field theory. Then the dipole moment of the system $\mathbf{D}=e\mathbf{r}/2$, where $\mathbf{r}=\mathbf{P}-\mathbf{N}$, and the required $\partial\mathbf{D}/\partial t$ can be calculated from the equations of motion of the heavy particle, namely:

$$\partial\mathbf{D}/\partial t = \frac{i}{\hbar}(H\mathbf{D}-\mathbf{D}H). \quad (2)$$

The Hamiltonian H contains the kinetic energy, and an exchange potential which (unlike an ordinary potential) does not commute with $\mathbf{r}$. One finds

$$\partial\mathbf{D}/\partial t = e\left\{\frac{\hbar}{Mi}\,\mathrm{grad}_r + \frac{\mathbf{r}}{i\hbar}J(r)\right\}, \quad (3)$$

where the first term, as is usual, comes from the kinetic energy term $-(\hbar^2/M)\Delta_r$ of H, while the new term with $\mathbf{r}J(r)$ arises from the exchange potential $J(r)P$, where P is an operator which exchanges neutron and proton. One may further transform the interaction energy

$$-(\partial\mathbf{D}/\partial t\cdot\mathbf{A})/c = -1/c\{\mathbf{D}\cdot\mathcal{E}+\partial/\partial t(\mathbf{D}\cdot\mathbf{A})\}, \quad (4)$$

where the last term will not contribute to radiative transitions. This provides a justification for the procedure of Breit and Condon,[1] who calculated the probability of the photodisintegration of the deuteron by the use of only the dipole moment operator $\mathbf{D}$ of the system. Naturally, the exchange currents still play a role, only this is now hidden in the effect of the exchange forces on the wave functions that are used in the calculation of the matrix elements. Investigation in which the scalar dynaton theory is used checks this result of Siegert in detail. The connection between exchange force and exchange current is given by the equality[15]

$$\int \mathbf{s}(x)d\tau = \mathbf{S}(r) = -ie\mathbf{r}J(r). \quad (5)$$

However, since the above relation between force and current depends on the validity of the conservation laws, one would not expect to be able to derive it on the basis of the electron-neutrino theory, and in fact, one cannot so derive it.

[14] A. J. F. Siegert, Phys. Rev. **52**, 787 (1937). We have enjoyed several helpful discussions with Dr. Siegert, and wish to thank him for them.

[15] We use "relativistic units" in what follows: $\hbar$ and c are set equal to unity.

We now consider the questions of the magnetic moment and magnetic dipole radiation in the deuteron. If a heavy-light particle coupling is used which gives isolated neutrons and protons a magnetic moment, we would expect extra terms to appear in the interaction of a deuteron with an electromagnetic field because of the magnetic moment of the exchange current. The six vector scalar dynaton, which gives a magnetic moment of the same sign and magnitude for neutron and proton, gives a magnetic moment operator for the deuteron of

$$\mu_{\text{deuteron}} = g\gamma\eta(M/16\pi em)(1-2e^{-mr})(\boldsymbol{\sigma}_N+\boldsymbol{\sigma}_P). \quad (6)$$

The interference term with e^{-mr} appears with a negative sign, which comes from the action of the exclusion principle on the heavy particles, and is related to the repulsive nature of the neutron-proton forces. With reasonable values of the constants, one can fit both the observed proton and deuteron magnetic moments. However, since $\boldsymbol{\sigma}_N+\boldsymbol{\sigma}_P$ is a constant of the motion, one could get magnetic dipole radiation from a transition between states of the deuteron only from an intrinsic magnetic moment of the proton; if this were about one n.m., it would be insufficient to account for the radiative capture of slow neutrons in paraffin. In the form of the electron-neutrino theory for which neutrons and protons have equal and opposite magnetic moments, there is no net extra magnetic moment for the deuteron, as the operator for the interaction energy with a magnetic field $\mathfrak{H}$ contains the spin matrices of the heavy particles only through $(\boldsymbol{\sigma}_N-\boldsymbol{\sigma}_P)\cdot\mathfrak{H}$ and $[\boldsymbol{\sigma}_N\times\boldsymbol{\sigma}_P\cdot\mathfrak{H}]$. Such terms will however give rise to extra magnetic dipole radiation, and for the capture of slow neutrons, the corrections to the probability are quite appreciable.

We must ask if it will be possible to retain a phenomenological description of magnetic dipole transitions involving the exchange force in a manner similar to the one Siegert found suitable for the electric dipole radiation. The answer seems to be in the negative. In the first place, it is possible in our field theory because of the space dependence of the interference magnetic moment operator, to obtain magnetic dipole radiation in the collision of a neutron and a proton even in order g^2e, while the possibility of this radiation in the usual phenomenological discussion depends both on the existence of magnetic moments (order g^2e) and the presence of Heisenberg exchange forces (order g^2). Second, if one does go to fourth order in g, the contributions of the exchange currents really do appear in addition to those of the currents about each heavy particle. Finally, the terms involving $[\boldsymbol{\sigma}_N\times\boldsymbol{\sigma}_P\cdot\mathfrak{H}]$ are quite unlike any that appear in the phenomenological treatment.

Hence it seems likely that processes involving the coupling of magnetic moments with the electromagnetic field should not be trusted when information about the position of the singlet level of the deuteron is desired. While it is known from scattering experiments that this level is close to zero potential, it may not be safe to infer from data on the probability of magnetic dipole capture alone that the level is a virtual one.[16] The possibility of complications of a similar nature may be expected and should be kept in mind when looking for regularities in the magnetic moments and magnetic multipole radiation of heavier nuclei.

Spin-Dependent Forces Between Elementary Particles

If one assumes that the force between neutron and proton is purely of Majorana type, and treats the heavy particles nonrelativistically, the singlet and triplet levels in the deuteron coincide;[17] from experiment, on the other hand, the singlet level is known to lie some two million volts higher. Bethe and Bacher[18] and Casimir[19] have estimated the splitting of the S term due to the magnetic interaction which is present if one assigns phenomenologically described magnetic moments to the particles, and although their

[16] This point will probably be settled definitely by a study of the scattering of slow neutrons by ortho- and para-hydrogen. (J. Schwinger and E. Teller, Phys. Rev. **52**, 286 (1937).) Even if the level should prove to be virtual, there seems to be some discrepancy between the observed and theoretical life times of neutrons in hydrogen, and this may be due to the phenomenon discussed above.

[17] We shall not consider here the spin-spin forces which arise from the many possible relativistic extensions of the two-body interaction, or even those which would arise in our calculations from a retention of the higher terms in the heavy particle velocities. See G. Breit, Phys. Rev. **51**, 248 (1937); **53**, 153 (1938). We are indebted to Professor Breit for several interesting communications dealing with these questions.

[18] H. A. Bethe and R. F. Bacher, Rev. Mod. Phys. **8**, 82 (1936).

[19] H. Casimir, Physica **3**, 936 (1936).

results differ by a factor of a thousand, both are too small (100 ev, 10^5 ev) to fit the experiments, and hence seem to require the admixture of some Heisenberg type interaction in the spin dependence of $J(r)$. In view of the above discrepancy, however, it seems of interest to examine the splitting predicted by one of the field theories which we have been considering.

Bethe and Bacher assumed a spin-spin coupling for neutron and proton

$$U_0=\mu_N\mu_P(\boldsymbol{\sigma}_N\cdot\boldsymbol{\sigma}_P/r^3-3\boldsymbol{\sigma}_N\cdot\mathbf{r}\boldsymbol{\sigma}_P\cdot\mathbf{r}/r^5) \quad (7)$$

based on the classical interaction of two point dipoles. Because of its angular dependence, this gives a splitting of the ground S state of the deuteron only in second order. It is obvious, however, that Eq. (7) is too singular at $r=0$ for unambiguous use in a perturbation calculation.

On the other hand, in his two particle equations, Casimir took the coupling energy appropriate for steady currents

$$-\int\frac{\mathbf{s}(N)\cdot\mathbf{s}(P)}{r}d\tau \quad (8)$$

and for the $\mathbf{s}$'s inserted the polarization currents corresponding to the observed magnetic moments, thus

$$\mathbf{s}(N)=\mu_N \text{ curl } \{\phi^*(N)\boldsymbol{\sigma}_N\phi(N)\} \quad (9)$$

and similarly for the proton. After partial integrations (in which surface terms also contribute), one finds an interaction containing besides the terms (7), a part independent of orbital angles and containing a delta-function of the separation $\mathbf{r}$ of the particles

$$U_s=U_0-\frac{4\pi}{3}\mu_N\mu_P\boldsymbol{\sigma}_N\cdot\boldsymbol{\sigma}_P\delta(\mathbf{r}) \quad (10)$$

so that a splitting of an S state results in first order.

However, with a phenomenological description of the magnetic moments, it is not possible unambiguously to deduce a magnetic interaction energy for the neutron and proton. Thus the sign and magnitude of the delta-function term in Eq. (10) would be changed[20] if one were to couple the single heavy particles to the electromagnetic field by their magnetic moments, taking for the interaction energy

$$-\{\boldsymbol{\mu}_N\cdot\mathfrak{H}(N)+\boldsymbol{\mu}_P\cdot\mathfrak{H}(P)\}, \quad (11)$$

where $\mathfrak{H}$ is the magnetic field, instead of a current coupling

$$-\{\mathbf{s}(N)\cdot\mathbf{A}(N)+\mathbf{s}(P)\cdot\mathbf{A}(P)\}, \quad (12)$$

which can be used when div $\mathbf{s}=0$ to derive Eq. (8). Of course, with the view that the magnetic moments of the single heavy particles arise largely from the light particle currents which surround them, one would tend to rule out the coupling (11).

Now it may be that a part of the proton's magnetic moment may be treated in analogy to the magnetic moment of an electron. For this part of μ_P, Eq. (8) is applicable, and gives a splitting analogous to that derived in hyperfine structure calculations. According to our model, however, the remaining magnetic moments arise from the light particle field, and the theory of this should be used to calculate the magnetic splitting.

According to an electron neutrino field model which gives neutron and proton equal and opposite magnetic moments,[21] a magnetic spin-spin coupling between neutron and proton arises in order g^4e^2, i.e., in a sixth-order perturbation calculation, and while one can, in fact, show that some of the terms in the calculation may be put into the form of Eqs. (8) and (9) with magnetic moments characteristic of the single heavy particles, there are also contributions from terms which correspond to an exchange of light particles between the two heavy particles. These in effect change the coefficient of the delta function in Eq. (10) by an amount of order unity. This will lead to a magnetic interaction which is in no simple way connected to the observed magnetic dipole moments; hence from this point of view, neither of the previously used magnetic

[20] G. Breit and F. W. Doermann, Phys. Rev. **36**, 1732 (1930).

[21] We abstract here from the complication that when the particular electron-neutrino coupling of Eq. (19) which gives neutron and proton oppositely equal magnetic moments is used, the cross terms in the coupling lead to Heisenberg forces. For in the above, we are particularly interested in magnetic spin-spin forces; furthermore, one could avoid the Heisenberg forces by a more general electron-neutrino coupling.

interactions is applicable. From an examination of typical terms in the field theoretic calculation when $r\sim 0$, it seems likely that there will be a coupling which is finite at $r=0$, and which also gives a first order splitting of S states from the anomalous part of the proton's magnetic moment and is probably not different in order of magnitude from Casimir's result.

In view of the considerable role of exchange in the magnetic interaction of neutron and proton, one may ask whether any appreciable changes are to be expected in the formula for the magnetic interaction of heavy particles and electrons, which is used in calculations of hyperfine structure and magnetic scattering of neutrons,[22] etc. In fact, there seems to be some evidence for this in the discrepancy between the values given by Stern[23] and by Rabi[24] for the magnetic moment of the proton. As Young[25] has pointed out, the differences in the apparent magnetic moment $\mu_P=2.46\pm 0.08$ and 2.85 ± 0.15 could be accounted for by an additional spin-dependent proton-electron coupling. If this discrepancy is real, it will suggest strongly that a theory of the electron-neutrino type is preferable to one of the dynaton type, for while with the latter, one would not expect any important new spin-dependent electron-proton forces, the electron-neutrino field theory which we have been investigating does lead in order g^2e^2 to such an additional interaction (arising from an exchange of the original electron and that emitted by the heavy particle.)[26] This leads one to expect deviations from the usual magnetic interaction of order $\sim e^2\sim 1/137$. We do not, however, regard the formalism as sufficiently reliable to justify a more accurate estimate of these deviations.

Appendix I

Interaction energy of a neutron and a proton

For the purposes of this section, we need consider only the scalar dynaton theory with the coupling energy

$$H_d=g\int[\phi_P^*(x)\beta\phi_N(x)]\phi_D(x)d\mathbf{x}+\text{conjugate.}\quad(13)$$

Here, ϕ_N, ϕ_P, ϕ_D are the neutron, proton, and dynaton wave functions, respectively, β is the Dirac matrix, and g is a dimensionless parameter measuring the strength of the coupling. "Relativistic units," in which $\hbar$ and c are set equal to unity, are used throughout. ϕ_D is assumed to satisfy the scalar relativistic wave equation investigated by Pauli and Weisskopf.[7] We use non-relativistic theory for the heavy particles, so that ϕ_N and ϕ_P are two component functions and the β connecting them may be set equal to the unit matrix.

Using the method of quantized waves,[27] we put

$$\phi_N(x)=\sum_\alpha A_\alpha u_\alpha(x),\quad \phi_P(x)=\sum_\beta B_\beta v_\beta(x),$$

where the u's and v's are complete orthonormal sets of state functions, and the A's and B's operate on the occupation numbers of neutrons and protons, respectively, in the Schrödinger functional and obey Fermi commutation rules. For the dynatons we follow Pauli and Weisskopf, and use plane waves normalized in the $\mathbf{k}$ scale

$$\phi_D(x)=\int(2\pi)^{-3}(2E_k)^{-\frac{1}{2}}(a_k-b_k^*)\exp(i\mathbf{kx})d\mathbf{x},$$

where $E_k=(k^2+m^2)^{\frac{1}{2}}$ is the dynaton energy, m the dynaton mass, and the a's and b's operate on the positive and negative dynaton occupation numbers, respectively, and obey Bose commutation rules. We adopt the convention that unstarred operators destroy particles, and starred operators (complex conjugates of the unstarred ones) create them. The coupling (13) then becomes

$$H_d=g\sum_{\alpha,\beta}\int\int(2\pi)^{-3}(2E_k)^{-\frac{1}{2}}v_\beta^*(x)u_\alpha(x)$$
$$\times\exp(i\mathbf{kx})B_\beta^*A_\alpha(a_k-b_k^*)d\mathbf{x}d\mathbf{k}+\text{conjugate.}$$

Here, the first term corresponds to a neutron changing into a proton with either the emission of a negative or the absorption of a positive

[22] F. Bloch, Phys. Rev. **51**, 994 (1937).
[23] I. Estermann, O. C. Simpson and O. Stern, Phys. Rev. **52**, 535 (1937).
[24] J. M. B. Kellogg, I. I. Rabi and J. R. Zacharias, Phys. Rev. **50**, 472 (1936).
[25] L. A. Young, Phys. Rev. **52**, 138 (1937).
[26] There is also a spin-spin interaction even in order g^2, but this must be assumed small due to the fact that the coupling of low energy electrons and heavy particles is known to be small from the observed slowness of β-decay.
[27] Reference 10, page 198.

dynaton; the complex conjugate term corresponds to a proton changing into a neutron with either the emission of a positive or the absorption of a negative dynaton. Because of the anti-commuting properties of the A's and of the B's, it is necessary to keep their order straight.

The matrix element of the interaction energy between a neutron and a proton is the second order perturbation energy computed from the transitions in which either (a) the proton emits a positive dynaton and changes into a neutron, the dynaton subsequently being absorbed by one of the neutrons; or (b) the neutron emits a negative dynaton and changes into a proton, the dynaton subsequently being absorbed by one of the protons. These two types of transition give the same formal result; we need consider only (a), and multiply the final answer by two. If the initial neutron and proton states are u_α and v_β, and their final states are u_η and v_γ, respectively, then the interaction energy is

$$-g^2\int d\mathbf{k}/(16\pi^3E_k^2)\Big\{\int v_\gamma^*(x)u_\alpha(x)\exp(i\mathbf{kx})d\mathbf{x}\times\int u_\eta^*(x')v_\beta(x')\exp(-i\mathbf{kx}')d\mathbf{x}'(1-\delta_{\alpha\eta})Q$$
$$+\sum_\xi\int v_\gamma^*(x)u_\xi(x)\exp(i\mathbf{kx})d\mathbf{x}\times\int u_\xi^*(x')v_\beta(x')\exp(-i\mathbf{kx}')d\mathbf{x}'\delta_{\alpha\eta}R\Big\}.$$

Here,

$$Q\equiv\Psi^*(1N_\eta,1P_\gamma)B_\gamma^*A_\alpha A_\eta^*B_\beta a_k a_k^*\Psi(1N_\alpha,1P_\beta)$$
$$=\Psi^*(1N_\eta,1P_\gamma)B_\gamma^*B_\beta(\delta_{\alpha\eta}-A_\eta^*A_\alpha)\times(1+a_k^*a_k)\Psi(1N_\alpha,1P_\beta)=\delta_{\alpha\eta}-1,$$
$$R\equiv\Psi^*(1N_\alpha,1P_\gamma)B_\gamma^*A_\xi A_\xi^*B_\beta a_k a_k^*\Psi(1N_\alpha,1P_\beta)$$
$$=\Psi^*(1N_\alpha,1P_\gamma)B_\gamma^*B_\beta(1-A_\xi^*A_\xi)\times(1+a_k^*a_k)\Psi(1N_\alpha,1P_\beta)=1-\delta_{\alpha\xi},$$

on making use of the commutation rules for the various operators; $\Psi(1N_\alpha,1P_\beta)$ and $\Psi(1N_\eta,1P_\gamma)$ are the Schrödinger functionals for the initial and final states respectively. The expression for the interaction energy thus becomes

$$+g^2\int d\mathbf{k}/(16\pi^3E_k^2)\Big\{\int v_\gamma^*(x)u_\alpha(x)\exp(i\mathbf{kx})d\mathbf{x}\times\int u_\eta^*(x')v_\beta(x')\exp(-i\mathbf{kx}')d\mathbf{x}'$$
$$-\delta_{\alpha\eta}\sum_\xi\int v_\gamma^*(x)u_\xi(x)\exp(i\mathbf{kx})d\mathbf{x}\times\int u_\xi^*(x')v_\beta(x')\exp(-i\mathbf{kx}')d\mathbf{x}'\Big\}.$$

Considering the second term of this expression, we can perform the sum over ξ by making use of the closure theorem, and thus obtain $-\delta_{\alpha\eta}\delta_{\beta\gamma}g^2\int d\mathbf{k}/(16\pi^3E_k^2)$; this is the negatively infinite "proper" energy of a proton in state v_β, and appears only in the diagonal elements, as it should. The first term in the above expression is readily evaluated and is

$$+\int\int u_\eta^*(x')v_\gamma^*(x)(g^2e^{-mr}/8\pi r)\times u_\alpha(x)v_\beta(x')d\mathbf{x}d\mathbf{x}',\quad \mathbf{r}\equiv\mathbf{x}-\mathbf{x}'.$$

This expression for the interaction energy has been given correctly by Serber[5] and by Yukawa and Sakata.[28] Other investigators, apparently, have not examined the structure of the term Q above carefully enough to realize that it has the effect of making the sign of the interaction energy just the opposite of what would be expected intuitively. The appearance of this sign derives from the fact that the exclusion principle is valid for the heavy particles, and is independent of the statistics obeyed by the light particles in the field. Thus the operator for the total interaction energy is

$$J(r)=+(g^2e^{-mr}/4\pi r)P^H,\qquad(14)$$

where P^H is the Heisenberg exchange operator; this is repulsive for a symmetric state. $J(r)$ is of the right order of magnitude if the phase integral $\int[MJ(r)]^{\frac{1}{2}}dr\sim1$, where M is the mass of the neutron or proton. This makes $g\sim1$.

For comparison, it is interesting to consider what form the Q and R above would have if neutrons and protons were to obey Bose statistics. Using Bose commutation rules for the

[28] H. Yukawa and S. Sakata, Proc. Phys.-Math. Soc. Japan, **19**, 1084 (1937).

A's and B's, we obtain

$$Q'=\delta_{\alpha\eta}+1, \quad R'=1+\delta_{\alpha\xi},$$

which result in the same proper energy as above, but change the sign of the interaction energy (14).

An exactly analogous calculation can be carried through with the electron-neutrino theory, in which the simplest coupling is used

$$H_a=g\int[\phi_N^*(x)\beta\phi_P(x)]$$

$$\times[\phi_n^*(x)\beta\phi_e(x)]d\mathbf{x}+\text{conjugate}, \quad (15)$$

where ϕ_e and ϕ_n are the electron and neutrino wave functions that satisfy the ordinary Dirac equation (with and without charge, respectively). In order to have a convergent theory, however, it is necessary to multiply electron and neutrino wave functions by a cut-off factor or finite distance operator of the general form $e^{-a|E|}$, where E is the light particle energy. The resulting interaction energy has the same sign and exchange character as (14); its range is $\sim a$, and its magnitude is $\sim g^2/a^5$. The phase integral condition on the magnitude of the interaction gives $g^2\sim a^2/M$.

Appendix II

Electric properties and Siegert's theorem

The expectation values of the charge and current density about a stationary neutron on the dynaton theory can be found by computing the diagonal matrix elements of the corresponding operators, which are given by Pauli and Weisskopf.[7] The calculations are straightforward, and result in a zero current density, and a charge density given by

$$\rho(r)=(eg^2m/16\pi^3r^2)K_1(mr)e^{-mr},$$

where r is the distance from the neutron, and K_1 is the Bessel function of imaginary argument.[29] The total charge corresponding to this charge density is infinite; but the expectation value of the charge on the heavy particle is also infinite, and it is easy to show that the two charges cancel term by term. On the electron-neutrino theory, with the coupling (15), the current density again vanishes. The expression for the charge density is quite complicated; however, its asymptotic form is

$$\rho(r)\sim-(eg^2a/r^8)\log(r/a), \quad r\gg a,$$

and the mean radius of the charge cloud is $\sim a$, where a is the parameter in the finite distance operator introduced in Appendix I. The presence of this parameter also makes the total charge in the field finite and $\sim eg^2/a^4\sim e/Ma\sim e/13$.

When a neutron and a proton are brought close together, as in a deuteron, the expectation value of any quantity can always be expressed as the sum of a "proper" part and an "interference" part. The proper part is just the sum of the expectation values for the quantity in question for the isolated neutron and proton; the interference part arises from the emission of light charged particles by one heavy particle and their absorption by the other, and hence depends on the distance between the heavy particles and vanishes rapidly as this distance becomes large. The charge density on either of our field theories is readily calculated, and it turns out that the interference part of its expectation value vanishes, since the neutron is just as likely to be emitting a negative particle as the proton is to be emitting a positive particle; the proper charge clouds about the heavy particles remain as before and give nothing new. The proper current density, on the other hand, vanishes, while the interference part of the current is appreciable. The calculation of this "exchange current" is analogous to that of the interaction energy (see Appendix I); the matrix elements of the total current operator are computed between Schrödinger functionals perturbed by either of the couplings (13) or (15). With the dynaton theory, the total current for a transition in which the initial neutron and proton states are u_α and v_β, and their final states are u_η and v_γ, respectively, is

$$-eg^2\int\mathbf{k}d\mathbf{k}/(16\pi^3E_k^4)\int v_\gamma^*(x)u_\alpha(x)e^{i\mathbf{k}}\,d\mathbf{x}$$

$$\times\int u_\eta^*(x')v_\beta(x')e^{-i\mathbf{k}x'}d\mathbf{x}'.$$

[29] Whittaker and Watson, *Modern Analysis*, fourth edition (1935), p. 373.

This can be simplified to

$$-\int\int u_\eta^*(x')v_\gamma^*(x) \times(ieg^2\mathbf{r}e^{-mr}/4\pi r)u_\alpha(x)v_\beta(x')d\mathbf{x}d\mathbf{x}'.$$

Thus the operator for the total current is

$$\mathbf{S}(r)=-(ieg^2\mathbf{r}e^{-mr}/4\pi r)P^H.$$

Comparison of this with the expression (2) for the interaction energy operator checks the relation

$$\mathbf{S}(r)=-ie\mathbf{r}J(r), \tag{16}$$

which is given by Siegert.[14]

Appendix III

Magnetic properties of neutron and deuteron

The scalar dynaton possesses no spin, and hence no magnetic moment. However, it is possible to introduce terms into the Hamiltonian so that it gives a magnetic interaction with the radiation field:

$$H_v=g\int[\phi_P^*\beta\phi_N]\phi_D d\mathbf{x}+\gamma\int[\phi_P^*\sigma_{\mu\nu}\phi_N]\phi_{\mu\nu}d\mathbf{x} +\eta\int\phi_D^*F_{\mu\nu}\phi_{\mu\nu}d\mathbf{x}+\text{conjugate}. \tag{17}$$

The first term here was present in Eq. (13) and represents the coupling between heavy particles and scalar dynaton; the second term gives the coupling between heavy particles and six-vector dynaton $\phi_{\mu\nu}$, each component of which separately satisfies the Pauli-Weisskopf equation; and the third term connects the two kinds of dynatons with the electromagnetic field tensor $F_{\mu\nu}$. The dynaton magnetic moment operator is thus

$$\eta(\phi_D^*\phi_{\mu\nu}+\phi_{\mu\nu}^*\phi_D),$$

besides this there will be an imaginary electric moment associated with the dynaton, which will, however, be of the order of the relativistic correction to the heavy particle motion, since it involves the space-like components of the Dirac α_μ matrices. Thus the dynaton cloud about a stationary heavy particle is capable of interacting with the magnetic vector of the radiation field in a way that is connected to the spin vector of the heavy particle. Although the total charge in the dynaton cloud about a single neutron is infinite, the total magnetic moment is not; this is because the dynaton charge density operator is $ie(\phi_D^*\partial\phi_D/\partial t-\partial\phi_D^*/\partial t\phi_D)$, which contains one less E_k in the denominator than the magnetic moment operator and thus causes the expression for the total charge to diverge at high dynaton momenta. The diagonal matrix element of the magnetic moment operator for a stationary neutron is readily calculated, and is to lowest order in the various coupling parameters $\boldsymbol{\mu}_N=(g\gamma\eta/32\pi m)(2M/e)\boldsymbol{\sigma}_N$ nuclear magnetons. This is of the right order of magnitude for the neutron moment if $g\gamma\eta$ is ~ 1. The magnetic moment of a proton at rest (aside from any intrinsic moment) is also given by the above expression, with the same sign. The appearance of both neutron and proton with the same sign of magnetic moment derives basically from the fact that the coupling with the electromagnetic field is through the field tensor $F_{\mu\nu}$, and not through the vector potential. Thus, interchanging positive and negative dynatons in (17) (i.e., replacing ϕ_D by ϕ_D^* and $\phi_{\mu\nu}$ by $\phi_{\mu\nu}^*$) and also interchanging neutron and proton, the magnetic field coupling terms as well as the light-heavy particle coupling terms remain unchanged. This gives positive and negative dynatons, and hence neutrons and protons, the same magnetic moment.

It is interesting to note that the γ terms in (17) lead to a mixed Majorana-Heisenberg interaction between a neutron and a proton

$$J(r)=(\gamma^2e^{-mr}/4\pi r)(2P^M-P^H),$$

which is again repulsive for a symmetric state. Thus by properly choosing g and γ, the unlike particle interaction can be made to have the right magnitude and exchange character, but still not the right sign.

On the electron-neutrino theory, any magnetic moment that might appear would come from the relativistic electron current, and thus the introduction of a new kind of particle is unnecessary. However, since the current density about a stationary neutron resulting from the coupling (15) vanishes, it is necessary to modify it so that a current appears that is coupled to the spin

axis of the neutron. The coupling term

$$H_b = g\int [\phi_N{}^*\beta\phi_e][\phi_n{}^*\beta\phi_P]d\mathbf{x} + \text{conjugate} \quad (18)$$

(which leads to a Majorana interaction between a neutron and a proton) serves to give the neutron a magnetic moment that is approximately

$$\mu_N \sim -(g^2e/a^3)(2M/e)\boldsymbol{\sigma}_N \text{ nuclear magnetons},$$

but gives the proton none since it clearly contains no connection between proton and electron. However, (18) can be modified so as to make it symmetric between neutron and proton:

$$H_c = H_b + \left\{ g'e^{i\theta}\int [\phi_N{}^*\beta\delta\tilde{\phi}_n{}^*] \times [\tilde{\phi}_P\beta\delta\phi_e]d\mathbf{x} + \text{conjugate} \right\}, \quad (19)$$

where $\tilde{\phi}$ is the transpose of ϕ, δ is Fermi's matrix and θ is any real number. When the two parameters g and g' are chosen equal, the magnetic moments of neutron and proton are equal and opposite in sign, except for a possible intrinsic magnetic moment of the proton.

When the two-body situation is considered, the total magnetic moment appears as the sum of the proper moments of the isolated particles, and an interference term which depends on their distance apart. With the dynaton theory, the matrix element of this interference term between initial neutron and proton states u_α and v_β, and final states u_η and v_γ, respectively, is

$$-\int\int u_\eta{}^*(x')v_\gamma{}^*(x)(g\gamma\eta M/8\pi em)e^{-mr}(\boldsymbol{\sigma}_N+\boldsymbol{\sigma}_P) \times u_\alpha(x)v_\beta(x')d\mathbf{x}d\mathbf{x}' \text{ nuclear magnetons.}$$

Thus the total magnetic moment operator, including the proper moments of the isolated particles, is

$$\mu_{\text{deuteron}} = (g\gamma\eta M/16\pi em) \times (1-2e^{-mr})(\boldsymbol{\sigma}_N+\boldsymbol{\sigma}_P) \text{ nuclear magnetons.}$$

Since this is proportional to $\boldsymbol{\sigma}_N+\boldsymbol{\sigma}_P$, which is a constant of the motion, it cannot give rise to radiative magnetic dipole transitions.

The electron-neutrino theory with coupling H_b of Eq. (18) leads to an interference magnetic moment operator for the deuteron

$$\mu_{\text{deuteron}} = (eg^2/4)\boldsymbol{\sigma}_N \cdot F(r),$$

where

$$F(r) = \sum_{s,\,t}[e^{i(\mathfrak{p}_s+\mathfrak{p}_t)\mathfrak{r}}/E_s(E_s+E_t)^2],$$

where the sum is over intermediate electron states s and anti-neutrino states t. $F(r)$ falls off rapidly for large r, and is $\sim g^2/a^3$ for $r=0$. We see that μ_{deuteron} has the form of an effective extra magnetic moment μ_N' for the neutron. If the neutron and proton were brought together ($r=0$), μ_N' would be of the order of μ_N for an isolated neutron. If we use the coupling (19), which is symmetric between neutron and proton, the proton will also have an extra moment $\mu_P' = -\mu_N'$. In addition, however, the cross terms of H_c lead to a coupling of the deuteron with the magnetic field

$$-(eg^2/4)\{(\boldsymbol{\sigma}_N-\boldsymbol{\sigma}_P)\cdot\mathfrak{H}\cos\theta + [\boldsymbol{\sigma}_N\times\boldsymbol{\sigma}_P]\cdot\mathfrak{H}\sin\theta\}F(r).$$

We see that, on the electron-neutrino theory with H_c, the extra magnetic moment operator for the deuteron has only off-diagonal elements, and thus can contribute only to magnetic dipole radiation and not to the net magnetic moment of the deuteron in either singlet or triplet states. In the limit $\alpha_t a \to 0$, $|\alpha_s| \ll \alpha_t$ (where the α's are the wave numbers corresponding to triplet and singlet states of the deuteron), one finds corrections to the transition rate of order $\alpha_t a$; for larger $\alpha_t a \to 1$, the corrections can become of order unity. (Actually $\alpha_t a \sim 0.6$.)

We are greatly indebted to Professor J. R. Oppenheimer and to Dr. Robert Serber for many helpful suggestions and for encouragement during the course of these investigations.

Self-Consistent Field for Iron

MILLARD F. MANNING, *Massachusetts Institute of Technology and University of Toledo*

AND

LEO GOLDBERG, *Harvard College Observatory*

(Received January 22, 1938)

This paper reports the results of self-consistent field calculations for the d^6s^2 configuration of iron. Preliminary calculations were made on the Massachusetts Institute of Technology differential analyzer. The final results were obtained by numerical integration. For all of the wave functions the discrepancy between final and semi-final values of Z is less than 0.010. A brief discussion of the relation of the results to spectroscopy and to Slater's theory of ferromagnetism is given.

THE group of atoms between potassium and zinc is one of the most interesting in the periodic table. The spectra of these elements are particularly interesting to astrophysicists, and the solids formed by these elements have many properties, particularly ferromagnetism, which have been studied experimentally and theoretically for many years. For a detailed quantum-mechanical discussion of the behavior of a particular element, a knowledge of the wave functions is usually necessary. In this paper are reported the results of calculations of the wave functions for iron as found by the Hartree self-consistent field method.

In this method the wave function of a many electron atom is written as a product of one-electron wave functions of the type,

$$\Psi_{n,l}=\Phi(\phi)\Theta(\theta)Y_{n,l}(r)/r^{\frac{1}{2}}, \qquad (1)$$

where $r^{\frac{1}{2}}Y_{n,l}$ has the same meaning as the $P_{n,l}$ used by Hartree.[1] In all other respects the notation used in this paper is the same as that used by Hartree.[1] The differential equation which a particular $Y_{n,l}$ satisfies is:

$$d^2Y/d\rho^2+[2rZ_p-\epsilon r^2-(l+\tfrac{1}{2})^2]Y=0. \qquad (2)$$

The substitutions $\rho\equiv\log_e r$ and $Y=Pr^{-\frac{1}{2}}$ were suggested by Hartree[2] in his report on self-consistent field calculations for mercury. The use of Y and ρ as variables is considerably more convenient than the use of P and r, because it is possible to carry out the entire range of integration with only one change of interval of the independent variable.

When the wave functions are known, the field due to a particular subshell of electrons, and the corresponding nuclear charge, is equal to $r^2Z^{n,l}$ and

$$Z_{n,l}=2(2l+1)\int_{\infty}^{\rho}Y^2e^{2\rho}d\rho/\int_{+\infty}^{-\infty}Y^2e^{2\rho}d\rho. \qquad (3)$$

The potential at a given radius due to a particular subshell and its associated nuclear charge is equal to $rZ_p{}^{n,l}$, where Z_p is found by solution of the differential equation:

$$dZ_p{}^{n,l}/d\rho=Z_p{}^{n,l}-Z^{n,l} \qquad (4)$$

subject to the condition that $Z_p{}^{n,l}\to 0$ at large values of r (or ρ).

The starting point in self-consistent field calculations is usually made by estimating the Z's of the separate subshells. In this case the method used was that described in a previous paper.[3] For the $1s$, $2s$, $2p$, $3s$, $3p$, interpolations between Ca and Cu^+ could be used. Estimates for the $3d$ were found by interpolating between Cr $(3d)^6$ and Cu^+, but since neither of these is a normal configuration, the initial estimates were not very satisfactory. It was also difficult to make a good first approximation for the $4s$. Because of these difficulties and because the $3d$ electron is so sensitive to the assumed field, a number of determinations of the $3p$, $4s$, and particularly $3d$,

[1] D. R. Hartree, Proc. Roy. Soc. **A141**, 285 (1933).
[2] D. R. and W. Hartree, Proc. Roy. Soc. **A149**, 210 (1935).
[3] Manning and Millman, Phys. Rev. **49**, 849 (1936). At this time we wish to thank Dr. Millman for his assistance in making the initial estimates.

wave functions had to be made before a reasonably consistent solution was obtained.

These early determinations were carried out under the direction of one of us on the Massachusetts Institute of Technology differential analyzer[4] which was very kindly placed at his disposal by Professor S. H. Caldwell of the department of electrical engineering.

The values of Y near $r=0$, are found by a power series expansion in r. The value of ϵ in Eq. (2) is to be so chosen that at large values of r, Y should approach zero. When using the differential analyzer, this condition is most readily satisfied by carrying solutions for a range of values of ϵ to a value of ρ just beyond the outermost maximum of the wave function. At this point, the numerical values needed for outward integration for intermediate values of ϵ are found by least squares interpolation. After successive trials, a value of ϵ is found for which the boundary condition is fulfilled. For further details the reader is referred to the paper on tungsten.[3, 5]

Since the application of the results of the self-consistent field calculations to spectroscopy and theories of ferromagnetism requires more accurate results than were needed for the proposed application of the tungsten results, a further set of approximations was obtained by numerical integration.

The remaining stages of integration have been carried out at Harvard Observatory and at the University of Toledo.[6] For the inner electrons, the general method was the same as that used on the differential analyzer—repeated trials until a solution satisfying the boundary conditions was found. For one- and two-quantum electrons this method is quite convenient. For the three- and four-quantum electrons this method suffers from at least two drawbacks. In the large number of separate stages of the step-by-step process of integration, there is considerable chance of an embarrassing accumulation of rounding-off errors. Another difficulty is that when it has been found that one value of ϵ is too large and another too small there is no satisfactory method of estimating the correct intermediate value. For the outer electrons a method suggested by Hartree[7] is preferable. For a particular ϵ, Eq. (2) is carried to a point just inside the outer point of inflection and the value of $dY/Yd\rho$ is computed. A transformed equation is then integrated inwards from a large value of ρ, where an asymptotic solution can be found. Several forms of transformed equation are possible, but the most satisfactory is that for $\eta(\equiv dP/Pdr)$ which is:

$$d\eta/d\rho=\epsilon r+l(l+1)/r-2Z_p-r\eta^2. \qquad (5)$$

The solution of this equation is carried to the same point as that for which $dY/Yd\rho$ has been found by outward integration. If the value of ϵ used is an eigenvalue, the relation between η and $dY/Yd\rho$ should be:

$$dY/Yd\rho=-\tfrac{1}{2}-r\eta. \qquad (6)$$

Both $dY/Yd\rho$ and η change very nearly linearly with ϵ and hence when integrations for two values of ϵ have been carried out, a very close estimate of the eigenvalue can be made. When previous stages of approximation are available, it is even possible to make very close estimates of the change of η and $dY/Yd\rho$ with ϵ.

In the actual numerical integration[8] the authors have differed slightly from the method described by Hartree.[7] They have made no use of so-called "variation" equations, but have preferred to carry out solutions for two values of ϵ which enclose the correct solution, and to interpolate between these at comparatively large values of ρ. Rather than to tabulate differences, they have preferred a modification of methods developed by Milne and Steffensen,

[4] For many suggestions about the use of the differential analyzer in solving this sort of problem, I wish to express my thanks to Professor Caldwell and Professor P. M. Morse. For their hearty cooperation and skillful operation of the differential analyzer I am greatly indebted to Mr. D. D. Terwilliger and Mr. Darrell Roots. (MFM)

[5] It should be pointed out that in the published diagram on page 850 of that paper the caption under the first integrator should read:

$$\int[2rZ_p-\epsilon r^2-(l+\tfrac{1}{2})^2]Yd\rho=0.$$

[6] The computations at the University of Toledo were carried out on a computing machine purchased with funds provided for the purpose by the Permanent Science Fund of the American Academy of Arts and Sciences.

[7] D. R. Hartree, Proc. Camb. Phil. Soc. **24**, 89, 111 (1928); D. R. Hartree, Proc. Manch. Lit. Phil. Soc. **77**, 91 (1933).

[8] The authors wish to express their thanks to Dr. G. E. Kimball, Dr. H. M. Krutter, Dr. J. Millman, and Dr. T. E. Sterne for many enlightening conversations on the subject of numerical integration.

TABLE I. *Values of the 2 Z_p's.*

ρ	$(1s)^2$	$(2s)^2$	$(2p)^6$	$(3s)^2$	$(3p)^6$	$(3d)^6$	$(4s)^2$	ρ	$(1s)^2$	$(2s)^2$	$(2p)^6$	$(3s)^2$	$(3p)^6$	$(3d)^6$	$(4s)^2$
0.0	3.899	3.978	11.936	3.993	11.981	11.987	3.999	5.6		0.428	0.903	2.477	7.596	8.397	3.609
.2	3.876	3.974	11.921	3.992	11.977	11.984	3.999	.7		.301	.630	2.342	7.200	8.034	3.569
.4	3.849	3.968	11.904	3.990	11.972	11.980	3.999	.8		.201	.419	2.194	6.763	7.641	3.525
.6	3.815	3.961	11.882	3.988	11.966	11.976	3.998	.9		.127	.264	2.030	6.281	7.218	3.476
.8	3.774	3.952	11.856	3.985	11.958	11.970	3.997	6.0		.076	.157	1.850	5.753	6.766	3.422
1.0	3.725	3.941	11.824	3.981	11.949	11.963	3.996	.1		.043	.087	1.653	5.182	6.288	3.362
.2	3.664	3.929	11.786	3.977	11.937	11.955	3.995	.2		.022	.045	1.443	4.575	5.789	3.297
.4	3.591	3.913	11.739	3.972	11.923	11.945	3.994	.3		.011	.021	1.224	3.946	5.274	3.226
.6	3.501	3.894	11.681	3.966	11.907	11.933	3.993	.4		.005	.009	1.005	3.314	4.750	3.148
.8	3.394	3.870	11.610	3.959	11.886	11.919	3.991	.5		.002	.003	0.795	2.701	4.224	3.063
2.0	3.264	3.842	11.524	3.950	11.861	11.901	3.989	.6		.001	.001	.603	2.128	3.706	2.971
.2	3.108	3.807	11.418	3.939	11.830	11.879	3.987	.7				.437	1.615	3.204	2.871
.4	2.927	3.766	11.289	3.926	11.792	11.852	3.984	.8				.301	1.177	2.727	2.761
.6	2.703	3.716	11.132	3.910	11.746	11.819	3.980	.9				.196	0.820	2.281	2.641
.8	2.453	3.656	10.940	3.891	11.691	11.779	3.975	7.0				.120	.544	1.873	2.508
3.0	2.171	3.586	10.705	3.867	11.622	11.730	3.970	.1				.069	.342	1.507	2.361
.2	1.861	3.502	10.419	3.839	11.538	11.668	3.963	.2				.037	.202	1.186	2.199
.4	1.532	3.403	10.070	3.805	11.436	11.597	3.955	.3				.018	.112	0.911	2.022
.6	1.198	3.288	9.646	3.764	11.312	11.508	3.945	.4				.008	.058	.682	1.831
.8	0.879	3.154	9.132	3.715	11.161	11.400	3.933	.5				.003	.028	.496	1.628
4.0	.595	2.995	8.512	3.655	10.977	11.266	3.918	.6				.001	.012	.350	1.418
.1	.472	2.905	8.157	3.621	10.871	11.189	3.910	.7					.004	.236	1.205
.2	.364	2.806	7.771	3.583	10.755	11.103	3.901	.8					.001	.157	0.997
.3	.273	2.697	7.353	3.541	10.628	11.009	3.891	.9						.099	.800
.4	.197	2.576	6.903	3.495	10.489	10.906	3.880	8.0						.060	.620
.5	.137	2.443	6.421	3.444	10.337	10.790	3.867	.1						.035	.462
.6	.091	2.297	5.910	3.388	10.172	10.663	3.853	.2						.019	.330
.7	.058	2.136	5.374	3.326	9.993	10.522	3.838	.3						.010	.225
.8	.035	1.961	4.819	3.258	9.799	10.367	3.821	.4						.005	.146
.9	.021	1.772	4.252	3.184	9.590	10.196	3.803	.5						.002	.089
5.0	.011	1.572	3.683	3.103	9.366	10.007	3.783	.6						.001	.051
.1	.005	1.365	3.121	3.016	9.125	9.798	3.761	.7							.027
.2	.003	1.156	2.586	2.923	8.866	9.568	3.736	.8							.013
.3	.002	0.952	2.088	2.823	8.587	9.314	3.708	.9							.006
.4	.001	.758	1.636	2.716	8.285	9.036	3.678	9.0							.002
.5		.582	1.239	2.601	7.956	8.731	3.645								

which is described in a note to the editor, published in this issue.

A check on the accuracy of the integration formulas used can be made by tabulating differences for typical cases or by using two different integration formulas involving different assumptions about higher-order differences. This latter method is particularly applicable to the integration of Eq. (2). Ordinarily the formula involving second differences of the second derivative is sufficiently accurate, but its range of applicability can be tested by using the formula involving fourth differences of the second derivative. With the interval change at $\rho=4.0$, it is for only a few points in this neighborhood and for the last few values of ρ for the $1s$, $2s$, $2p$ functions that the correction is at all appreciable.

In self-consistent field calculations, considerable time and effort can be saved by estimating at the end of one approximation what is likely to happen during the next. If a given set of values for the Z_p of a given type of electron is assumed, and a wave function, charge density, and new Z_p calculated, the correct value of Z_p will, except possibly for indirect effects from other types of electron, lie somewhere between these values. With the results of the separate stages of calculations for two transition metals available, some general suggestions about other transition metals, particularly those having about the same atomic number as iron, are ventured. For the $1s$, $2s$, $2p$, $3s$, and even $4s$ electrons, the best estimate that can probably be made is to use the results of one stage of approximation as the initial values for the next approximation. For the $3p$ this process would yield an answer eventually, but a more rapid convergence is obtained if a value about two-thirds of the way from the assumed to the calculated value is used as the initial field for the next approximation. For the $3d$ electrons a straight iterative process would probably never

give a self-consistent solution. A process of halving the difference each time is bound to converge, and our experience indicates that once an approximately self-consistent field has been found, this process converges reasonably rapidly.

Results

Tables are given of the values of Y, $2Z$, $2Z_p$, for each type of electron as a function of ρ. Tables of ϵ, $\int_\infty^0 Y^2 e^{2\rho} d\rho$, and $-2v_0$ for each type of electron are also included. In the tables ρ stands for $\log_e 1000r$. In the actual integrations one and usually two more significant figures have been carried in the calculations than are tabulated. The consistency aimed at was the same as that obtained by Hartree[1] for Cu^+—namely, 0.01 in Z for any one type of electron. (This is essentially the same as a consistency of 0.01 in $2Z_p$.) Actually, the final calculations for even $3p$ and $3d$ are well within this tolerance. As Hartree[9] has pointed out, the changes that would be produced by the introduction of exchange corrections will be several times as large as this. However, he suggests that if accurate results for self-consistent field calculations are available, very good estimates of the exchange corrections can be made if Fock equations for neighboring atoms in the periodic table have already been studied.

The results give support to suggestions that have been made by Slater[10] about the explanation of ferromagnetism. In a crystal,* the discrete atomic levels of the valence electrons are per-

[9] D. R. Hartree and W. Hartree, Proc. Roy. Soc. **A157**, 490 (1936).

[10] J. C. Slater, Phys. Rev. **36**, 57 (1930); J. C. Slater, Phys. Rev. **49**, 537 (1936).

TABLE II. *Values of the Y's.*

ρ	$(1s)^2$	$(2s)^2$	$(2p)^6$	$(3s)^2$	$(3p)^6$	$(3d)^6$	$(4s)^2$	ρ	$(1s)^2$	$(2s)^2$	$(2p)^6$	$(3s)^2$	$(3p)^6$	$(3d)^6$	$(4s)^2$
0.0	2240	2240	20.00	2240	40.00	0.0300	2240	6.0	2	1744	1931	1493	5146	7366	1669
.2	2461	2461	26.92	2461	53.84	0.0484	2461	.1		1337	1473	2255	6723	7648	2402
.4	2701	2701	36.21	2701	72.42	0.0791	2701	.2		976	1081	2876	7981	7822	2963
.6	2960	2959	48.67	2959	97.34	0.1296	2959	.3		684	760	3321	8864	7875	3310
.8	3237	3236	65.36	3236	130.70	0.2128	3236	.4		452	510	3571	9342	7803	3417
1.0	3532	3530	87.66	3530	175.31	0.3492	3530	.5		284	325	3626	9417	7610	3280
.2	3843	3840	117.41	3840	234.8	0.5728	3840	.6		167	195	3504	9122	7307	2914
.4	4166	4162	157.0	4162	313.9	0.9384	4162	.7		92	110	3236	8518	6912	2351
.6	4499	4491	209.5	4490	418.9	1.5354	4490	.8		48	56	2864	7681	6444	1637
.8	4832	4820	278.8	4819	557.5	2.508	4818	.9		23	25	2433	6695	5927	821
2.0	5158	5138	369.9	5136	739.6	4.088	5135	7.0		10	11	1983	5642	5379	−43
.2	5464	5431	488.9	5427	977.5	6.647	5427	.1		4	4	1551	4596	4820	905
.4	5734	5681	643.3	5675	1285.9	10.777	5674	.2		2	1	1163	3671	4263	1720
.6	5949	5864	841.8	5855	1682.2	17.407	5854	.3		1		834	2745	3720	2451
.8	6086	5954	1094.1	5939	2186	28.00	5937	.4				571	2005	3201	3067
3.0	6122	5916	1410.5	5893	2816	44.79	5891	.5				372	1406	2714	3547
.2	6033	5715	1800.6	5681	3592	71.20	5678	.6				229	943	2263	3879
.4	5797	5317	2271	5266	4525	112.34	5261	.7				133	603	1855	4058
.6	5402	4691	2825	4617	5616	175.67	4609	.8				73	367	1492	4088
.8	4850	3820	3453	3715	6853	211.7	3704	.9				37	211	1174	3981
4.0	4162	2708	4135	2567	8173	415.0	2551	8.0				18	114	904	3756
.1	3778	2074	4484	1911	8836	510.0	1894	.1				8	58	679	3437
.2	3379	1396	4829	1214	9477	624.3	1194	.2				3	27	497	3050
.3	2971	689	5162	488	10079	760.8	466	.3				1	12	354	2623
.4	2564	−35	5473	−251	10615	922.7	−274	.4					5	244	2184
.5	2169	758	5751	983	11059	1113.2	1006	.5					3	162	1758
.6	1794	1460	5984	1684	11379	1335.7	1707	.6					1	104	1363
.7	1453	2120	6161	2329	11545	1593.1	2349	.7						63	1016
.8	1136	2717	6270	2890	11526	1887.9	2907	.8						37	726
.9	865	3229	6300	3341	11292	2222	3351	.9						21	494
5.0	638	3637	6243	3655	10817	2597	3657	9.0						11	320
.1	453	3925	6095	3811	10084	3011	3800	.1						6	195
.2	310	4085	5855	3793	9083	3463	3765	.2						3	112
.3	202	4112	5525	3591	7818	3949	3543	.3						2	60
.4	126	4010	5115	3207	6304	4461	3136	.4						1	30
.5	74	3791	4637	2653	4574	4991	2555	.5							14
.6	41	3474	4113	1953	2676	5526	1827	.6							6
.7	21	3081	3553	1140	673	6050	988	.7							3
.8	11	2643	2990	−260	−1357	6546	−87	.8							1
.9	5	2190	2442	+636	3328	6991	+819								

turbed so much by the interaction with neighboring atoms that the discrete levels become a finite band of levels. If it were not for exchange effects, the normal state in an electronic energy band arising from an incomplete shell of electrons would contain equal numbers of electrons of each spin, and the state with more spins in one direction than in the other would have a greater energy. The contributions to the energy due to exchange effects give a lower energy when some spins are reversed. The question of whether or not an element is ferromagnetic depends upon whether this exchange energy is greater or less than the other energy changes produced by reversing some of the spins from the normal state. If the overlap of the wave functions of adjacent atoms is small, the perturbation of the energy levels is small, and the band of energies in the crystal is narrow. It is only under these conditions that exchange effects can predominate and a spontaneously magnetized condition can exist. In metallic iron the half-distance between nearest atoms corresponds to $\rho = 7.8$. A study of the tables of $2Z$ shows that only a few percent of the total charge of the $3d$ atomic electrons lies outside of this radius. It is thus reasonable to expect that the corresponding band of energies in the crystal will be narrow—thus affording the essential feature of an explanation of the ferromagnetic behavior of iron.

The results show something of the change in character of the $3d$ wave functions in this row of the periodic table. For potassium, calcium, and scandium, a d electron is a loosely bound, series electron with a small eigenvalue. For Cu the d electrons are core electrons and the normal

TABLE III. *Values of the 2Z's.*

ρ	$(1s)^2$	$(2s)^2$	$(2p)^6$	$(3s)^2$	$(3p)^6$	$(3d)^6$	$(4s)^2$	ρ	$(1s)^2$	$(2s)^2$	$(2p)^6$	$(3s)^2$	$(3p)^6$	$(3d)^6$	$(4s)^2$
0.0	4.000	4.000	12.000	4.000	12.000	12.000	4.000	5.5	0.002	2.235	4.914	3.792	11.389	11.924	3.991
.2	4.000							.6	.001	1.836	3.947	3.769	11.367	11.881	3.990
.4	4.000							.7		1.440	3.041	3.756	11.360	11.818	3.989
.6	4.000							.8		1.070	2.237	3.752	11.348	11.726	3.989
.8	3.999							.9		0.755	1.559	3.751	11.330	11.596	3.989
1.0	3.998							6.0		.495	1.026	3.740	11.259	11.418	3.989
.2	3.997							.1		.306	0.631	3.696	11.093	11.181	3.986
.4	3.995							.2		.173	.361	3.599	10.785	10.873	3.981
.6	3.991	3.999						.3		.090	.189	3.427	10.283	10.485	3.973
.8	3.984	3.999						.4		.043	.090	3.167	9.573	10.014	3.961
2.0	3.973	3.998		4.000				.5		.017	.038	2.822	8.664	9.457	3.946
.2	3.953	3.996		3.999				.6		.007	.014	2.409	7.582	8.821	3.931
.4	3.921	3.993		3.999				.7		.003	.004	1.960	6.387	8.115	3.918
.6	3.868	3.989		3.998				.8		.001	.001	1.512	5.159	7.355	3.909
.8	3.785	3.981	12.000	3.997				.9				1.100	3.980	6.559	3.904
3.0	3.657	3.971	11.999	3.996				7.0				0.752	2.921	5.748	3.904
.2	3.468	3.955	11.997	3.994	12.000			.1				.480	2.033	4.943	3.903
.4	3.203	3.935	11.992	3.991	11.999			.2				.284	1.326	4.163	3.893
.6	2.849	3.910	11.981	3.987	11.997			.3				.156	0.807	3.428	3.865
.8	2.405	3.883	11.956	3.983	11.994			.4				.078	.462	2.753	3.806
4.0	1.894	3.859	11.905	3.980	11.987		4.000	.5				.036	.245	2.151	3.702
.1	1.627	3.847	11.858	3.979	11.981		3.999	.6				.015	.119	1.631	3.544
.2	1.363	3.844	11.791	3.978	11.972		3.999	.7				.005	.053	1.197	3.322
.3	1.109	3.842	11.697	3.978	11.960		3.999	.8				.002	.022	0.847	3.038
.4	0.873	3.841	11.567	3.978	11.943		3.999	.9					.007	.576	2.698
.5	.663	3.839	11.390	3.978	11.921		3.999	8.0					.003	.376	2.317
.6	.483	3.835	11.153	3.977	11.892	12.000	3.999	.1					.001	.233	1.915
.7	.336	3.820	10.844	3.974	11.855	11.999	3.999	.2						.138	1.517
.8	.221	3.784	10.449	3.968	11.810	11.998	3.999	.3						.077	1.145
.9	.138	3.718	9.955	3.957	11.755	11.997	3.998	.4						.040	0.820
5.0	.081	3.611	9.355	3.941	11.692	11.994	3.997	.5						.020	.553
.1	.044	3.449	8.645	3.918	11.624	11.990	3.996	.6						.009	.350
.2	.022	3.232	7.757	3.890	11.554	11.982	3.995	.7						.004	.206
.3	.010	2.949	6.857	3.857	11.487	11.971	3.994	.8						.001	.111
.4	.004	2.616	5.898	3.823	11.431	11.952	3.992	.9							.055
								9.0							.025
								.1							.010
								.2							.005
								.3							.002
								.4							.001

state is a $d^{10}s$. For Fe, the normal state is d^6s^2. For d^7s configuration the effective potential would be greatly changed, and the eigenvalue would be decreased in magnitude. Since the eigenvalue is the negative of the energy, this corresponds to an increase in the energy. This increase in the energy of the six d electrons would more than compensate for the decrease in energy of the electron which was changed from an s to a d electron. It may not be superfluous to point out that even though the $3d$ eigenvalue in $3d^74s$ were greater than the $4s$ eigenvalue, it would not necessarily follow that the d^7s configuration would be lower in energy than the d^6s^2. It is hoped to establish more detailed relations between these results and the iron spectrum in a future paper.

The relative positions of the $3d$ and $4s$ eigenvalues give some indication of the potential to be used in calculations for metallic iron. Since the $4s$ wave functions for metallic iron overlap considerably, the $4s$ band will be broadened into a truly metallic band. If the band broadens symmetrically and is filled up to the eigenvalue, there will be about one electron per atom in this band. On the other hand, because of the small overlap, the $3d$ band probably broadens less than 0.2 of a unit on each side of the $3d$ eigenvalue. Under these circumstances, there will be vacant places in the d band for ten electrons, all having energies lying below the $4s$ eigenvalue. It thus seems reasonable that in metallic Fe the s band will contain less than one electron per atom, in accordance with assumptions that are usually made.

TABLE IV. *Values of* ϵ, $\int_\infty^0 Y^2\epsilon^{2\rho}d\rho$, *and* $2v_0$.

	ϵ	$10^{-6}\int_\infty^0 Y^2\epsilon^{2\rho}d\rho$	$-2v_0$
$(1s)^2$	523.0	0.07791	101.5
$(2s)^2$	60.79	0.8789	21.6
$(2p)^6$	53.02	1.5728	64.5
$(3s)^2$	6.973	6.078	6.8
$(3p)^6$	4.600	46.89	18.83
$(3d)^6$	0.7578	51.44	13.44
$(4s)^2$	0.4836	126.9	1.34

The authors wish to thank Professor J. C. Slater for his helpful advice about many points in this paper.

LETTERS TO THE EDITOR

Prompt publication of brief reports of important discoveries in physics may be secured by addressing them to this department. Closing dates for this department are, for the first issue of the month, the eighteenth of the preceding month, for the second issue, the third of the month. Because of the late closing dates for the section no proof can be shown to authors. The Board of Editors does not hold itself responsible for the opinions expressed by the correspondents.

Communications should not in general exceed 600 words in length.

The Demonstration of the Existence of Permanent Volume Polarization in Certain Types of Multilayers

During the past few years Langmuir, Blodgett and Schaefer have described in a number of journals[1] the technique developed by them for depositing multilayers of oriented long chain molecules. They reported the formation of two types of multilayers, the *Y* type and the *X* type. They were able to deposit the former on polished surfaces of glass and of a number of metals under certain conditions but the latter only on polished metal surfaces under certain other conditions. In the *Y* type multilayer the molecules in successive layers are oppositely oriented whereas in the *X* type they are oriented alike. The former is therefore electrically neutral because of internal compensation just as are natural stearic acid crystals, for example. The *X* type structure, on the other hand, should have a volume polarization and this should be permanent so long as this structure is preserved; insofar as we know this type of structure has no natural prototype.

Recently Porter and Wyman,[2] using a method devised by one[3] of us measured the potential difference between the opposite faces of a calcium stearate *X* type multilayer of 170 layers deposited on a chromium surface and obtained a value of approximately 8.6 volts.

A calculation from their data indicates that the component of the electric moment perpendicular to the surface is about 0.027×10^{-18} e.s.u. per molecule and therefore the intensity of permanent electrostatic polarization is about 55 e.s.u. per cm^3.

Impressed with the possibility of preparing from *X* layers an electrostatic analog to a permanent magnet, we commenced experimental work on the electrical properties of these *X* type films with reference to the intensity of volume polarization.

It was found necessary first to investigate the practicality of various insulating materials as "plating" surfaces on which a large number of *X* layers could be deposited and we succeeded in doing this on mica, ebonite, and cellulose triacetate (previous published efforts by others had been made only on metallic surfaces and furthermore Porter and Wyman reported difficulty in obtaining more than 170 successive layers).

A hemicylindrical coating of 340 *X* layers of calcium stearate on an ebonite cylinder was suspended by a galvanometer suspension (torsion constant 0.16 dyne-cm per radian) between two parallel metal plates, and a small mirror was attached to the suspension. The hemicylindrical coating covered an area of 2.3 cm^2. The cylinder was adjusted in such a manner that the polar axis of the multilayer was perpendicular to the field when in the zero position and the angle of deflection, θ, was read from this position. When a d.c. field of 100 volts per cm was applied to the plates the cylinder rotated in the field and gave a steady deflection of 16 cm on a scale one meter distant. When the field polarity was reversed the cylinder rotated an equal amount in the opposite direction. This rotation was, moreover, approximately reproducible. On varying the P.D. impressed across the two plates we observed a change in the magnitude of the deflection which was directly proportional to the field intensity. The observed steady deflection can be made to change by dipping a cylinder in water or in dilute acid. Preliminary experiments indicate these changes are due to the adsorption on the surface of the *X* layer of ions or water molecules. Dipping the cylinder in mercury results in the formation of extremely large electrostatic charges on the surface of the *X* layer. Preliminary experiments indicate that part of this effect is due to frictional electrification caused by the motion of the *X* layer through the mercury, and part may be due to charging by induction. Similar results were obtained in experiments with three other cylinders coated in the same way with calcium stearate. No change which would indicate a deterioration or breakdown of the polarized property of the *X* layers has occurred in a period of over one month.

Our previously computed value of the deflection to be expected in the electric field, after introducing a small correction for the effect of the induced polarization of the cylinder and a larger correction for the effect of the curved surface of the cylinder on the orientation of the molecules, is 5 cm if the moment per molecule perpendicular to the surface is 0.27×10^{-19}. Our observed deflection corresponds to a moment of about 0.1×10^{-18}.

Further work is in progress on the above and other properties of these *X* type deposits or electrets and will be reported at length in the near future.

ROY W. GORANSON
W. A. ZISMAN

Geophysical Laboratory,
Carnegie Institution of Washington,
Washington, D. C.
April 1, 1938.

[1] K. Blodgett, J. Am. Chem. Soc. **57**, 1007 (1935); K. Blodgett and I. Langmuir, Phys. Rev. **51**, 964 (1937); I. Langmuir and V. Schaefer, J. Am. Chem. Soc. **59**, 2401 (1937).
[2] E. Porter and J. Wyman, J. Am. Chem. Soc. **59**, 2746 (1937).
[3] W. Zisman, Rev. Sci. Inst. **3**, 7 (1932); H. Yamins and W. Zisman, J. Chem. Phys. **1**, 656 (1933).

The Thermal Expansion of the Alkalis

At the New York meeting of the American Physical Society during February Bardeen[1] suggested the semi-empirical equation

$$W/V_0 = A(V_0/V) + B(V_0/V)^{\frac{1}{3}} - C(V_0/V)^{\frac{1}{3}} \qquad (1)$$

for the energies of the alkali metals. This equation is based upon a wave mechanical treatment of the alkalis by Frohlich.[2] Since this relation reproduces the relative change of volume with pressure in close agreement with Bridgman's[3] results, it seems reasonable to suppose that it represents the form of the potential energy curve in the neighborhood of the minimum with reasonable accuracy.

The combination of this idea with Debye's[4] idea that the thermal expansion of a solid is determined essentially by the anharmonic terms in the potential energy allows one to compute the thermal dilatation of the alkalis from Eq. (1). If one assumes that Debye's method applies to the energy expression (1), the thermal expansion formula thereby derived should be in fair agreement with the observed thermal expansion, since the thermal expansion depends on the form of the energy curve in the neighborhood of V_0. As is to be expected, this formula to a first approximation is Grüneisen's law[5]

$$\Delta V/V_0 = KE \qquad (2)$$

where $\Delta V/V_0$ is the thermal dilatation measured from 0°K and E is the corresponding increment to the thermal energy. The constant K is given by

$$K = \frac{9}{4V_0}\left[\frac{10A + 4B - C}{(6A + 3B - C)^2}\right]. \qquad (3)$$

The advantage of this method for computing the thermal expansion from Eq. (3) rests in the fact that K is expressed directly in terms of the potential energy constants of the crystal lattice.

Dr. Bardeen[6] was kind enough to provide me with his values of A, B, C for the alkali metals. They give for K the values:

Element	Li	Na	K	Rb	Cs
10^6K	6.28	6.23	6.78	7.19	7.36

K is in (joule)$^{-1}$.

In order to compare the results with experiment, one must have the values of both $\Delta V/V_0$ and E over a temperature range which is well below the melting point. (At higher temperatures second-order terms in Eq. (2) become more important.) The only substance for which these data appear to be available is sodium. The *International Critical Tables* yield a value of $\Delta V/V_0$ for the temperature range −191 to 16°C. Recent preliminary work of Quimby and Siegel[6] gives values of $\Delta V/V_0$ for the range 79 to 192°K and 192 to 273.1°K. A summary of the results for sodium follows:

Range °K	$10^3\Delta V/V_0$(obs.)	$10^3\Delta V/V_0$(calc.)
82.2–289.2	38.6	32.6
79 –192	19.3	17.1
192 –273.1	16.3	13.3

Dr. Bardeen reports that his values of A, B and C agree fairly well with the theoretical values of Frohlich. However, Frohlich's values of A, B and C yield thermal expansion values for sodium which disagree with experiment by a factor of three. Since the thermal expansion is thus seen to be a very sensitive function of A, B and C the above agreement appears to be fairly good.

I am grateful to Drs. Bardeen, Quimby and Siegel for the data they supplied.

LEWIS BALAMUTH

College of the City of New York,
New York, New York,
March 23, 1938.

[1] Bardeen, Bull. Am. Phys. Soc., Abstract No. 46, N. Y. Meeting (1938); Phys. Rev. **53**, 683 (1938).
[2] Frohlich, Proc. Roy. Soc. **A158**, 97 (1937).
[3] Bridgman, Proc. Am. Acad. (in press).
[4] Debye, *Atomtheorie des Festes Zustandes*, M. Born, second edition, Vol. 30, p. 667.
[5] *Handbuch der Physik*, Bd. X (1926), p. 41.
[6] Quimby and Siegel, to be published.

Heavy Beta-Rays?

Experiments by Schonland[1] and a recent paper by Chalmers[2] indicate that the scattering of beta-rays from metals is diffuse with a considerable fraction of the beta-rays being scattered through angles ranging from 90° to 180°. For ordinary electrons to produce the B band shown in a previous letter[3] they must, according to Zahn,[4] be produced by scattering within the selector. Compton[5] concurs in the possibility of this alternative explanation. The intensity which I obtain requires something like specular reflection rather than the diffuse scattering of Chalmers and Schonland for its explanation. As noted by Flammersfeld[6] the backward scattering from the base upon which the RaE is mounted affects considerably the $H\rho$ spectrum of the rays. In my experiments this backward scattering removes the possibility of showing that $p/(1-\beta^2)^{\frac{1}{2}}$ is a constant. Even though this may be the case as the beta-rays start out from the parent atoms the scattering from the base will on account of the attendant absorption give a range of values of p for each β. A table by O'Connor[7] shows a wide variation of values for the high energy end point and for the energy of the most prevalent rays but perhaps the most prevalent energy corresponds to $H\rho = 2000$ and this for ordinary electrons gives $\beta = 0.76$. If therefore the magnetic field is kept constant (340 gauss) and β_s first put at $0.76 - 0.16 = 0.60$ and then at $0.76 + 0.16 = 0.92$ the two pictures of the B band should on the internal reflection hypothesis be similar. Actually when $\beta_s = 0.92$ the B band was pretty well removed. With our latest selector ($l = 5$ cm, $w = 0.044$ cm and made of aluminum), we have found high energy beta-rays with $p = 0.12$ cm. This line appears when $H = 340$ gauss, $V = 3000$ volts but disappears when $H = 340$ gauss, $V = 4560$ volts. Are these then heavy electrons with p of about 8? The source was a mixture of RaD and RaE on a base of nickel. Distance from plates to film was 3.5 cm.

G. E. M. JAUNCEY

Washington University,
St. Louis, Missouri,
April 1, 1938.

[1] Schonland, Proc. Roy. Soc. **108**, 187 (1925).
[2] Chalmers, Phil. Mag. **25**, 322 (1938).
[3] Jauncey, Phys. Rev. **53**, 265 and 319 (1938).
[4] Zahn, Phys. Rev. **53**, 431 (1938).
[5] Compton, Phys. Rev. **53**, 431 (1938).
[6] Flammersfeld, Physik. Zeits. **23**, 973 (1937).
[7] O'Connor, Phys. Rev. **52**, 303 (1937).

Role of Oxidation in Arc Cathodes

We have recently made some observations which point to the importance of an oxide film on the cathode of arcs in the atmospheric pressure range. The experimental arrangement was similar to that used by Stolt,[1] except that the electrode and pole structure were enclosed so that gases other than air could be used. A typical observation with copper electrodes is the following: At a current of a few amperes and an electrode separation of 2 mm, and with a given magnetic field strength, the arc will rotate regularly in air or in nitrogen of 98 percent purity. If, however, oxygen-free dry hydrogen is used in the tube, an initial arc rotational velocity is found which is ten times as high as for the same current and magnetic field in impure nitrogen or air. In the course of a few minutes this high velocity decreases by a factor of about 100 times, however, coincident with the appearance of a bright "etched" condition of the electrode.

The arc, if it persists, follows the outer boundary of the clean (oxide-free?) electrode area, and when this becomes extensive, the arc changes to a striated glow discharge (glow II).[2] With pure hydrogen and with electrodes which have been cleaned in this way, it is then impossible to strike the arc form in this current range (1–10 amperes), the striated glow being the common and a self-sustaining form. If the current is increased in an attempt to find an arc in the 10–100 ampere range, an incipient discharge is produced which takes a long path to uncleaned portions of the electrode, or to the magnetic pole pieces which are well oxidized. If oxygen-free dry nitrogen is now used with electrodes which have been cleaned by hydrogen, it is found that the "arc" discharge is very unstable and prefers (1) to revert to a glow, or (2) to take a 20 mm path between the oxidized magnetic poles in preference to the 2 mm path between the cleaned electrodes.

Similar observations apply to silver electrodes, where it is impossible to produce anything but the glow form in the 1–10 ampere range in hydrogen. Arcs in these pure gases with a thermionic (C or W) cathode are, of course, quite stable.

We believe that these results point definitely to the importance of an oxide film in the case of cold cathode arcs. A likely interpretation is that with electrode materials like Ag and Cu (in this current range) the cathode cannot supply sufficient emission without an oxide mechanism, possibly identical with that studied by Güntherschulze and Fricke.[3] This result agrees with calculations (e.g., Lüdi's[4]) of field emission for cold cathode arcs which have always shown that the available field is too small.

Druyvesteyn[5] suggested the possibility of this mechanism in the arc cathode, but apparently his suggestion was not supported by experimental evidence.

Doan and Myer[6] and later Doan and Thorne[7] reported experiments in pure argon, helium, and neon, which showed that the normal stability of these arcs is destroyed by purifying the gas. They attributed the effect to "purity of the gas," but did not identify oxygen as the important agent. From studies of the electrical characteristics of arcs (with thermionic cathodes) in many of the common gases[8] we know that argon in particular shows the greatest arc stability, e.g., lowest gradient, of all the common gases except mercury vapor. This is the "gas effect," and, in view of this and the present results, the experiments of Doan, *et al.*, should be interpreted as an "electrode effect," probably an effect of oxide on the cathode.

It is a fact well known to welders and easy of verification that in air attempts to strike an arc between clean, bright iron welding rods and a clean, steel plate are unsuccessful until, by repeatedly restriking an incipient discharge, a visible oxide layer is formed on the cathode (the plate). This observation is also susceptible to the interpretation given above.

Research Laboratory,
General Electric Company,
Schenectady, New York,
March 23, 1938.

C. G. SUITS
J. P. HOCKER

[1] Stolt, Ann. d. Physik **74**, 80 (1924).
[2] Suits, Phys. Rev. **53**, 609 (1938).
[3] Güntherschulze and Fricke, Zeits. f. Physik **86**, 451, 821 (1933); Fricke, Zeits. f. Physik **92**, 728 (1934).
[4] Lüdi, Zeits. f. Physik **82**, 815 (1933).
[5] Druyvesteyn, Nature **137**, 580 (1936).
[6] Doan and Myer, Phys. Rev. **40**, 36 (1932).
[7] Doan and Thorne, Phys. Rev. **46**, 49 (1934). See also experiments of Schrum and Wiest, Elec. Eng. **50**, 827 (1931).
[8] Suits, Phys. Rev. **52**, 245 (1937).

Seasonal Variation in F_2 Ionization

Opportunity is taken to remark briefly on new data of variations in F_2 ionization in the light of the theory of a recent paper,[1] the data having become available after the paper was written. I refer to monthly average $f_{F_2}{}^x$ data through February, 1938, for Washington, D. C., U. S. A. (latitude 38° 50′ N) of the U. S. National Bureau of Standards,[2] and $f_{F_2}{}^0$ data through December, 1936, for Watheroo, Western Australia (latitude 30° 19′ S) of the Department of Terrestrial Magnetism,[3] Carnegie Institution. For comparison the average monthly noon data were converted to equivalent electron densities y_e by the usual formulae and are plotted in Fig. 1 with one point for each month; a scale of $f_{F_2}{}^x$ cycles sec.$^{-1}$ is appended.

Disregarding the general increase of y_e with increasing sunspots from 1934 to 1938 we note in Fig. 1 the summer minimum and winter maximum of the Washington curve, and the small dip in the summit of the maximum in December or January. The small dip marked "1" is

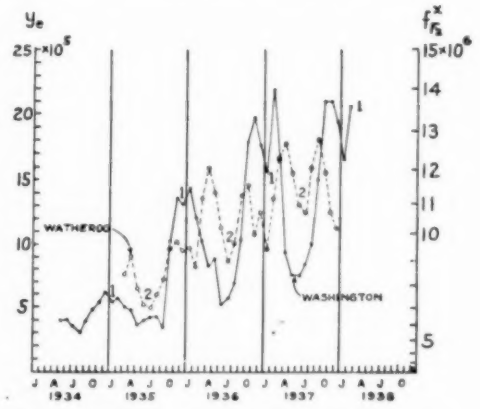

FIG. 1. Monthly average noon ionization of F_2 region.

repeated for four years; it appears real and has been mentioned by the authors of the data.[2] In explanation we recall two hypotheses of the theory,[1] (a) that the ionization is caused by the ultraviolet light of the sun, (b) that the distribution in height of the ionization is modified by winds and expansion of F_2 region resulting from heating and dissociation by solar radiation. y_s varies with the solar zenith angle ζ in opposite sense for (a) and (b), and its march with ζ depends on the relative importance of (a) and (b). For (a) more important than (b) y_s increases as ζ decreases and hence is a maximum in summer; for (b) more important than (a) the reverse is true. To account for the Washington curve we assume that (b) is the more important, hence securing agreement with the winter maximum; but not quite important enough entirely to conceal the influence of (a), thereby obtaining agreement with the small dip in the winter maximum. Turning to the Watheroo curve the same situation exists except that the winter (July) dip is more pronounced than the dip of the Washington curve, because of the difference in relative importance of (a) and (b) occasioned by the difference in absolute latitude of the two observing stations.

Thus the dips 1 of the Washington curve find their counterpart in the dips 2 of the Watheroo curve. It is concluded that apart from magnetic and solar activity features F_2 variations are seasonal, in accord with Goodall's portrayal,[4] and fall in with the qualitative pattern of the theory. If the conclusion is true the contours of the curves should be repetitive in future years. Knowledge of world-wide F_2 variations would be greatly supplemented by data from southern latitudes above 40° and from northern latitudes between 20° and 30°. Quantitative exposition of the theory will require hypotheses of intensities and penetrating power of solar wave-lengths which cause ionization, dissociation, and heating with consequent photochemical processes, winds and diffusive mixing in F_2 region; winds may be particularly important and are difficult to calculate for a rotating earth. Until such hypotheses are developed the theory remains euphemistic but hardly eclectic.

Naval Research Laboratory,
Washington, D. C.,
March 24, 1938.

E. O. HULBURT

[1] Hulburt, Phys. Rev. **53**, 344 (1938).
[2] Gilliland, Kirby, Smith and Reymer, Proc. Inst. Rad. Eng. 1937, *et seq.*
[3] Berkner, Wells and Seaton, Terr. Mag. **41**, 173 (1936); Berkner and Wells, ibid. **43**, 15 (1938).
[4] Goodall, Proc. Inst. Rad. Eng. **25**, 1414 (1937).

An Improved Wigner-Seitz Method for the Calculation of Electronic Energy Bands

In a recent article in this journal, Shockley showed[1] that the Wigner-Seitz method for the calculation of energy bands in crystals is subject to serious limitations. He proved it by applying the scheme to an "empty" lattice, i.e., to electrons moving in a field-free space, into which an artificial lattice structure was introduced.

Fortunately, I have been able to remove this discrepancy by a slight reshuffling of the original method. The W-S method is a departure from the standard mathematical procedure, because it solves the Schrödinger equation of the problem first and then, by superposition, tries to satisfy the boundary conditions, i.e., to fit the W-S cell.

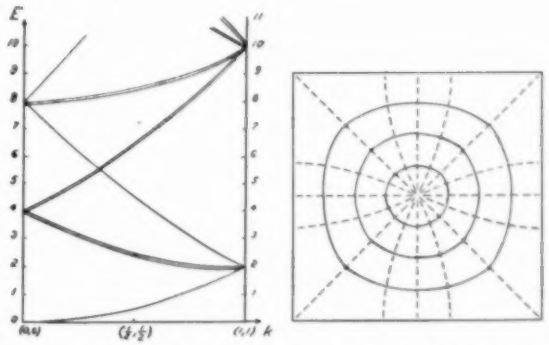

FIG. 1. (left) Energy E vs. wave vector k. FIG. 2. (right) Distorted "polar" coordinates that fit the cell.

The modified method reverts to the standard procedure. First of all, coordinates are designed which fit the cell; they yield automatically wave functions with the correct behavior at the boundary. Then approximate methods are used to solve the wave equation.

The method was tested by applying it to an "empty" two-dimensional simply-quadratic lattice, for which the W-S cell and the first Brillouin zone are squares. The true relation between energy E and wave vector k in the (1, 1) direction is plotted in Fig. 1. The points to the extreme right and left of this diagram were calculated with the new method. The coordinates ρ and ϕ that fit the cell are of a distorted "polar" type (Fig. 2). The calculations suggest quite naturally the spherical harmonics

$$P_{lm}(\cos\rho)\cdot\begin{matrix}\cos\\ \sin\end{matrix} m\phi$$

as zero-order eigenfunctions, and first-order energies can be obtained by calculating the average value of the Hamiltonian for each of them. The following table shows that the values thus obtained are in surprisingly good agreement with the true values:

E_{true}	$E_{\text{approx.}}$	E_{true}	$E_{\text{approx.}}$
0	0.00	8	7.30
		8	8.23
2	2.00	8	—
2	2.12		
2	2.28	10	10.16
4	4.20	16	15.13
4	—		
4	4.41		

It may be noticed that in a few cases no approximate energy values are given; this is the case when the boundary conditions are different along different sides of the square. It is hoped that a logical way to include this case will be found.

The above energies can be further improved by a variation scheme of the Hylleraas type. The level 4.41, e.g., could thus be depressed to 4.22.

There are some technical difficulties to be surmounted before results for three-dimensional lattices and actual crystals can be given, but the work is in progress at this university.

University of Pittsburgh,
Pittsburgh, Pennsylvania,
March 31, 1938.

G. WANNIER

[1] Shockley, Phys. Rev. **52**, 866 (1937).

The Absolute Measurement of Resistance and Reactance at Frequencies of the Order 300 mC/second

The characteristic impedance of a parallel wire transmission line can serve as an absolute impedance with which may be compared any unknown impedances. Schmidt[1] has shown the application of this for a partial range of pure resistances and pure reactances. Labus[2] has developed an absolute method for measuring pure resistances at medium frequencies. A theory by Hempel[3] is similar to that of Schmidt with slight extension. Other theories and methods, notably those of King,[4] have been concerned with the comparison of different unknown impedances at very high frequencies.

The formula for the complex current amplitude at any point of a parallel wire line which is terminated in arbitrary impedances, and which has an e.m.f. applied in series with one of the terminations,[5, 6] is used to develop a general theory and a simplified experimental procedure which permit the simultaneous measurement of the resistive and reactive components of any complex impedance in terms of the characteristic impedance of the line. The theories of Schmidt and Hempel are seen to be special cases of the general theory.

The experimental procedure is to connect the unknown impedance as one termination of a parallel wire line, the other end of which is terminated in a low impedance thermocouple. A high frequency e.m.f. is induced in the circuit by coupling to an oscillator, in such a way that the effective e.m.f. acting in the circuit is that induced in the unknown terminal impedance. Observation of the resonance curve of current through the thermocouple on varying the line length, and of the length of the line at maximum current, permits the determination of the magnitude and phase angle of the product of the complex reflection coefficients at the two ends of the line (XY in Pierce's notation). If the unknown impedance is replaced by a large copper disk through the center of which the parallel wire line passes normally, the value of X can be taken as unity and Y can be determined in magnitude and phase angle. Hence the value of X for any unknown impedance can be determined. From the complex value of X and the characteristic impedance of the line the resistive and reactive components of the unknown impedance can be easily and directly calculated.

The method is symmetrical in inductive and capacitive reactances and also shows a form of symmetry for any two impedances whose product is equal to the square of the characteristic impedance.

The accuracy of the method depends on the accuracy of the measurement of line length and other line dimensions. The possible accuracy varies widely over the whole field of resistance and reactance. Measurements at a frequency of 377 mC/sec. indicate an accuracy of about 1 percent for resistance component from a few ohms to a few thousand ohms. Low reactance components combined with resistance components up to several hundred ohms can be measured within 1 ohm or less. Least accurate is the determination of small values of either component when combined with values of the other component of several hundred ohms or greater. High reactance components with low resistance components can be measured within about 1 percent up to several thousand ohms.

The permeability of ferromagnetic substances can be measured with considerable accuracy if one assumes the validity of existing classical formulas for the effect of permeability on the skin effect and inductance of fine straight wires at these frequencies.

Full details of the experimental method together with measurements made on a number of different forms of impedance and a number of different wire samples are to be published later.

Cruft Laboratory,
Harvard University,
Cambridge, Massachusetts,
March 30, 1938.

R. A. CHIPMAN

[1] Otto Schmidt, Hochfreq. und Elektroak. **41**, 2 (1933).
[2] J. W. Labus, Proc. I. R. E. **19**, 452 (1931).
[3] Werner Hempel, E. N. T. **14**, 33 (1937).
[4] R. King, Proc. I. R. E. **23**, 885 (1935).
[5] G. W. Pierce, *Electric Oscillations and Electric Waves* (New York, 1920), Eq. (30), p. 330.
[6] J. R. Carson, *Electric Circuit Theory and Operational Calculus* (New York, 1926), Eq. (243), p. 133.
The equations in the last two references are developed by different approaches, but are identical.

Rotational Transitions Associated with Radiation in Water Molecules in Nonpolar Solvents

In our previous report[1] upon the apparent rotational structure in the 1.87, 1.38, and 1.13μ absorption bands of water molecules in carbon disulfide solution we stated that carbon tetrachloride is an unsuitable solvent because of the low solubility of water in this liquid. Some months later we learned that the solubility datum given in the reference cited in the earlier paper is in error, and that the solubilities in carbon tetrachloride and carbon disulfide are, in fact, comparable. We, therefore, repeated our experiment with the new solvent and wish to make this very brief report pending a fuller account which will include, we hope, a study of deuterium oxide.

The 1.87 and 1.38μ bands show the same sorts of structures in the two solutions; the improved plot of the 1.87μ band reveals a long wave portion which had been obscured previously by a deep overlapping solvent band. We believe we can now say with confidence that the bands, shifted toward longer waves in solution, have vapor-like structure with partially developed P, Q, and R branches. However, the intensity of the Q branch is very greatly enhanced over that in the vapor bands. Two alternative interpretations of this enhancement seem possible. First, that there is a marked departure from the usual statistical distribution over rotational states, that $J''=0$ states and consequently $J''=0\rightarrow J'=0$ transitions predominate. Second, that there is no appreciable alteration of the statistical distribution and hence that $J''>0$ states and $\Delta J=0$ transitions predominate. If the selection rule for gaseous molecules that forbids $J''=0\rightarrow J'=0$ transitions is applicable here, the second interpretation must be the correct one.

University of California,
Los Angeles, California,
March 24, 1938.

J. W. ELLIS
E. L. KINSEY

[1] Kinsey and Ellis, Phys. Rev. **51**, 1074 (1937).

Note on Numerical Integration

In the numerical solution of a differential equation, two different approaches are possible. A method using backwards differences only has been suggested by Adams, and a method based upon an estimate of the derivative at the next step has been suggested by Störmer, Milne, Hartree, and others.[1] In either case, the actual integration formula can be expressed either in terms of differences or by using a polynomial as suggested by Steffensen. A very satisfactory combination of the Milne and Steffensen viewpoints which is applicable to many homogeneous equations has been found by the authors. Since this type of differential equation is met very frequently in self-consistent field calculations, and the simplification has not been found in any of the standard treatises, it is outlined here.

Consider the differential equation

$$d^2P/dr^2=P''=f(r)P. \tag{1}$$

If the integration table is complete to P_n, the integration formula for obtaining P_{n+1} is:

$$P_{n+1}=2P_n-2P_{n-1}+(h^2/12)(P''_n+10P''_n+P''_{n+1}) \tag{2}$$

where h stands for Δr, the increment of the independent variable. In practice, $(h^2/12)P''$, P, and $(h^2/12)f(r)$ are tabulated.

Ordinarily, in using this formula, it is necessary to estimate the value of P''_{n-1} and then check. The authors have found that frequently considerable time can be saved by combining Eqs. (1) and (2) to obtain:

$$P_{n+1}=\frac{2P_n-P_{n-1}+(h^2/12)P''_{n-1}+10(h^2/12)P''_n}{1-(h^2/12)f_{n+1}(r)}. \tag{3}$$

If $(h^2/12)f(r)$ and $1-(h^2/12)f_{n+1}(r)$ are tabulated before starting the integration, the above formula can be applied very conveniently. Other types of differential equation for which this method is applicable are readily recognized and the extension of the method to these equations is easily made.

WILLARD F. MANNING*
JACOB MILLMAN†

Massachusetts Institute of Technology,
Cambridge, Massachusetts,
January 22, 1938.

* Now at University of Toledo, Toledo, Ohio.
† Now at the College of the City of New York, N. Y. C.

[1] A. A. Bennett, W. E. Milne, and H. Bateman, "Numerical Integration of Differential Equations," Bulletin of the National Research Council, No. 92. See particularly Chapter III, Section 3.4.2.

On the Penetrability of a Simple Type of Potential Barrier

In view of possible applications in the calculation of nuclear radii it seems of interest to call attention to the existence of a potential barrier with Coulomb tail for which the transmission coefficient can be expressed exactly in terms of known functions. The potential referred to is the negative of the Kratzer potential joined to a square well near the origin, and may be written in the form

$$V(r)=-V_0, \qquad r\leq r_0,$$
$$V(r)=A/r-B/r^2, \quad r>r_0.$$

It is well known that the corresponding Schrödinger radial equation is soluble by Whittaker functions in the region $r>r_0$ and for all values of the angular momentum.

The transmission coefficient T (incident flux at r_0 divided by outgoing flux) for particles of zero angular momentum, mass M, and energy E, proceeding outward from the origin is readily shown to be

$$T=\frac{4\mu e^{-\pi\eta}}{|\mu W_{\kappa,m}(a)-iW'_{\kappa,m}(a)|^2},$$

where $\mu=(1+V_0/E)^{\frac{1}{2}}$, $a=kr_0$, $k=(2ME)^{\frac{1}{2}}/h$, $\eta=MA/h^2k$, $\kappa=-i\eta$, $m=(\frac{1}{4}-2MB/h^2)^{\frac{1}{2}}$, $W_{\kappa,m}$ is the Whittaker W function and $W'_{\kappa,m}$ is its derivative with respect to kr. For incident particles of angular momentum lh a slightly more complicated form is necessary with

$$m=[(l+\tfrac{1}{2})^2-2MB/h^2]^{\frac{1}{2}}.$$

In the case of a pure Coulomb field ($B=0$) the result takes the form $T=4[\mu(F^2+G^2)+(1/\mu)(F'^2+G'^2)+2]^{-1}$ where F and G are the functions computed and tabulated by Yost, Wheeler and Breit.[1] When $l=0$ and $B=0$ the result is identical with that obtained by Sexl.[2]

Suitable methods for the computation of the complex W functions have been devised.

F. C. HOYT

Ryerson Physical Laboratory,
University of Chicago,
Chicago, Illinois,
March 31, 1938.

[1] Wheeler and Breit, Phys. Rev. **49**, 174 (1936).
[2] Sexl, Zeits. f. Physik **56**, 62 (1929).

Comparison of Intensities of Spectral Lines

Among the methods for comparing the intensities of spectral lines the ones most commonly used involve the use of a rotating logarithmic or stepped sector disk for the purpose of producing a known distribution of intensity along the slit of the spectrograph. If the arc is imaged on the slit, practical considerations require the employment of a central segment of the arc which is a considerable fraction of its total length. The intensity of the arc varies along this segment and this distribution of intensity is superposed on that introduced by the disk. If the effect were the same for all spectral lines there would be no difficulty; but we have observed that there is a considerable variation in the distribution of intensity along the arc from line to line. This variation produces errors in the apparent relative intensities as determined by the logarithmic method and changes in the slopes of the apparent sensitometric curves of individual lines which are difficult to interpret or eliminate from the data in the case of the sector method.

It is possible to overcome these serious difficulties by means of a simple method of illuminating the slit which produces uniform illumination for all spectral lines and at

the same time satisfies the requirements with regard to angular aperture and provides lines of whatever length may be desired.

The method of illumination that we have used is familiar to students of other branches of optics. Two converging lenses are used between the arc and the slit. The arc and the second lens are confocal with respect to the first lens, and the first lens and the slit are confocal with respect to the second lens. In this manner each point of the source illuminates all points of the slit. Light from only the desired short central segment of the arc is selected by means of a stop placed at either the arc or its enlarged image on the second lens. Doubtless there are other ways to achieve uniform illumination of the slit from a nonuniform source, such as by the use of astigmatic lenses. There are advantages in mounting the sector at the first lens rather than at the slit.

DONALD FOSTER
H. W. HIGHRITER

Boonton, New Jersey (DF),
Lamp Division, Westinghouse Electric and Mfg. Co.,
Bloomfield, New Jersey (HWH),
March 28, 1938.

APRIL 15, 1938 PHYSICAL REVIEW VOLUME 53

Proceedings of the American Physical Society

MINUTES OF THE NEW YORK MEETING FEBRUARY 25–26, 1938

THE 219th regular meeting of the American Physical Society was held in New York on Friday and Saturday, February 25–26, 1938 as a joint meeting with the Optical Society of America. The presiding officers at the sessions of the Physical Society were Dr. Lyman J. Briggs, President of the Society, Professor John T. Tate, Vice President, Dr. Walter H. Brattain, Dr. Karl K. Darrow and Professor H. W. Webb. All sessions were held in the Pupin Physics Laboratories of Columbia University.

The joint session with the Optical Society of America was held on Friday morning at nine-thirty o'clock. This session was a symposium on *The Optical Properties of Metals*. The President of the Optical Society, Professor R. C. Gibbs, presided. The invited papers were as follows: *Some Simple Concepts in the Quantum Theory of Metals* by L. A. DuBridge, University of Rochester; *The Experimental Determination of Optical Constants of Metals—Methods and Results* by J. B. Nathanson, Carnegie Institute of Technology; and *Derivation of Properties of Electrons in Metals from Optical Constants* by H. A. Bethe, Cornell University. The attendance at this symposium was about three hundred and fifty.

On Friday evening the Society joined with the Optical Society for dinner at the Columbia University Faculty Club. This dinner was attended by two hundred guests. The President of the Physical Society, Dr. Lyman J. Briggs, presided and called upon Professor R. C. Gibbs, President of the Optical Society of America, to speak. After the dinner the two societies went to the Museum of Natural History to hear the Adolph Lomb Memorial Lecture given by Dr. Harlow Shapley, Director of the Harvard University Observatory, on *The Debt of the World to Optical Science.*

Meeting of the Council. At its meeting on Friday, February 25, 1938, the Council elected one candidate to fellowship, transferred two candidates from membership to fellowship, and elected thirty-five candidates to membership. *Elected to fellowship:* J. Franklin Carlson. *Transferred from membership to fellowship:* John H. Manley and John C. Steinberg. *Elected to membership:* Henry E. Bent, John L. Binder, T. Bjerge, W. A. Bruce, George E. Crouch, Jr., Richard B. Dow, Mark G. Foster, Carl Gamertsfelder, Donald H. Hamsher, John M. Harding, Lawrence Harris, George B. Hoadley, Arthur

V. Hollenberg, Oscar B. Jackson, Vincent P. Jacobsmeyer, Morton H. Kanner, Albert E. Kempton, James S. Koehler, Willis E. Lamb, Jr., Paul S. Lester, Lefler H. McKee, J. E. Morgan, Albert G. Oswald, Syoji Ozaki, F. A. Paneth, Gaylord W. Penney, Thomas Perry, M. A. Pittman, Marguerite M. Rogers, Alden H. Ryan, Donna J. Seaman, Hugh A. Shadduck, C. D. Thomas, Raymond E. Wilson, and Seitaroe Yamaguchi.

The regular scientific program of the American Physical Society consisted of seventy-one contributed papers of which numbers 14, 67, 69, 70 and 71 were read by title. The abstracts of the contributed papers are given in the following pages. An Author Index will be found at the end.

W. L. SEVERINGHAUS, *Secretary*

ABSTRACTS

1. A Scale for Predicting Nuclear Transformations. VLADIMIR KARAPETOFF, *Cornell University.*—Let atoms of an element X, of atomic weight A and atomic number Z, be bombarded by particles (or radiation) P of atomic weight a and atomic number u. Let the final product be an element Y and let the ejected particle (or radiation) be Q, of atomic weight b and atomic number v. Then

$$X_Z{}^A + P_u{}^a \rightarrow Y_{Z+u-v}^{A+a-b} + Q_v{}^b.$$

The sum of the weights on both sides of the equation is $A+a$, and the sum of unit electric charges is $Z+u$. A table of isotopes is constructed.[1] Let the bombarding particles be

$He_2{}^2$	$H_1{}^1$	$\gamma_0{}^0$
$He_2{}^3$	$H_1{}^2(D)$	$n_0{}^1$
$He_2{}^4$	$H_1{}^3$	$n_0{}^2$

These nine names are written on a piece of a thin celluloid scale in the positions indicated above, at the same distances as the elements in the table of isotopes, with a sharp point below each name on the scale. By placing a desired bombarding particle on the scale over any desired isotope in the table, the resulting products and the ejected particles may be read off directly.

[1] See, for example, Rasetti, *Elements of Nuclear Physics*, p. 154.

2. Maximum Energy of Ions from the Cyclotron. M. E. ROSE, *Cornell University.*—The magnetic fields giving the greatest ion energy from the cyclotron are those which effect some compromise between the conflicting requirements of focusing and resonance.[1] The principal conditions for the magnetic field are (a) focusing force everywhere positive and (b) phase changes $\leqslant\pi$. It is also advantageous to make the field too large for exact resonance near the center of the cyclotron and too small farther out; then the phase changes will partially cancel. Three types of magnetic fields have been investigated: (1) homogeneous field (phase change $\leqslant\pi/2$), (2) radially decreasing field with linear gradient and (3) the field which gives a constant total (electric+magnetic) focusing force. The energy in all cases is proportional to $(V_0AZ)^{\frac{1}{2}}$ where V_0 is the accelerating voltage, Z the atomic number and A the atomic weight of the ion. For protons and 50 kv dee voltage the maximum energies for the three fields are 11, 14, and 15 Mev, respectively. These energies may be obtained with intensities of about one-quarter the intensities obtained at low energy. However, very accurate shimming will be necessary to produce the required magnetic fields.

[1] H. A. Bethe and M. E. Rose, Phys. Rev. **52**, 1254 (1937); M. E. Rose, Phys. Rev. to appear shortly.

3. Possible Deviations from the Evaporation Model of Nuclear Reactions. H. A. BETHE, *Cornell University.*—If a nuclear particle of energy E comparable with the nuclear interaction energy V (or smaller) strikes a nucleus, it will lose practically all its energy in the "surface layer" of the nucleus. This process will cause an intense "local heating" of the part of the nucleus struck. The "heat" will then gradually spread over the whole nucleus. Since the local temperatures reached are very high it seems possible that a particle evaporates from the heated spot before the whole nucleus has come to thermal equilibrium. The probability of this occurrence depends on the heat conductivity k of the nucleus and is about $p=(a^2\omega/2\pi k)\times(2E/A)^{4/3}$ where a is the distance of neighbors, ω the natural frequency of vibration, and A the dissociation energy of the nucleus. For a solid body model, $k=\frac{1}{3}lu$ where $u\approx a/\omega$ is the "velocity of sound" and l the mean free path of elastic waves. l will certainly be small; assuming $l=a$ and $E=A$, we get $p\approx 1$. Thus many of the particles produced in reactions with heavy nuclei may have energies considerably higher than those calculated from the assumption of uniform nuclear temperature, although much lower than the energy of the incident particle. These "too fast" particles will be emitted preferably in the backward direction.

4. The Nuclear Isomers of In^{116}. ALLAN C. G. MITCHELL AND L. M. LANGER, *New York University.*—The isomeric periods of In^{116} (13 seconds and 54 minutes), produced by the capture of slow neutrons by In^{115}, have been studied with the purpose of determining the energy level scheme for In^{116}. The γ-ray of energy 1.4 Mev previously measured by the authors has been shown to have a period of 54 minutes. No γ-ray of 13-second period could be found. The percentage transmission by boron of resonance neutrons which effect the two periods has been measured and found to be the same within the experimental error, for both periods. The value obtained for the percentage transmission of 0.0252 g/cm² B (uncorrected for obliquity) is 73.5 ± 3.0. The branching ratio $(R(13\text{ sec.}))/(R(54\text{ min.}))$ has been shown to be independent of the method of excita-

tion and has the value 1.12 ± 0.06. From the known beta-ray end points and the energy of the gamma-ray an energy level diagram has been drawn up which accounts for all the experimental facts. The two excited levels of In^{116} from which disintegration takes place are separated by 0.3 Mev, the level corresponding to the 13-second period lying higher. Gamma-ray transitions between these two levels can be forbidden by choosing quantum numbers which differ by 5 units.

5. A Method for Measuring the Nuclear Recoil in Beta-Ray Emission. J. HALPERN AND H. R. CRANE, *University of Michigan.*—The length of track produced in a cloud chamber by the recoil nucleus resulting from a beta-ray disintegration is too small to measure directly, even at the lowest pressure at which a cloud chamber can be operated. However, the recoil nucleus produces a number of ion pairs in the gas. For radio-chlorine, which has a 6 Mev upper limit, a maximum of about 15 ion pairs is expected, which is as many as the beta-ray produces in $\frac{1}{2}$ cm path in air. The method of the present experiment is as follows. A gas containing radio-chlorine is placed in a cloud chamber. The clearing field is removed long enough before the expansion to allow the ions to spread out so that the resulting droplets can be seen individually. In many of the cases obtained, a small cluster of droplets appears at the beginning of the track. From the number of droplets an estimate is made of the kinetic energy of the recoil nucleus, and this is compared with that calculated from the observed energy of the beta-ray. Photographs will be shown of some of the tracks obtained.

6. Collimation of Slow Neutrons. J. G. HOFFMAN AND M. STANLEY LIVINGSTON, *Cornell University.*—A collimated beam of slow neutrons with an angular spread of 9 degrees is produced and analyzed with the aid of absorbers of B_4C and Cd, and detected in a BF_3 gas chamber actuating a linear amplifier and counter. The cylindrical collimators are made of concentric brass tubes between which B_4C is packed and around which Cd is fastened. The Cd (0.58 g/cm²) absorbs 91.6 percent of slow neutrons detected in the BF_3 chamber; the B_4C (0.65 g B/cm²) an additional 5.7 percent.[1] One collimator is fixed to the slow neutron source, the second collimator and detecting chamber are arranged to be swung about an axis midway between the two collimators. At zero angle a 260 mC Rn-Be source in the howitzer produces a beam of 285 counts/minute with a neutron background of 10 counts/minute. About ten times this intensity is obtained with the 1.2 Mev cyclotron as a neutron source. Variation of angles shows the collimation expected from the ratio of diameter to length of the collimator tubes. The instrument is being used to study the angular distribution of slow neutrons scattered from magnetized iron and other scatterers placed between the collimators.

[1] Hoffman and Livingston, Phys. Rev. **52**, 1228 (1937).

7. The Scattering of Fast Neutrons. R. F. BACHER AND D. C. SWANSON, *Cornell University.*—With a lithium target in the deuteron beam, the Cornell cyclotron has been used as a source of fast neutrons. It has been found that a large water shield placed close to the cyclotron forms quite a good fast neutron screen. A pressure cloud chamber filled with either helium or hydrogen has been used to observe the recoils produced. Expansions behind the shield show only occasional tracks whereas in front of a hole through the shield large numbers of recoils are observed. Without any scatterer the recoils produced with the chamber in the "beam" show neutron energies up to 13 Mev. A scatterer of iron or lead of thickness, which on the basis of the known cross section was expected to scatter about one-quarter of the incident neutrons, was placed in the port, flush with the surface of the shield. Numerous tracks in the cloud chamber were now observed behind the shield and it was found that these led to neutron energies from 1 to 2 Mev. This indicates that the neutrons must lose a large amount of their energy in a single nuclear collision. This large energy loss, in turn, points to large interactions of the nuclear particles such as those which appear in the Bohr nuclear model.

8. Range and Specific Ionization of Alpha-Particles. M. G. HOLLOWAY AND M. STANLEY LIVINGSTON, *Cornell University.*—A shallow ionization chamber operating a linear pulse amplifier and counter is used for a study of the extreme end of the range of Po alpha-particles. The output pulses as measured by a variable thyratron bias are strictly proportional to the ionization in the chamber. Using 1 mm and 2 mm deep chambers the ionization near the end of the range is determined. For particles which stop in the chamber the ionization is directly proportional to the residual energy at the face. The difference in ionization in the two chambers gives directly the range-energy relation within the last mm. Ionization measurements in the 1 mm chamber were also taken throughout the last 2.8 cm of range, and the Bragg curve obtained. By combining these data a range-energy relation is computed, extending to within 0.005 cm of the end of the range, with an average error of less than 0.5 percent. The energy measurements are accurate to ± 5 kilovolt (assuming the average energy loss per ion pair formed to remain constant), and the relative range measurements to ± 0.004 cm. The mean range of Po alphas is found to be 3.802 ± 0.010 cm.

9. Induced Radioactivity in Tellurium. GERALD F. TAPE AND J. M. CORK, *University of Michigan.*—In continuing the detailed study of induced radioactivity, tellurium has been bombarded in the cyclotron with (6 Mev) deuterons, with slow neutrons and with fast (Li) neutrons and observations made of the radioactive isotopes formed. In addition, the heavier element, iodine, and the lighter element, antimony, have been similarly treated. Chemical separation of the tellurium specimen after deuteron bombardment yields radioactive tellurium isotopes of half-lives: 66 min., 10 hr. and 8 days. The same bombarded specimen gives certain active iodine isotopes by proton capture. Bombardment by lithium neutrons yields activities in the tellurium whose half-lives are: 66 min., 10 hr. and 31

days. The antimony precipitate from the tellurium bombarded with deuterons gives the previously reported period of 60 days. Iodine bombarded with fast neutrons yields the well-known 26-min. period due to I^{128} and an activity of half-life 13 days undoubtedly attributable to I^{126}. Cloud chamber observations show that all of these radioactive elements emit negative electrons. It is thus reasonable to associate the 8-day period with Te^{131} and the 66 min. and 10 hr. activities with Te^{127} and Te^{129}. The 31-day Te activity, produced only by fast neutrons, is thought to be due to Te^{121} and is negative active because of the capture of K electrons followed by partial internal conversion. Gamma-rays are also observed as might be expected in this case. Since iodine has but a single stable isotope, it is evident that there are here two induced chain reactions. The active Te^{131} and Te^{129} emit electrons and become I^{131} and I^{129}. These in turn emit beta-particles and end as stable Xe^{131} and Xe^{129}.

10. Electron Pair Theory of Heavy Particle Interaction and the Rabi Effect. R. E. Marshak and H. A. Bethe, *Cornell University.*—Rabi's atomic beam determination of the magnetic moment of the proton gave a value about 15 percent larger than Stern's, this discrepancy apparently lying outside the limits of experimental error. Young[1] suggested that an additional spin-spin interaction between proton and electron could account for the discrepancy. By coupling the heavy particles with the electron-positron field to get nuclear forces (Gamow-Teller[2] theory) one has at the same time the physical mechanism for the desired proton-electron interaction. The Hamiltonian (nonrelativistic approximation for heavy particles) was taken as

$$H=G\{C_1\Psi^*\Psi\psi^*\beta\psi+C_2\Psi^*\Psi\psi^*\psi+C_3\Psi^*+\Psi\psi^*\beta+\psi + C_4\Psi^*+\Psi\psi^*+\psi\}$$

where Ψ is the quantized wave function of the heavy particle and ψ that of the electron. The diagonal element of this interaction with the electron eigenfunction in the hydrogen atom was calculated. The constants were deduced from the best values for heavy particle interaction, *viz.* ${}^3V_{NP}=75\ mc^2$, ${}^1V_{NP}=40\ mc^2$, range $=2.25\times10^{-13}$ cm. Assuming $C_3=C_4$, one finds $G=1.25\times10^{-6}\ (mc^2)(\hbar/mc)^3$ and $C_3=C_4=0.25$. With these values one obtains $V_{P_4}=0.0052\ \text{cm}^{-1}$, which is 12 percent h.f.s. splitting. This is just what is required to explain Rabi's result although the exact quantitative agreement is of course accidental. The effect being of first order in G is not equivalent to the hyperfine structure caused by the magnetic moment of proton which is $\sim G^2$.

[1] L. A. Young, Phys. Rev. **52**, 138 (1937).
[2] G. Gamow and E. Teller, Phys. Rev. **51**, 289 (1937).

11. Factors Governing Yield from Ion Sources Using Focused Beams. Lloyd P. Smith and G. W. Scott, Jr., *Cornell University.*—An analysis of ion sources in which ions are produced by a focused beam of electrons has been made. It is found that with usual electrode arrangements the effect of space charge on the number of electrons effective in producing ions together with the ionization cross section as a function of electron energy leads to a certain interelectrode potential at which the maximum ion yield is obtained. In particular, for the case of coaxial cylindrical electrodes, one of which is the cathode, the number of ions produced per unit volume per unit time varies approximately as $I_0^{1/2}V^{7/4}$ $(V<V_m)$ and as $I_0^{1/2}V^{-1/4}$ for $V>V_m$ where V is the potential difference between cathode and anode, I_0 the saturated cathode current per unit area, and V_m is the electron voltage for which the ionization cross section for the particular gas under consideration is a maximum.

12. A Linear Accelerator Using a Quarter Wave-Length Transmission Line. Paul L. Hartman and Lloyd P. Smith, *Cornell University.*—A linear accelerator has been constructed with coaxial cylindrical electrodes mounted alternately on each side of a parallel transmission line so that the electrodes and line form a quarter wave-length resonant system. The part of the line carrying the electrodes is enclosed in an evacuated envelope made of glass tubing six inches in diameter. The radio-frequency voltage is applied to the transmission line near the short circuited end, thereby obtaining voltages across the electrodes considerably greater than that applied to the line. The radio-frequency (10 megacycles) voltage is generated by a three stage power oscillator. The present accelerator is designed to produce a beam of deuterons with an energy of about a half million electron volts. This type of accelerator has the advantage that the ion source and target are at ground potential and very accessible.

13. Stereoscopic Viewing and Measuring Instrument for Cloud Chamber Photographs. Creighton Jones and Arthur Ruark, *University of North Carolina.*—This instrument was conveniently built by using an old photostat machine as a basis. It makes possible four types of measurement: (1) full-size images of the chamber can be viewed stereoscopically; (2) track curvatures can be measured; (3) a translucent screen can be made to coincide with the real image of a track, so that angles between branches can be determined; (4) the direction of a track relative to axes fixed in the chamber can be measured directly on quarter-degree protractors. The important feature is the ease and speed with which measurements can be made. Slides will be shown.

14. Investigation of Hyperfine Structure of Spectral Lines from Atomic Beams. K. W. Meissner, *Frankfurt/Main.* (*Introduced by R. Ladenburg.*)—Atomic beams excited by electron impact and observed under 90° with respect to their motion give the sharpest spectral lines known, as they are nearly free from Doppler effect broadening. It is found that it is possible to get separation for lines which are only 2.5 thousands of an angstrom unit apart. In this way some "complete doublets" of different subordinate series were resolved for the first time and the splitting of their levels determined; furthermore new hyperfine structure patterns and isotopic shift of different elements were measured and the corresponding nuclear spins and moments calculated.

15. The Interval Rule in Hyperfine Structure. D. H. TOMBOULIAN AND R. F. BACHER, *Cornell University.*—Interferometric measurements have been carried out on λ7182 ($5s6p^3P_1 \rightarrow 5s6s^3S_1$) and λ7276 ($5s6p^3P_0 \rightarrow 5s6s^3S_1$) of In II to supplement the grating measurements of Paschen. Most of the states of In II have hyperfine structures which show deviations from interval rule arising either from perturbations of nearby states or from the electric quadrupole moment of the nucleus. The $5s6s^3S_1$ state is unusual in that there should be no quadrupole effect and the nearest neighboring states are about 3000 cm^{-1}. From λ7182, the $^3S_1$ separations are found to be 2.2088 cm^{-1} (11/2−9/2) and 1.8081 cm^{-1} (9/2−7/2). These give a ratio 1.2216 which agrees with the expected ratio 1.2222 from the interval rule, to 0.05 percent. From λ7276, the $^3S_1$ separations can be checked and are found to be 2.2081 and 1.8096 cm^{-1}. These measurements are essentially in agreement with the measurements above, the differences probably being due to the presence of the nearby helium line. From the observed separation one can conclude that the magnetic dipole interaction which gives rise to the interval rule is remarkably successful in accounting for the relative level spacing when there are no quadrupole effects and perturbation effects are negligible.

16. Spectra of Rare Earth Oxides. WILLIAM W. WATSON, *Yale University.*—Emission bands are reported for CeO and PrO. Vibrational quantum assignments have been made for four sparsely developed systems of CeO and one of PrO. Comparison of these is made with two known GdO systems (Piccardi) and one LuO system (Watson and Meggers). Nd has no evident oxide spectrum in the flame of the arc, and Meggers and Scribner report none for Yb. Many previously reported oxide spectra of rare earth elements are shown to be due to YO, LaO or to chlorides. Lower state vibrational frequencies range from 864 cm^{-1} for CeO to 842 cm^{-1} for LuO. The scarcity of bands, the general absence of long sequences, the usual singlet character and the frequently diffuse appearance of the bands for the oxides of the rare earths, all in marked contrast with the numerous systems of well-developed oxide bands for La which has the same outer electron configuration (ds^2), are attributed to the great prevalence of predissociation because of a high density of repulsion states. Where present these bands serve as easily identified spectral frequencies for chemical analysis.

17. The Optical Constants of Liquid Thallium. A. P. FRIESEN, *Bethel College, Newton, Kansas.*—Thallium was melted in a specially constructed furnace having glass observation windows free from strain. A steady flow of hydrogen kept the metal surface optically clean. The source of light was a mercury arc. The optical system consisted of the usual train for the reflection method. Measurements were made for wave-lengths 5790A and 5461A. The values obtained for the indices of refraction were 1.304 and 1.153 respectively, while the extinction coefficients were 4.094 and 3.786, respectively. The reflecting powers were 76.35 percent and 75.78 percent, respectively.

18. The Relative Luminosity of the Yellow and Green Mercury Lines. W. E. FORSYTHE, B. T. BARNES AND ANN L. SHRIDER, *General Electric Co., Nela Park, Cleveland, Ohio.*—The relative luminous intensity of the yellow and the green mercury lines from an H-1 lamp was measured, with an Ives-Brady flicker photometer that has a 2° field using Corning glass filters to separate the lines, by sixteen selected observers. The Y/B[1] of the observers ranged from 0.667 to 1.113 with an average of about 0.99. The ratio for the two lines (yellow/green) found was 1.356. The ratio calculated from the spectral transmission of the screens, the average spectral intensity of three H-1 lamps and the standard I.C.I. luminosity factors was 1.332. This is not in agreement with results reported by Dresler;[2] however, he used a smaller field.

[1] Ives and Kingsbury, Trans. I. E. S. **10**, 103 (1915).
[2] Das Licht **7**, 81 (1937).

19. The Absorption Spectra of SrH and SrCl. KENNETH R. MORE* AND S. D. CORNELL, *Yale University.*—A high temperature vacuum furnace using a coil of molybdenum wire as a heating element was constructed for use in spectroscopic investigations. A temperature of about 1800°C has been attained with a power consumption of 2.5 kw. Strontium metal was placed in the core tube and the furnace filled with hydrogen to a pressure of about 60 cm of mercury. The band systems of SrH reported by Watson, Fredrickson and Hogan are observed in absorption. The analysis of the D system is extended by the use of known lower state combination differences. The appearance of lines of the C system arising from transitions to levels for which K' is greater than 18 shows the effect of pressure on the predissociation limit. The SrCl bands observed in emission by Parker are also observed and some of the sequences extended. The Boltzmann factor at the temperature used is such that appreciable fractions of the molecules in the ground electronic state exist in levels with values of v'' as high as 12. This makes it possible to observe in absorption sequences extending to members as high as (12, 12).

* Sterling Fellow.

20. Determination of Widths of Energy States: Argon K Absorption Limit. F. K. RICHTMYER AND L. G. PARRATT, *Cornell University.*—One must know the width of one x-ray energy state before one can construct from the observed widths of x-ray emission lines the complete diagram of widths of energy states (single ionization). Early investigations showed hope of obtaining directly this state width from the contour of an absorption limit. Recent work with solid absorbers indicates that profuse fine (sub-Krönig) structure completely obscures the width of the energy state in question. This is illustrated with the contour of the L_{III} limit for silver. Parenthetically, such fine structure is very promising as indicating possibilities in studies of energy zones of the solid state. With a gaseous absorber argon, free from the solid state structure, several resonance absorption lines are found due to optical levels, superimposed on the K absorption limit. The width of each of these absorption lines, one of which is sharp and

easily measured, gives directly the width of the K state of argon. The true K absorption discontinuity (complete ionization), an arctangent curve having this measured width, may be sketched in at the atom's periphery and three or more component resonant lines resolved.

21. Widths of Double-Ionization X-Ray Energy States. L. G. PARRATT, *Cornell University.*—Just as the energy level diagram is used to "explain" wave-lengths of x-ray lines, a diagram of *widths* of energy states (single-ionization) has been used to account for the *widths* of simple x-ray lines. An extension of this correlation to atomic states of double-ionization and the widths of the double-ionization (satellite) lines is attempted. Because of the uncertainties in the observed widths of most satellites, due to unresolvably overlapping adjacent components, one cannot ascertain from observed satellite widths the corresponding state widths. However, one might assume that the state of double-ionization has a width equal to the sum of the widths of each of the two single-ionization states involved. This says that the absence of the second electron does not influence the probability per unit time that either one of the vacancies will be filled. Then, knowing the single-ionization state widths, one might predict widths of satellite lines and use these widths as criteria (?) for sketching in under the observed complex contour *more* component lines than one finds direct experimental evidence for. Of 20 AgL series satellite lines measured, the width of one, $L\beta_2'$, 3.2 ev, is *less* than the width of the "parent" line, $L\beta_2$, 3.7 ev, which is tentatively ascribed to a decrease in the Auger width of N_V due to the $M_{LV,V}$ vacancy. This is, then, one case in which the above assumption is not valid.

22. Absorption of Soft X-Rays in Beryllium, Carbon, Aluminum, Copper, Silver and Gold. C. L. ANDREWS, *Cornell University.* (*Introduced by F. K. Richtmyer.*)—Absorption measurements for beryllium, carbon, aluminum, copper, silver and gold have been made for x-rays of wavelength 1.5A to 8.3A. Monochromatization was obtained with a modified Siegbahn-Thoraeus spectrometer, and the intensities measured with the aid of an ionization chamber. Most of the absorbing foils were made by evaporation of the metal onto a glass plate. A plot of log $\mu A/\rho z$ against log $z\lambda$ according to Jönson's rule for a universal absorption curve brings the data for all the elements except beryllium along a smooth curve. The curve for beryllium lies above the universal absorption curve. Since it is impossible to make sufficiently accurate chemical analysis for the impurity in the small amount of beryllium foil, no corrections for the impurities have been made. Plots of the absorption curve for beryllium in the neighborhood of the K discontinuity of iron show that much of the iron impurity is removed by fractional evaporation of the beryllium.

23. The Mean Life of Rubidium 87. E. J. KONOPINSKI* AND H. A. BETHE, *Cornell University.*—Recent experiments[1] have shown that naturally radioactive rubidium is definitely Rb^{87}, having a mean life of 10^{11} years. The spin of Rb^{87} is known to be 3/2 while that of Sr^{87} has recently been determined by Kopfermann to be 9/2. Thus, for the first time, the spin change taking place during a "forbidden" β-decay process is known. With the experimental value of 250 kv for the maximum energy of the β-rays, the theoretical lifetime comes out to be $10^{10}/|M|^2$ years for the Fermi theory and about 1/10 as long with the Uhlenbeck-Konopinski modification or with the spin-dependent interaction of Gamow and Teller.[2] M is the nuclear matrix element and is expected to be less than unity so the agreement is satisfactory. The parities of the initial and final nuclei were assumed to be different so that the product of the nuclear wave functions contains spherical harmonics of order $L=3$ (and higher). Equal parities would make $L_{\min}=4$ in the F and KU theories and $L_{\min}=2$ in the GT theory, giving too long and too short a life, respectively.

* National Research Fellow.
[1] Mattauch, Hahn, *et al.*, Naturwiss. **25**, 189 (1937).
[2] Phys. Rev. **49**, 895 (1936).

24. Evidence Against the Existence of Heavy Beta-Particles. ARTHUR RUARK AND CREIGHTON C. JONES, *University of North Carolina.*—Jauncey suggested[1] that the slower beta-particles from a radioactive source may have rest masses greater than m_0, the electronic mass. On this basis $R\gamma=\gamma_m$; where Rm_0 is the mass, $\gamma=(1-\beta^2)^{-\frac{1}{2}}$, and βc is the velocity. γ_m is the value of γ for a beta-particle at the upper end of the velocity spectrum. For Ra E, $\gamma_m=3.44$. We have analyzed Champion's photographs[2] showing collisions of Ra E beta-particles with electrons. In 14 collisions of good quality, interpreted on the above basis, $R\gamma$ ranges from 1.65 to 2.74, most of the values being below 2. This is conclusive evidence against the hypothesis of heavy beta-particles; obviously it has no bearing on the possibility that the heavy cosmic-ray particles are electrons of exceptional rest mass.

[1] Phys. Rev. **53**, 106 (1938).
[2] Proc. Roy. Soc. **136**, 630 (1932).

25. On the Theory of the Neutral Particle. W. H. FURRY, *Harvard University.*—In a recent paper[1] Majorana has shown that by the use of a special set of Dirac matrices the symmetry properties of the Dirac equations can be used to obtain a theory of the neutral particle in which neither negative energy states nor antiparticles ("holes") occur. If one introduces either a charge or a magnetic moment on the particle, it becomes necessary to admit the existence of antiparticles. The only other possibility of subjecting the particles to a force having a classical analogue is to use a "nonelectric force" as suggested some time ago by the writer.[2] The theory is here carried through without restriction on the form of the Dirac matrices, and for the case of a nonelectric force field. In spite of the fact that the theory does not admit the existence of antiparticles, pairs of particles can be produced by the field.

[1] Nuovo Cimento **14**, 171 (1937).
[2] Phys. Rev. **50**, 784 (1936).

26. Transmutation of Scandium by Th C′ Alpha-Particles. ERNEST POLLARD, *Yale University.*—The emission of protons from scandium under bombardment by Th C′ alpha-particles according to the reaction

$$Sc^{45}+He^4 \rightarrow Ti^{48}+H^1$$

has been observed. The energy distribution of the protons is complex, consisting of at least two groups with nuclear energy change $[Q]$ values -1.0 ± 0.4 Mev and -2.9 ± 0.4 Mev with some evidence of a more energetic group of $+1.0\pm0.5$ Mev energy change. Using this, together with Dempster's recent value for the mass of Ti^{48}, the value 44.9687 can be deduced for the mass of Sc^{45}.

27. Variations in the Relative Abundances of the Lead Isotopes. ALFRED O. NIER,* *Harvard University.*—A mass-spectrographic study of the isotopes of *common* lead shows that the relative abundances vary considerably in spite of a nearly constant atomic weight. The table below gives the results for several minerals. The numbers given are reproducible within at least one percent. A possible explanation for the variations is found if we consider the two oldest samples as primeval lead and the others as primeval lead contaminated by uranium and thorium lead. As the minerals listed are all essentially free from thorium and uranium, this may mean that the lead in them became contaminated before the mineral was formed. In view of these results the conclusions of Holmes[1] may have to be modified, inasmuch as he used the alleged constancy of common lead as an argument against the derivation of lead ores from acid or basic magmas. The samples were furnished and prepared by Professor G. P. Baxter.

MINERAL	GEOLOGICAL AGE IN M. Y.	204	206	207	208
Galena, Gr. Bear Lake	1300	1.00	15.9	15.3	35.3
Cerussite, N. S. W.	950	1.00	15.9	15.3	35.3
Galena, Germany	240	1.00	18.1	15.6	37.9
Galena, Joplin, Mo.	230	1.00	21.6	15.8	40.6
Cerussite, Wallace, Ida.	80	1.00	16.0	15.1	35.3
Wulfenite and Vanadinite, Arizona	25	1.00	18.4	15.5	38.2

* National Research Fellow.
[1] Holmes, Economic Geology **32**, 763 (1937).

28. The Scattering of Neutrons by Gases. H. CARROLL, P. N. POWERS, H. G. BEYER AND J. R. DUNNING, *Columbia University.*—It has been found possible to investigate the scattering of neutrons by gases through the use of a high pressure gas scattering cell. A collimated beam of neutrons about one meter long, from Rn—Be source to BF_3 pressure ion chamber, was utilized. Scattering measurements were made by interposing in the beam the high pressure scattering cell containing the gas to be investigated, and comparing the measurements with those having a calibrated "dummy" cell interposed. Approximately 300 K neutrons were utilized by making readings with and without Cd in the beam. Measurements have been made with a large number of gases. Preliminary results show that the proton (using H_2 in gas form) has a cross section of about 35×10^{-24} cm² compared with 45.0×10^{-24} cm² for the proton in CH_4.

29. The Scattering of Slow Positive Ions at Very Small Angles. A. G. EMSLIE, *Williams College.*—Scattering experiments with electrons and x-rays show that it is only in the angular region where diffraction or interference effects occur that the scattering is at all sensitive to the finer details of the fields of force involved. For positive ions, with their very short de Broglie wave-lengths, this important region is too small to be investigated by the usual electrical methods of recording, because of the relatively wide beams necessary to give measurable currents. A new method has been tried which avoids this difficulty and allows the critical angular region to be explored. The scattered ions are accelerated by a high voltage electrostatic lens and recorded on a photographic plate. The lens produces an angular magnification of the scattered pattern but does not distort it. The unlimited sensitivity of photographic recording permits a very fine beam to be used. Photographs of 150 to 300 volt lithium ions scattered by sodium vapor or by a polished nickel target show an unexpected uniform scattering up to angles of about half a degree. At greater angles the intensity falls off abruptly. With sodium vapor the plates also show a faint halo around the inner uniform disk.

30. On the Scattering of Neutrons by Paramagnetic Media. J. H. VAN VLECK, *Harvard University.*—Whitaker's experiments[1] have failed to reveal any excess of neutron scattering in paramagnetic materials over that calculated from the sum of the cross sections for purely nuclear scattering. Halpern and Johnson[2] showed that due to interaction between the neutron's magnetic moment and electron spin a large excess is to be expected if the wave-length λ of the neutron is large compared with the orbital radius r of the paramagnetic electrons. They note that negative experimental results are probably attributable to the form factor, i.e., nonfulfillment of the condition $\lambda/2\pi\gg r$. However, if the scattering is computed on the usual basis that the atoms can be treated as free independent units, the reduction due to the form factor disappears for forward scattering. The present paper shows that exchange coupling between the paramagnetic atoms makes them tend to scatter inelastically rather than elastically. The mean energy change is estimated to be roughly $k\cdot200°$ (140 cm^{-1}) for the materials used by Whitaker. In consequence the reduction due to the form factor is greater than for free atoms and persists even in the forward direction. The preponderantly inelastic character of the collisions thus makes it easier to understand the negative outcome of Whitaker's experiments.

[1] M. D. Whitaker, Phys. Rev. **52**, 384 (1937).
[2] O. Halpern and M. H. Johnson, Phys. Rev. **52**, 52 (1937).

31. Note on the Hartree Approximation Method for Calculating Nuclear Energies. V. F. WEISSKOPF, *University of Rochester.*—A method is given for estimating the order of magnitude of the successive approximations to the nuclear energy as given by the Hartree method. For nuclear potentials of the form Ae^{-r^2/a^2} the nth approximation, E_n, to the binding energy per particle is given by the expressions:

$$E_1\cong c_1A\,;\quad E_2\cong c_2A^2Ma^2/\hbar^2\,;$$
$$E_n\cong c_nA^n(Ma^2/\hbar^2)^{n-1}(r_0/(9\pi)^{\frac{1}{3}}a)^{n-1}\cdots(n\text{ odd})\,;$$
$$E_n\cong c_nA^n(Ma^2/\hbar^2)^{n-1}(r_0/(9\pi)^{\frac{1}{3}}a)^{n-2}\cdots(n\text{ even}).$$

In these formulas $N^{\frac{1}{3}}r_0$ is the radius of a nucleus with N

particles. The c_n are constants which vary as n^3. E_1 and E_2 have been calculated explicitly by Euler.[1] If $r_0/(9\pi)^{\frac{1}{3}}a$ can be considered as small, the first two approximations alone contribute essentially to the energy. It is possible by means of similar methods to compute the level density of the nucleus in the successive Hartree approximations, and to correct in this way the result of Bethe[2] for the free particle nuclear model. According to Bardeen[3] the first approximation leads to a decrease of the level density. The present calculations show that the second approximation compensates this decrease completely and may even indicate a higher level density than that of Bethe's formula. As the above expressions show, the Hartree method converges only when $r_0/(9\pi)^{\frac{1}{3}}a$ is small and in this case the approximations beyond the second do not contribute appreciably to the level density.

[1] H. Euler, Zeits. f. Physik **105**, 553 (1937).
[2] H. Bethe, Phys. Rev. **50**, 332 (1936).
[3] J. Bardeen, Phys. Rev. **51**, 799 (1937).

32. Multipole Radiation Probabilities in Light Nuclei. M. PHILLIPS, *Connecticut College.*—According to the Hartree approximation the lowest group of levels in each of the nuclei Li^6, B^{10}, N^{14} contains both triplets and singlets described by the same space wave functions.[1] Between such states there should be magnetic dipole radiation corresponding to the proton and neutron magnetic moments. Application of the ordinary radiation formula yields the transition probability:

$$A=\frac{mce^2}{3\hbar^2}\left(\frac{m}{M}\right)^2\epsilon^3\left|\sum_{p,\,n}(g_p\boldsymbol{\sigma}_p+g_n\boldsymbol{\sigma}_n)\right|^2,$$

where ϵ is the energy difference between singlet and triplet levels expressed in mc^2. Since $\epsilon\sim 6$ the consequent width of the singlet levels may be as large as a few tenths of a volt. The electric quadrupole radiation probabilities for transitions between levels having the same spin but different orbital angular momentum have also been estimated, and are somewhat smaller. The latter transitions would occur within the lowest group of states in all the nuclei considered in reference 1. The broadening in such deep lying metastable states may be surprising in view of level widths in the slow neutron range, and may again raise the question of the applicability of ordinary radiation formulae to nuclear processes.

[1] Feenberg and Wigner, Phys. Rev. **51**, 95 (1937); Feenberg and Phillips, Phys. Rev. **51**, 597 (1937).

33. Beta-Radiation from Activated Isotopes of Arsenic. B. R. CURTIS AND J. M. CORK, *University of Michigan.*—Although arsenic has but one stable isotope As^{75} there are at least three radioactive isotopes. These are as follows: (a) As^{76} from As^{75} by slow neutron capture (n, γ) or by deuteron bombardment (H^2, H) or from Br^{79} by fast neutrons (n, α); (b) As^{78} from Br^{81} by fast neutron bombardment (n, α), and (c) As^{74} produced by fast neutrons on As^{75} $(n, 2n)$. The half-lives of these activities are, respectively, 26 hr., 80 min. and 13.5 days. The first two emit negative electrons while the very long 13.5-day activity emits both positives and negatives. The form of the beta-distribution for such a heavy long period positive emitter should be of particular interest. Measurements from the histograms indicate an upper limit of 0.65 Mev for the positron spectrum and about 2.3 Mev for the 26 hr. negative activity.

34. The Disintegration of Be by Alpha-Particles. H. L. SCHULTZ,* *Yale University.*—The excitation function for the emission of neutrons from Be under alpha-particle bombardment has been studied. Measurements of other observers have been extended by using the more energetic particles from Ra C′ and Th C′. Neutrons from a 4 mm air-equivalent Be layer were detected with the aid of a BF_3-filled ionization chamber surrounded by paraffin. The data obtained by this method give a pronounced resonance maximum in the yield curve at an alpha-particle range of 1.2 cm. The presence of a weaker resonance effect near the top of the barrier reported by Bernardini has not been confirmed. Above 4 cm range the yield is found to remain approximately constant until 7 cm range where it again appears to decrease. Interpretation of this behavior above the barrier height will be discussed.

* Sterling Fellow.

35. The Apparent Discrepancy Among the Experimental Measurements of the Atomic Constants. RICHARD A. BETH, *Worcester Polytechnic Institute.*—The work of Birge and others[1] has emphasized that probably (on the basis of the statistical theory of errors) our present interpretation of experimental measurements of R_∞, e, e/m, and h/e is not consistent with our present views of the theoretical interrelations among these quantities. This situation is depicted by means of a new form of diagram, based on $R_\infty=2\pi^2me^4/ch^3=109737.42$ cm^{-1}, which treats all other atomic constants of the form $f=kc^\alpha h^\beta m^\gamma$ (in particular, e, m, h, e/m, h/e, h/mc, $he/4\pi mc$, $8\pi^2m/h^2$, and $hc/2\pi e^2$) in a mathematically similar way. This largely avoids a tendency to bias the question as to where the indicated difficulty may lie, in the form of its presentation. The diagram shows probable errors of measured quantities and permits a graphical estimate of probable errors of dependent quantities. It permits a simple graphical determination of any f from given values of any two others. Its relation to the Birge-Bond diagram[2] can be expressed in simple mathematical terms.

[1] R. T. Birge, Phys. Rev. **49**, 204 (1936), Nature **137**, 187 (1936) and Phys. Rev. **52**, 241 (1937). R. Ladenburg, Ann. d. Physik **28**, 458 (1937). J. DuMond and V. Bollman, Phys. Rev. **51**, 427–9 (1937). F. G. Dunnington, Phys. Rev. **52**, 501 (1937). J. DuMond, Phys. Rev. **52**, 1251 (1937).
[2] R. T. Birge, Science **79**, 438 (1934).

36. The Photon Emission of the Sun. ARTHUR E. HAAS, *University of Notre Dame.*—Quantum-theoretical computations lead to the result that the total number of photons emitted per sq. cm per sec. by a black-body in thermodynamical equilibrium is equal to $(4\pi\beta k^3T^3)/(h^3c^2)$, where k and h denote Boltzmann's and Planck's constants, respectively, T the absolute temperature, c the velocity of light, and $\beta=1/1^3+1/2^3+\cdots=1.20206$. This yields a value of $1.5\times10^{11}\times T^3$ photons per sq. cm per sec. The average energy of a photon in thermodynamical equi-

librium is thus equal to $3kT\times\alpha/\beta$, where $\alpha=\pi^4/90=1.0823$. If we consider the sun as a black-body in thermodynamical equilibrium having a surface temperature of about 6000°K, we find the total emission to be about 2×10^{45} photons per sec. The sun would send about two photons per sec. through a sq. cm area at a distance of 10,000 light years (about 10^{22} cm). The total number of photons emitted by the sun in a period of about 20,000 years equals the total number of protons and neutrons contained in the sun. This fact seems to lead to some new aspects concerning the question of the photon production in the sun.

37. On the Theory of the Emissivity of Metals. EUGENE GUTH, *University of Notre Dame. (Introduced by George B. Collins.)*—(1) H. A. Lorentz derived for his free electron metal model the radiation law of Rayleigh-Jeans by computing explicitly the emissivity and the absorption of his metal model and then applying Kirchhoff's law. The derivation of Planck's law by considering an arbitrary body, e.g. any metal, can be obtained by a simple extension of Einstein's derivation of Planck's law. (2) The simplest radiation law based on correct approximations holds for the spectral emissivity of metals for long waves and at low temperatures, the dependence of the electric resistance of the metal on the frequency being neglected. Simple laws can also be derived by taking into account this dependence and neglecting the jumping of electrons in other energy bands which may eventually occur along with an excitation of the whole lattice. (3) More general laws can be obtained semi-empirically by using simple representations of the dependence of the optical constants of metals on the frequency. In the selection of these expressions, the results theoretically obtained for simplified models can be used.

38. Suggested Explanation of the Contradiction Between the Rayleigh-Jeans Formula and Experiment. PRESTON B. CARWILE, *Lehigh University.*—According to classical theory, degrees of freedom for radiant energy in a finite volume of free space may be thought of as modes of resonance for plane waves in the space. Resonance, however, depends on the existence of definite relationships at every instant of time, between incident and emergent waves at the boundary surface, as regards frequency, amplitude, phase, direction of propagation and state of polarization. It may be shown on classical grounds that these relationships do not exist at an interface between free space and a material substance. Therefore, modes of resonance in space have no meaning, and the Rayleigh-Jeans formula is not applicable to the partition of energy between space and a material body.

39. The Intensity of the Primary Cosmic Radiation and Its Energy Distribution. THOMAS H. JOHNSON, *Bartol Research Foundation, The Franklin Institute.*—The number of primary cosmic rays incident upon one horizontal square centimeter at the top of the atmosphere is computed by dividing the total energy spent in ionization in an infinitely deep column of air by the average energy of a single primary ray. The energy is found by integrating under the ionization-depth curves of Bowen, Millikan, Neher and Haynes[1] and the average energy per ray is computed from the minimum energy of the Lemaître and Vallarta theory, with a suitably chosen energy distribution function. Evidence for a low energy limit at about 4.0×10^9 volts is found. The number of primary cosmic rays increases from 0.03 per cm² per sec. at the equator to 0.36 per cm² per sec. at latitudes above 45°. The total cosmic-ray current to the earth, if all rays are positive, is 0.13 ampere or 8×10^{17} rays per sec. The distribution function for the number of rays can be represented by AV^{-n} where n is equal to or slightly less than 3, and V is the energy of a single ray.

[1] Bowen, Millikan and Neher, Phys. Rev. **52**, 80 (1937). Bowen, Millikan, Neher and Haynes, Phys. Rev. **50**, 992 (1936).

40. The Multiplicative Theory of Showers as Applied to Large Bursts of Cosmic-Ray Ionization. C. G. MONTGOMERY AND D. D. MONTGOMERY, *Bartol Research Foundation of The Franklin Institute.*—The energy spectrum of the electrons incident upon a small thickness of material is calculated, by means of the Bhabha-Heitler theory, from the observed frequency distribution of bursts of ionization produced by 100-ray showers, the effect of fluctuations being taken into account. The energy distribution obtained is of the form $1/E^{\alpha}$ where α is 2.5 for energies of the order of 10^9 volts and decreases slowly with increasing energy, in agreement with the energy distribution calculated by Heitler to explain the variation of cosmic-ray intensity with altitude. The number of electrons necessary to give the observed frequency of bursts is only about 1 percent of the total number of particles at sea level in the energy range 10^9 to 10^{10} volts. The incident energy spectrum found in this way is then used to calculate the number and frequency distribution of large bursts at large thicknesses of material. These calculated values differ considerably from the experimental ones. It may be concluded that, although the theory is satisfactory as a description of the building-up process of a large shower, some modification must be introduced to account for the penetration of showers through large thicknesses of matter.

41. On Sidereal Diurnal Variation in Cosmic-Ray Intensity. S. E. FORBUSH, *Department of Terrestrial Magnetism, Carnegie Institution of Washington. (Introduced by John A. Fleming.)*—Important implications concerning the origin of cosmic rays would follow were a sidereal diurnal variation in the observed cosmic-ray intensity definitely established. In addition to the possibility of emission or absorption in the Milky Way, there exists the apparent effect of galactic rotation investigated by A. H. Compton and I. A. Getting.[1] Modern statistical methods, developed by J. Bartels,[2] have been applied to data for 595 days from continuous records obtained from a Compton-Bennett precision recording cosmic-ray meter at Cheltenham, Maryland. The results indicate that if a 24-hour sidereal wave in cosmic-ray intensity actually exists, the data for 595 days at this station are statistically inadequate to establish the fact. This conclusion is substantiated by analysis of data for 396 days from a similar instrument at Huancayo, Peru. Results for these two stations are com-

pared with those which have been published for other stations.

[1] Phys. Rev. **47**, 817–821 (1935).
[2] Terr. Mag. **40**, 1–60 (1935).

42. Cesium Discharges Under Conditions of Nearly Complete Ionization.—FRED L. MOHLER, *National Bureau of Standards, Washington, D. C.*—The absolute intensity and intensity distribution of the continuous recombination spectrum have been used to measure the electron concentration and electron temperature in a high current discharge through a capillary 1 mm or more in diameter. In the pressure range 0.1 mm to 7 mm the intensity at high currents varies as the square of the pressure. At constant pressure the intensity rises to a flat maximum and then decreases with increasing current, the current density for the maximum ranging from 40 to 100 amperes per cm². The electron temperature is nearly independent of the pressure and increases nearly linearly with the current from 3100°K at 30 amperes per cm² to 7500°K at 200 amperes per cm². The intensity variation with pressure and current can be accounted for by Saha's equation with the assumption that the gas temperature is equal to the electron temperature. The maximum intensity is attained when about 0.9 of the gas is ionized and further increase in current lowers the ionization by pure temperature effect. Over a wide range of pressure and current nearly complete single ionization can be attained.

43. The Use of Isotopes in the Study of Ionization Processes of Polyatomic Molecules. J. M. DELFOSSE AND J. A. HIPPLE, JR., *Princeton University.*—In recent studies of hydrocarbons with the mass spectrometer, it has been shown that there are a great many different ions formed when the molecule is dissociated by electron impact. In many cases the appearance potential may be interpreted uniquely and the actual process may be determined. A greater insight into the processes occurring may be obtained from an additional study of the heavy hydrocarbons. An example of this is the study of the size of the peaks observed in *cis* and *trans* $C_2H_2D_2$. The ratio, (mass 15/mass 16) = 10, obtained with the mass spectrometer indicates that the most probable process is a splitting of the molecule into the two CHD radicals rather than CD_2 or CH_2. The ratio CHD^+/CD_2^+ is actually greater than the above figure since the impurities would tend to increase mass 16 more than mass 15. One of these impurities is perhaps asymmetric $C_2H_2D_2$. Other processes in this gas may be interpreted by the same method.

44. Ionization and Dissociation by Electron Impact in CCl_2F_2 and in CCl_4 Vapor. RICHARD F. BAKER AND JOHN T. TATE, *University of Minnesota.*—In the table is given the relative abundance of the ions formed in these gases at an electron energy of 75 ev. The appearance potentials are also given. The process $CCl_4 \rightarrow CCl_3^+ + Cl^-$ is a very probable one. An upper limit of 1.7 volts is fixed for the electron affinity of Cl_2. The heat of formation of CCl_2F_2 is calculated to be 4.7±1 volts (108±23 kcal).

Ion	Int.	A.P. (volts)	Ion	Int.	A.P. (volts)
CCl_4^+	0.02	11.0±1.0	$CCl_2F_2^+$	0.3	11.7±0.5
CCl_3^+	100.0	12.2±0.2	CCl_2F^+	8.0	15.4±0.2
CCl_2^+	23.5	16.0±0.2	$CClF_2^+$	100.0	12.8±0.2
CCl^+	27.8	17.1±0.2	$CClF^+$	4.3	18.1±0.2
		19.5±0.2	CF_2^+	15.0	18.1±0.2
Cl_2^+	0.35	16.4±0.5	CCl^+	6.4	17.0±0.5
		23.0±1.0	CF^+	20.0	19.5±0.5
Cl^+	27.6	19.1±0.2	Cl_2^+	0.3	16.7±1.0
C^+	14.4	23.5±0.2	F_2^+	0.4	16.0±1.0
CCl_3^{++}	1.6	31.8±1.0	Cl^+	18.5	21.0±0.2
CCl_2^{++}	0.8	34.0±1.0	F^+	1.2	31.5±0.5
Cl^-	99.5	1.3±0.5	C^+	9.0	26.5±1.0
		5.8±0.5	CCl_2F^{++}	0.7	19.3±1.0
		12.4±0.2	$CClF_2^{++}$	0.9	35.5±1.0
Cl_2^-	0.1	4.8±1.0	F^-	7.0	1.4±0.5
		17.0±0.5			15.3±0.5
C^-	0.01	—			
CCl^-	0.005	—	Cl^-	16.0	2.9±1.0
					13.0±0.5
			C^-	0.05	31.0±1.0

45. The Energy Loss of Electrons in Lead. A. J. RUHLIG AND H. R. CRANE, *University of Michigan.*—Continuing previous work[1] on the absorption in carbon and lead of electrons having energies from 2 to 11 Mev, the losses in lead of electrons with energies both above and below this range have now been measured. For the low energy range electrons from radioactive P^{32} were sent through lead laminae of two thicknesses placed in the center of a cloud chamber. For the high energy group the electrons and positrons produced by the $Li+H^1$ gamma-radiation were used. The values found are again considerably greater than those predicted by theory, but are in good accord with the previous experimental values.

	Thickness of Pb	Average Incident Energy	Average Energy Loss
Electrons	0.038 mm	0.82 Mev	0.12 Mev
	0.066 mm	0.82 Mev	0.20 Mev
	0.38 mm	9.4 Mev	1.1 Mev
		12.7 Mev	2.3 Mev
Positrons	0.38 mm	5.8 Mev	1.1 Mev
		9.5 Mev	1.5 Mev
		12.3 Mev	2.3 Mev

[1] Turin and Crane, Phys. Rev. **52**, 63 (1937); **52**, 610 (1937).

46. Compressibility of the Alkali Metals. J. BARDEEN, *Harvard University.*—As a further test of the method of Wigner and Seitz[1] (for the calculation of the energies of the monovalent metals), the pressure variation of the compressibilities of the alkali metals is determined and compared with recent experimental results of Bridgman[2] which extend to pressures of the order of 45,000 kg/cm². Improved calculation of the variation of the energies of Li and Na with volume yields the results given in the following table. Here v_0 is the volume at zero pressure and v is the actual volume; the smaller volumes in each case correspond to a pressure of about 40,000 kg/cm². The observed results are all extrapolated to $T=0$°K. The ion-core fields used by Wigner and Seitz were also used in the present calculation.

	Lattice Constant	Heat of Sublimation (kcal./mole)	Compressibility $\times 10^{12}$ (abs. c.g.s. units)	
			$v/v_0=1$	$v/v_0=0.808$
Li (exp.)	3.46A	46	7.4	4.2
Li (calc.)	3.49A	34	8.4	5.2
			$v/v_0=1$	$v/v_0=0.745$
Na (exp.)	4.25A	30	12.3	5.0
Na (calc.)	4.53A	23	12.0	4.6

A simplified method was used to determine the Fermi energy. Frohlich's[3] approximate analytic expression for the energies of the alkali metals suggests the following semi-empirical form:

$$W=a/v+b/v^{\frac{1}{3}}-c/v^{\frac{1}{2}}.$$

If the parameters are determined from (1) the lattice constant, (2) the energy, and (3) the compressibility (all taken at $p=0$) the expression gives values for the relative change of volume with pressure in close agreement with Bridgman's results. The constants so determined agree fairly well with Frohlich's theoretical values.

[1] Wigner and Seitz, Phys. Rev. **43**, 804 (1933); **46**, 509 (1934); Seitz, Phys. Rev. **47**, 400 (1935); Wigner, Phys. Rev. **46**, 1002 (1934).
[2] Proc. Am. Acad. (in press).
[3] Proc. Roy. Soc. **158A**, 97 (1937).

47. The Fine Structure of the Nuclear Ground Level of Li^7. G. Breit, *University of Wisconsin*, and J. R. Stehn, *Harvard University*.—To throw light on the form of the interaction energy between pairs of nuclear particles, the "approximately relativistic" equations[1] are applied to the fine structure of the ^2P ground level of the Li^7 nucleus. Since in this theory the requirements of relativistic covariance do not determine the spin-orbit interactions uniquely, there are adjustable parameters which are essentially coefficients of invariant additions to the Hamiltonian. These parameters are chosen to obtain agreement with the observed fine structure. Both the potential energies and the single-particle wave functions are assumed to have the customary Gaussian variation with space. The results are sensitive to the over-all wave function used and are thus of only qualitative significance. For the two p neutrons coupled into a ^1S state, the parameters can be ~ 1. But with the more likely symmetric-coordinate function of the three p particles (a linear combination of ^1S and ^1D for the neutrons), the parameters must be ~ 3. This does not correspond to the picture of one particle moving in a scalar field due to another; it requires instead an additional interaction having the transformation properties of an electromagnetic field.

[1] G. Breit. Phys. Rev. **51**, 248 (1936).

48. On the Saturation of Nuclear Forces. C. Critchfield and E. Teller, *George Washington University*.—Nuclear forces have saturation character as shown by the facts that both the total binding energies and the volumes of heavy nuclei are roughly proportional to the number of elementary particles (protons and neutrons) contained in the nucleus. The usual explanation is that the interaction between the heavy elementary particles is of the exchange type. An alternative explanation can be given with the help of the following assumptions: (1) a neutron or a proton can emit an electron-positron pair into one definite (or a few definite) quantum state of finite extension, L (this assumption violates relativity but secures convergence); (2) the average kinetic energy of the electron and positron in this state, E_{kin}, is small compared with the matrix element H' giving rise to pair emission. These assumptions lead to a potential which can not be written as a sum of interactions between pairs of heavy particles. If all particles are closer to each other than the extension, L, of the state into which the light particles may be emitted, the total potential is proportional to the number of particles. Setting $L\sim$electron radius this potential per particle is $\sim 137\ mc^2$ in rough agreement with experience.

49. On the Rotation of Atomic Nuclei. E. Teller, *George Washington University*, and J. A. Wheeler, *University of North Carolina*.—In Bohr's droplet model of the nucleus rotation of the nucleus as a whole should lead to levels lying only a few kilovolts above the fundamental state. Such levels would give rise to difficulties in the theory of the fine structure of radioactive decay and of metastable nuclear states. The Bohr model can be reconciled, however, with the absence of these low excitations since certain rotational states may be missing if some rotations amount merely to exchanges of nuclear constituents. Although this argument excludes a sufficient number of levels only for very symmetrical rigid geometrical configurations the rotational exchange becomes equally important for all other cases if the amplitudes of the zero-point vibrations of the constituents are comparable to their separations. Then, owing to the difficulty of identifying the path of a definite particle, the rotation of the droplet loses all similarity to rigid rotation unless the rotational quantum number, J, becomes higher than a certain $J_{\min}$ (for heavy nuclei $J_{\min}\sim 8$). Under such circumstances the lowest excited state of the Bohr model will be inversely proportional to the mass of the nucleus, giving $\sim 10^5$ volts for the heaviest nuclei. Similar values are obtained from the independent particle picture.

50. The Rotational Transition in Solid Methane. John A. Wheeler and C. V. Cannon, *University of North Carolina*.—The face-centered crystal CH_4 shows a single transition at 20°K associated with an energy increase of 15.7 cal./mole. Clusius has recently found that CD_4 gives two transitions (21°K and 26°K; total energy increase of 78.5 cal./mole). We attribute the different *energy content* of light and heavy methane at low temperatures to the different zero point energy of their torsional vibrations, and thus determine for the ordered state how fast the rotation potential

$$V(\theta_x, \theta_y, \theta_z)=\text{const.}+2W(\theta_x^2+\theta_y^2+\theta_z^2)$$

increases for small rotational displacements θ_x, θ_y, θ_z from equilibrium. The simplest potential having the tetrahedral symmetry of the molecule and the symmetry demanded by the ordered state is

$$V(\theta, \varphi, \chi)=W\{[5\sin^4(\theta/2)-6\sin^6(\theta/2)]\cos 2(\chi-\varphi) + [5\cos^4(\theta/2)-6\cos^6(\theta/2)]\cos 2(\chi+\varphi)\},$$

where W has the same meaning as above. The rotational energy levels of the molecule are split in the proper way by this field to account for the entropy $R\ln 16$ observed for CH_4 at low temperatures. Calculation of the position of the altered energy levels and the mutual influence between molecules makes it possible to obtain a reasonable estimate of the heat content and degree of order at various temperatures and to check in order of magnitude the transition temperature calculated from the difference in zero point energies against the observed transition points.

51. The Potential Barrier in Ethylene Chloride. J. Y. BEACH AND K. J. PALMER, *Princeton University and California Institute of Technology.*—An electron diffraction investigation has been carried out on ethylene chloride to determine the extent of internal rotation around the carbon-carbon bond. Photographs taken at Princeton and at Pasadena both lead to the same result—that the potential barrier is 5 kcal. or greater. The procedure adopted was to calculate theoretical intensity curves assuming the potential function $A \sin \phi$. ϕ is the relative orientation of the two CH_2Cl groups. A is the height of the potential barrier and was varied from zero to infinity. Tetrahedral bond angles and covalent bond radii were assumed for the calculation. The *trans* model (A equal to infinity) is in good agreement with the photographs. The steric repulsion of the chlorine atoms was calculated by the method of Eyring and was found to give a potential barrier of 4.5 kcal. These values are compared with the value obtained by Altar from a Fourier analysis of the dipole moment data.

52. Nuclear Quadrupole and Magnetic Moments. KATHARINE WAY, *University of North Carolina.*—Observations of nuclear electric quadrupole moments, q, reveal a lack of spherical symmetry in the distribution of positive charge, the more frequently found positive q indicating an elongated and the less common negative q a flattened shape. Nuclear models which have been proposed may be classified under (1) single particle model, (2) liquid drop model, and (3) central core plus single particle model. Rose and Bethe[1] have shown that model (1) will account for magnetic moments of light nuclei but to make predictions about q from this model seems difficult. Model (2) has been known to give magnetic moments, μ, of the correct order of magnitude. However, calculations will be presented showing that its q values are very much too small. Schmidt[2] points out that the interaction of an extra neutron or proton with an elongated core (variety of model (3)) accounts qualitatively for variation of μ with spin and for positive q's. Fano[3] suggests that the core has an α-particle structure which for maximum number of bonds will have an elongated more often than a flattened shape. It is concluded that model (3) seems the most promising.

[1] Phys. Rev. **51**, 205 (1937).
[2] Zeits. f. Physik **106**, 358 (1937).
[3] Naturwiss. **37**, 602 (1937).

53. Analysis of Hyperfine Structure of Mn I and an Indicated Value for the Nuclear Magnetic Moment. RUSSELL A. FISHER AND EDSON R. PECK, *Northwestern University.*—New measurements of the hyperfine structure in visible lines of the Mn I spectrum provide a check upon disagreements reported by previous workers[1] as well as some new data. The observations are in general agreement with those of White and Ritchl and with their assigned value of $I=2\frac{1}{2}$ for the Mn nucleus but yield some additional details of structure not previously reported. With the new data and graphical methods of analysis, we obtain values for the separation factors of 24 different hyperfine multiplets arising in configurations d^6s, d^5s^2, d^5sp, d^5ss and d^6p. Much of the analysis is supported by observations of the Bock-Goudsmit effect in Mn I lines.[2] Formulas expressing the observed splittings in terms of coupling coefficients of individual electrons are consistent with the data and provide experimental values for the electron coupling coefficients. All interactions are detectable but that of a $4s$ electron is most prominent, providing a coupling coefficient which depends somewhat upon the total configuration. If the ionization energy of the $4s$ electron in each configuration is taken as a measure of its coupling with the nucleus we obtain by Goudsmit's methods[3] values for the nuclear magnetic moment. Three computations based on independent data agree within ten percent upon a value of 1.1 for the nuclear g-factor.

[1] White and Ritchl, Phys. Rev. **35**, 1146 (1930). Mohammad and Sharma, Phil. Mag. **18**, 144 (1934).
[2] Fisher, Platt and Fry, unpublished data.
[3] Goudsmit, Phys. Rev. **43**, 636 (1933).

54. Hyperfine Structure of Boron, Yttrium, Rhodium and Palladium. D. T. WILLIAMS AND L. P. GRANATH, *New York University.*—The spectra of boron, yttrium, rhodium and palladium have been investigated for hyperfine structure in the region 2400–4000 angstroms with a 20 cm quartz Lummer-Gehrcke plate. A Schuler tube with uncooled cathode was used as a source of radiation. The boron resonance doublet at λλ2497.73 and 2496.78 appeared too broad to reveal any asymmetry. Twenty-one lines in the yttrium first spark spectrum showed no significant h.f.s. Of seventy-one lines in the rhodium arc spectrum, only four, which end on the resonance level, appeared complex. The doublet structure observed seems to be due to absorption. A report by Sebaiya of recent date giving the same lines a genuine h.f.s. prompted the authors to obtain photographs using a tube with a water-cooled aluminum cathode as source. These photographs show no structure in the resonance lines. Twenty-six lines in the palladium arc spectrum revealed no significant hyperfine structure. It is estimated that any structure of magnitude greater than 0.05 cm^{-1} would be observable in the photographs of the three latter spectra, taken with the uncooled source. During the course of the research the iron spectrum was found to be excited when the current through the source was about 1.5 amperes. The average half-breadth of two of the stronger unreversed lines, chosen at random, was 0.10 cm^{-1}.

55. Alkali Halide-Thallium Phosphors. FREDERICK SEITZ, *General Electric Co.*—An attempt is made to interpret the properties of alkali halide-thallium phosphors. The experimental basis of this interpretation is the work of Pohl and his numerous collaborators on these sub-

stances. It is concluded that the long wave-length absorption peaks of the phosphors which are not contained in the pure alkali halides are to be attributed to the excitation of the thallium ions. These are assumed to be distributed throughout the crystal, replacing alkali metal ions. The structure of the observed peaks is interpreted in terms of the details of the spectrum of Tl^+ and the probable effects of crystalline perturbations. The nature of the fluorescent and phosphorescent spectra is then correlated with the behavior of the normal and excited levels during the time after absorption and before optical radiation in which the crystal again comes to mechanical equilibrium. Distinction is drawn between two cases: That in which the excited Tl ion has no thallium ions among its twelve positive ion neighbors and that in which it has one. It is concluded tentatively that excitation to the lowest excited levels, associated with a triplet in the free ion, will give rise to fluorescence in either case, and that excitation to the higher, singlet level will lead to the alternative possibility of phosphorescence in the second case, but not in the first. The theoretical justification of these tentative conclusions involves assuming that the interactions corresponding to homopolar forces between the excited ion and its neighbors depress singlet excited levels more than triplet excited levels, and that singlets are depressed more when one of the neighbors of a Tl ion is another Tl ion than when none are.

56. Heavy Particle Interactions. D. R. INGLIS, *Princeton University.**—The simplest combinations of exchange operators in a symmetrical nuclear Hamiltonian give important results relating the stability of isobars. One may enquire what other combinations would be as satisfactory. From a simplified treatment of the instability of odd-odd nuclei, one has *two* approximate conditions on the coefficients, $g_q > g$ and $g_q > g + 2g_\sigma$ (remarks[1] to the contrary notwithstanding). The first arises from a singlet and the other from a triplet state of the unstable nucleus. These and a third condition, derived earlier for the proper stability of isobars, are all amply satisfied by a combination of operators giving as much binding as possible subject to the well-known conditions that there shall be no very heavy nuclei, whether "ferromagnetic" or not. (In this combination, the space-exchange term is not overwhelmingly predominant, the spin-exchange term being half as large.) This emphasizes the point that the remarkable success[1] of the simplest combination of operators does not conclusively favor it as a close approximation.

* On leave of absence from the University of Pittsburgh.
[1] E. Wigner, Phys. Rev. **51**, 947 (1937), especially footnote 10.

57. Rate of Recrystallization in Polycrystalline Solids. L. A. YOUNG, *Carnegie Institute of Technology.*—A theory of rate curves for the transformation of a polycrystalline solid A into an allotropic modification B has been developed. For usual cases this will occur by nucleation and subsequent growth of these nuclei. We designate by $F_B(t)$ the fraction of A transformed to B at a time t after the transformation is initiated. Then $F_B(t) = n(t)\ g(t)$, where $n(t)$ represents the fraction of crystalline grains in which nucleation has occurred prior to t, and $g(t)$ the average fractional transformation of such grains at this time. Simple expressions for $n(t)$ and $g(t)$ have been derived. The first involves λ, the probability per unit time of nucleation occurring in a given grain; the second, a quantity T representing the average time necessary for complete transformation of a grain after nucleation. By proper choice of λ and T the function $F_B(t)$ can be made to fit experimental rate curves. Thus it is possible to determine separately the effect of impurities, change of temperature, etc., on the rate of nucleation and on the rate of growth of nuclei. This is of particular importance in gaining a better understanding of transformations in metals and alloys.

58. Relationship Between Internal Friction and Cold Work in Metals. CLARENCE ZENER, *College of the City of New York.*—A cold worked metal has residual internal stresses. When such a metal is vibrating, these internal stresses give rise to local heat currents, which in turn give rise to an increase in entropy. Hence these residual stresses are a source of internal friction. A quantitative theory of this internal friction is here given. Several experimental investigations have already shown that the internal friction of metals is increased by a large factor when cold worked. The theory here presented will enable one to interpret measurements of internal friction, made over a wide frequency range, in terms of the residual internal stresses. From such measurements it will be possible to calculate not only the energy associated with these stresses, but also the average dimensions of these stresses.

59. Some Unusual Demonstrations with Piezoelectric Resonators. K. S. VAN DYKE, *Wesleyan University.*—All of the following experiments, except 3, have been demonstrated at Scott Laboratory for a number of years but have not previously been shown outside. 1. *Spinning and translatory motions of a quartz sphere.*[1] In a field produced by a 1000-volt generator tuned to certain of the sphere's natural modes of vibration, a 4 cm sphere resting on an eighth-inch hole in the bottom brass electrode orients itself so as to select a vertical axis about which it then spins at a rate of one to two revolutions per second. If the atmospheric pressure is reduced, the glow discharge patterns which appear on the surface of the spinning sphere are very striking. In another mounting the sphere progresses along a level track by sliding without rolling. 2. *The friction between a vibrating quartz surface and a stationary surface is almost zero.* 3. *A steel ball dropped onto a vibrating quartz crystal may rebound to a greater height than that from which it fell.* 4. *Spraying a liquid from a vibrating surface,* the vibrating crystal being the atomizer, and the burning of the fingers on touching a cold vibrating quartz resonator were first observed in 1924 with a low power generator. They are similar to some of the effects described later by Wood and Loomis[2] but produced by them on a much larger scale.

[1] Proc. I. R. E. **16**, 706 (1928).
[2] R. W. Wood and A. L. Loomis, Phil. Mag. **4**, 417 (1927).

60. The Velocity of Sound in Air. R. C. COLWELL, A. W. FRIEND AND D. A. MCGRAW, *West Virginia University.*—

The velocity of sound in air has frequently been measured over long distances by means of explosives and chronometers. With modern electrical devices, the velocity may be found over short distances in a laboratory. An electron tube is connected in a circuit to produce 60 short pulses a second in a loud speaker. The sound pulses are received in a microphone and applied to the deflecting plates of a cathode ray oscillograph. A synchronous sweep is produced with a sixty cycle sine wave. When the microphone is moved approximately 5.75 meters, the pulse deflection moves along the sweep and returns to its original position on the screen. The time represented by this motion is one-sixtieth of a second. The average velocity for 100 measurements (ten readings at ten different temperatures) was found to be 331.54 meters/sec. at 0°C. By the use of the same sweep circuit in conjunction with a synchronous 3000-cycle timing wave, it is possible to measure the velocity of sound when the microphone is displaced a distance of 11–12 cm.

61. A New Electrostatic Method for the Determination of Young's Modulus. ROBERT B. JACOBS AND DENNISON BANCROFT, *Harvard University.*—A variable frequency precision oscillator is used to vibrate the sample through an electrostatic drive. The condition of resonance is ascertained by an electrostatic pickup feeding into the high impedance first stage of a 100-decibel amplifier. This method of drive and pickup has obvious advantages over either the piezoelectric or magnetic method, since each of the latter becomes ineffective at high temperatures. The present method has no such limitation and should be very valuable for the study of elastic properties of materials at very high temperatures. A further advantage, where metallic samples are concerned, is that they are used unloaded, thus obviating the usual load correction. The method is a rapid one, since the only adjustment necessary is a slight movement of the electrodes to compensate for the expansion or contraction of the sample at the different temperatures. Utilizing a steel cylinder ($\frac{1}{4}$″ diam., 4″ long) Young's modulus has been measured in the temperature range from 85°–373° absolute. The accuracy is of the order of one part in ten thousand.

62. Electric Impedance of *Nitella* During Excitation. KENNETH S. COLE AND HOWARD J. CURTIS, *College of Physicians and Surgeons, Columbia University.*—The membrane impedance characteristics of the long single cells of the fresh water plant *Nitella* are practically identical with those of single nerve fibers,[1] and their propagated waves of excitation are similar except for velocity. The changes in the alternating current impedance during this excitation wave in *Nitella* have been measured with the current flow normal to the cell axis and at 7 frequencies from 0.10 to 10 kilocycles per second. At each frequency the resting cell was balanced in a Wheatstone bridge with a cathode ray oscillograph, and the changes in the complex impedance during activity were determined from the bridge unbalance recorded by motion pictures of the oscillograph figure. An extension of the previous technique of interpretation of the transverse impedance shows that the dielectric impedance of the membrane which normally corresponds to a capacity of 0.9μf/cm^2 decreases about 15 percent without change of phase angle while the membrane resistance decreases from probably $2 \cdot 10^5$ ohm cm^2 to about 10^3 ohm cm^2 at the height of the excitation wave. The time relations of these changes and the accompanying action potential form a basis for the quantitative theory of nervous conduction.

[1] H. J. Curtis and K. S. Cole, Phys. Rev. **52**, 244 (1937). H. J. Curtis and K. S. Cole, in press.

63. A Stabilized a.c. Operated Ultramicrometer. DAVID L. ARENBERG AND PERCY M. ROOPE, *Clark University.*—An improved type of direct recording (Dowling) ultramicrometer was designed that reduced the difficulties found in the previous use of this instrument at high sensitivity. Two triode operated 6F6 vacuum tubes having a common power supply were placed as complex impedances in two arms of a Wheatstone bridge and operated as separate oscillators; the remaining arms were pure resistances. When the tubes were operated at such close frequencies that their heterodyne beat note disappeared, the balance was found to be extremely sensitive to frequency shifts in this locked region. Motion of condenser plates *vs.* galvanometer deflection gave sensitivities of 4×10^{-10} cm/mm and showed much higher sensitivity possible. To eliminate mechanical difficulties of producing small displacements only a portion of the total capacity was varied. Because of the symmetry of the circuits, both oscillators gave the same reaction to conditions of temperature, voltage, stray capacity, aging, etc., and eliminated these through their differential action. Tuned grid circuits of 3 megacycles were used and the set fed through a 110-volt a.c. voltage regulator.

64. A 600 kv a.c. Generator for the Production of Neutrons. T. R. FOLSOM, *Memorial Hospital, New York City.*—A novel method of cascading conventional x-ray transformers to produce potentials of 600 kvp is described. Eight 75 kv, 40 ma transformers of the radiographic type are assembled in oil tanks made from ordinary earthenware jars and mounted in cascade on an insulated frame. The primaries of transformer units at different potential levels are energized and regulated by alternators driven through insulated shafts by synchronous motors. The voltage is applied to a two-stage, short-gap discharge tube with ion-source in the high voltage terminal and target at ground potential.

65. A Wide Range Ionization Current Meter. G. FAILLA, *Memorial Hospital, New York.*—The well-known (null) method of measuring very small unidirectional currents by varying the voltage across a condenser, has the drawback of requiring close and continuous manual operation during the compensation period, which in turn must be timed carefully. This practical difficulty may be overcome by using a potentiometer of uniform resistance and moving the slider at a constant speed by means of a synchronous motor and suitable speed reducer. The desired value of the compensating current is obtained simply by adjusting the voltage applied to the potentiometer. For some purposes

it is desirable to be able to vary at will the speed of the slider from zero to a convenient upper limit. This may be done by a gear system like the automobile differential. Assuming that the drive shaft speed is constant, the speed of one driven shaft (carrying the potentiometer) may be varied from *zero* to any desired value by relatively small percentage changes in the speed of the other driven shaft—which may be brought about by simple means. Using an FP-54 detector a 10,000-fold current range may be obtained readily with a single condenser of fixed capacity.

66. A Vacuum Type High Speed Electrostatic Motor. C. S. SMITH, *University of Virginia. (Introduced by J. W. Beams.)*—A blade mounted on a tubular steel shaft was held between quadrant plates by a modified Holmes[1] magnetic suspension. The changes included passing the light beam under the control vane and elimination of all batteries. The blade was charged negatively and driven by alternating voltages on the quadrants generated in any one of three ways. Two of these involved automatic synchronization of the rotor, accomplished respectively by interruption of a beam of light and by an electrostatic pickup. The third consisted of synchronization with an independent oscillator. A rotor has been spun up to 3200 rev./sec, with approximately constant acceleration.

[1] F. T. Holmes, R. S. I. **8**, 444 (1937).

***67. An Alternative Description of the Compound Nucleus.** H. A. BETHE AND E. J. KONOPINSKI,[1] *Cornell University.*—The usual formulation of the theory of the compound nucleus meets with difficulties in joining the compound wave function at the surface to the wave function of the separated system. Consequently, (1) it is difficult to estimate the width of the compound levels, and (2) the method becomes unsatisfactory for very high energies when the widths are large and phase relations between incident and produced particle exist. These difficulties are avoided when the compound wave function is expanded as a sum of products of wave functions of residual nucleus and incident particle. The latter will obey a system of Schrödinger equations which are strongly coupled together, the strength of the coupling causing the "compound" character of the complete wave function. The coupling coefficients are certain integrals over the wave functions of the residual nucleus, and depend on the position of the incident particle in the nucleus. As an approximation, it is proposed to neglect this latter dependence. Then the coupled Schrödinger equations can be solved, the widths under various circumstances (high and low energy, with and without potential barrier, few and many possible states of the residual nucleus) can be estimated, and the transition to the Born approximation at high energies can be described.

* Paper No. 67 to be called for after paper No. 12.
[1] National Research Fellow.

***68. On the Diffraction of Electromagnetic Waves by Small Obstacles.** EUGENE GUTH, *University of Notre Dame. (Introduced by George B. Collins.)*—The special case, where the optical constants of a small obstacle differ but little from those of the surrounding medium, is treated by a method of successive approximations similar to Born's wave mechanical method. The new method is applicable to all forms of the obstacle as, for instance, for spheres, cylinders, ellipsoids. It is also applicable if the refractive index varies with the distance or with the direction. The results can also be obtained by replacing the wave equation for the Hertzian vector by an integral equation. This presentation reveals the relationship between the method of successive approximations and that of particular solutions, i.e., spherical harmonics developments, etc. Criteria for the applicability of the method are given. The method may be used for treating the transmission of light through turbid media containing small obstacles.

* Paper No. 68 to be called for after paper No. 44.

***69. The Lorenz-Lorentz Constant for Paraffin Oil Between 30 and 115 Degrees Centigrade.** A. P. FRIESEN, *Bethel College, Newton, Kansas.*—To measure the optical constants of certain liquid alloys underneath a protecting layer of paraffin oil it was necessary to measure the index of refraction of the oil at various temperatures. As a check the Lorenz-Lorentz constant was determined at each temperature. Only apparatus found in any sophomore physics laboratory was available. A telescope and a scale, illuminated by sodium light, were supported about two meters above a container in which a small mirror, silvered face up, formed a liquid wedge between mirror and the free surface of the oil. The distance between the mirror and the scale and readings of the reflected scale, with and without oil in the container, were the data needed for calculating indices of refraction. Densities were measured with a Mohr balance. Eight determinations between 30 and 115 degrees centigrade gave a value of 0.3211 ± 0.0005 for the Lorenz-Lorentz constant. This is in fair agreement with 0.3245 ± 0.0006, the value obtained by Poulter, Ritchey, and Benz[1] for constant temperature and pressures between 1 and 13,585 atmospheres.

* Paper No. 69 to be called for after paper No. 22.
[1] C. Poulter, Carter Ritchey and Carl A. Benz, Phys. Rev. **41**, 366 (1932).

***70. Optical Constants and Intermetallic Compounds.** A. P. FRIESEN, *Bethel College, Newton, Kansas.*—Determination of optical constants of liquid alloys seems to be a powerful method of detecting so-called intermetallic compounds. Large changes in the neighborhood of concentrations where compounds are known to exist were reported previously.[1] Work is in progress to determine these changes more in detail. The optical constants of twelve liquid thallium-bismuth alloys, between 0 and 30 atomic percent bismuth, have been determined. In this range the usual melting point curves indicate no compounds. If a compound exists, it must be highly dissociated. However, the optical constants decidedly change in the neighborhood of 25 atomic percent bismuth in a manner similar to the changes that occur for the sodium amalgams. Some evidence for the compound Tl_3Bi in e.m.f. data has been reported.[2] Work is begun in determining the changes of the optical constants of liquid thallium amalgams in the neighborhood of 33.3

atomic percent of thallium, where the highly dissociated compound Hg_2Tl is supposed to exist in the liquid state.

* Paper No. 70 to be called for after paper No. 69.
[1] Bull. Am. Phys. Soc. **10**, 13.
[2] R. Kremann and A. Lobinger, Zeits. f. Metallkunde **12**, 246 (1920).

71. Spectrographic Study of the Distribution of Mineral Elements in Sugar Cane. STANLEY S. BALLARD, *University of Hawaii.*—Samples of the ash of various portions of a single sugar cane stalk have been analyzed by the qualitative spectrochemical methods developed in the spectroscopic laboratory of the Experiment Station of the Hawaiian Sugar Planters' Association.[1] The presence in sugar cane of eighteen metals and semi-metals has been established. Large differences were found between the numbers and amounts of elements occurring in the several parts of the plant tested (the leaves, the growing point region, and various sections of the stalk). The results for the common plant constituents phosphorus, potassium, calcium, magnesium, silicon and iron conformed to what the plant physiologist would expect, but data on the less common elements were more striking. More critical analyses of this type are now in progress. Their improvements over the preliminary analyses lie in better sampling, in more careful preparation of samples (including ashing at 300°C), in using weighed portions of ash that are computed in terms of equal dry weights of the original plant materials, and in the use of a more exhaustive spectrographic technic which should reveal the presence of very small traces of the minor elements. Samples were prepared with the aid of Arthur Ayres, Assistant Chemist, Experiment Station H.S.P.A.

[1] S. S. Ballard, Phys. Rev. **52**, 253A (1937).

AUTHOR INDEX TO ABSTRACTS OF NEW YORK MEETING

Andrews, C. L.—No. 22
Arenberg, David L. and Percy M. Roope—No. 63

Bacher, R. F.—see Tomboulian, D. H.
—— **and D. C. Swanson**—No. 7
Baker, Richard F. and John T. Tate—No. 44
Ballard, Stanley S.—No. 71
Bancroft, Dennison—see Jacobs, Robert B.
Bardeen, J.—No. 46
Barnes, B. T.—see Forsythe, W. E.
Beach, J. Y. and K. J. Palmer—No. 51
Beth, Richard A.—No. 35
Bethe, H. A.—see Konopinski, E. J.
—— see Marshak, R. E.
——No. 3
—— **and E. J. Konopinski**—No. 67
Beyer, H. G.—see Carroll, H.
Breit, G. and J. R. Stehn—No. 47

Cannon, C. V.—see Wheeler, John A.
Carroll, H., P. N. Powers, H. G. Beyer and J. R. Dunning—No. 28
Carwile, Preston B.—No. 38
Cole, Kenneth S. and Howard J. Curtis—No. 62
Colwell, R. C., A. W. Friend and D. A. McGraw—No. 60
Cork, J. M.—see Curtis, B. R.
—— see Tape, Gerald F.
Cornell, S. D.—see More, Kenneth R.
Crane, H. R.—see Halpern J.
—— see Ruhlig, A. J.
Critchfield, C. and E. Teller—No. 48
Curtis, B. R. and J. M. Cork—No. 33
Curtis, Howard J.—see Cole, Kenneth S.

Delfosse, J. M. and J. A. Hipple, Jr.—No. 43
Dunning, J. R.—see Carroll, H.

Emslie, A. G.—No. 29

Failla, G.—No. 65
Fisher, Russell A. and Edson R. Peck—No. 53
Folsom, T. R.—No. 64
Forbush, S. E.—No. 41
Forsythe, W. E., B. T. Barnes and Ann L. Shrider—No. 18
Friend, A. W.—see Colwell, R. C.
Friesen, A. P.—Nos. 17, 69, 70
Furry, W. H.—No. 25

Granath, L. P.—see Williams, D. T.
Guth, Eugene—Nos. 37, 68

Haas, Arthur E.—No. 36
Halpern, J. and H. R. Crane—No. 5
Hartman, Paul L. and Lloyd P. Smith—No. 12
Hipple, J. A., Jr.—see Delfosse, J. M.
Hoffman, J. G. and M. Stanley Livingston—No. 6
Holloway, M. G. and M. Stanley Livingston—No. 8

Inglis, D. R.—No. 56

Jacobs, Robert B. and Dennison Bancroft—No. 61
Johnson, Thomas H.—No. 39
Jones, Creighton C.—see Ruark, Arthur
—— **and Arthur Ruark**—No. 13

Karapetoff, Vladimir—No. 1
Konopinski, E. J.—see Bethe, H. A.
—— **and H. A. Bethe**—No. 23

Langer, L. M.—see Mitchell, Allan C. G.
Livingston, M. Stanley—see Hoffman, J. G.
—— see Holloway, M. G.

McGraw, D. A.—see Colwell R. C.
Marshak, R. E. and H. A. Bethe—No. 10
Meissner, K. W.—No. 14

Mitchell, Allan C. G. and L. M. Langer—No. 4
Mohler, Fred L.—No. 42
Montgomery, C. G. and D. D. Montgomery—No. 40
Montgomery, D. D.—see Montgomery, C. G.
More, Kenneth R. and S. D. Cornell—No. 19

Nier, Alfred O.—No. 27

Palmer, K. J.—see Beach, J. Y.
Parratt, L. G.—see Richtmyer, F. K.
——No. 21
Peck, Edson R.—see Fisher, Russell A.
Phillips, M.—No. 32
Pollard, Ernest—No. 26
Powers, P. N.—see Carroll, H.

Richtmyer, F. K. and L. G. Parratt—No. 20
Roope, Percy M.—see Arenberg, David L.
Rose, M. E.—No. 2
Ruark, Arthur—see Jones, Creighton
—— **and Creighton C. Jones**—No. 24
Ruhlig, A. J. and H. R. Crane—No. 45

Schultz, H. L.—No. 34
Scott, G. W., Jr.—see Smith, Lloyd P.
Seitz, Frederick—No. 55
Shrider, Ann L.—see Forsythe, W. E.
Smith, C. S.—No. 66
Smith, Lloyd P.—see Hartman, Paul L.
—— **and G. W. Scott, Jr.**—No. 11
Stehn, J. R.—see Breit, G.
Swanson, D. C.—see Bacher, R. F.

Tape, Gerald F. and J. M. Cork—No. 9
Tate, John T.—see Baker, Richard F.
Teller, E.—see Critchfield, C.
—— **and J. A. Wheeler**—No. 49
Tomboulian, D. H. and R. F. Bacher—No. 15

Van Dyke, K. S.—No. 59
Van Vleck, J. H.—No. 30

Watson, William W.—No. 16
Way, Katharine—No. 52
Weisskopf, V. F.—No. 31
Wheeler, J. A.—see Teller, E.
—— **and C. V. Cannon**—No. 50
Williams, D. T. and L. P. Granath—No. 54

Young, L. A.—No. 57

Zener, Clarence—No. 58

Proceedings of the Metropolitan Section of the American Physical Society

Meeting of March 25, 1938

THE second meeting of the Metropolitan Section of the American Physical Society for the season 1937–1938 was held on Friday, March 25, 1938, in the Pupin Physics Laboratories of Columbia University. The following papers were presented:

Afternoon session, 3:00 P.M.

The Fluorescence of Solids Caused by Ultraviolet Light. S. G. Hibben
Cathodo-Luminescence of Inorganic Crystalline Solids. L. B. Headrick, H. W. Kaufmann and H. W. Leverenz
The Interpretation of Some Types of Crystal Fluorescence. F. Seitz

Evening session, 8:00 P.M.

The Physics of Microphonic Contacts. F. S. Goucher

The following officers were elected for the season 1938–1939:

Chairman—C. J. Davisson
Vice Chairman—I. I. Rabi
Secretary-Treasurer—W. S. Gorton
Members of the Executive Committee: B. Kurrelmeyer, L. A. Turner

W. S. Gorton,
Secretary-Treasurer